EFFECTS OF AGING, DIET AND POTENTIAL GENETIC INTERVENTIONS ON THE LEVELS OF SMURF2 AND ITS INTERACTING PARTNERS IN ZEBRAFISH (*DANIO RERIO*) BRAIN

A DISSERTATION SUBMITTED TO

THE GRADUATE SCHOOL OF ENGINEERING AND SCIENCE

OF BILKENT UNIVERSITY

IN PARTIAL FULFILLMENT OF THE REQUIREMENTS FOR

THE DEGREE OF

DOCTOR OF PHILOSOPHY

IN

NEUROSCIENCE

By

Melek Umay Tüz Şaşik

September, 2020

EFFECTS OF AGING, DIET AND POTENTIAL GENETIC INTERVENTIONS ON THE LEVELS OF SMURF2 AND ITS INTERACTING PARTNERS IN ZEBRAFISH (*DANIO RERIO*) BRAIN

By Melek Umay Tüz Şaşik

September, 2020

We certify that we have read this dissertation and that in our opinion it is fully adequate, in scope and in quality, as a thesis for the degree of Doctor of Philosophy.

_____

Michelle Marie Adams (Advisor)

_____

Urartu Özgür Şafak Şeker

_____

Hatice Güneş Özhan

_____

Özlen Konu Karakayalı

_____

Çağdaş Devrim Son

Approved for the Graduate School of Engineering and Science

_____

Ezhan Karaşan
Director of the Graduate School

ABSTRACT

EFFECTS OF AGING, DIET AND POTENTIAL GENETIC INTERVENTIONS ON THE LEVELS OF SMURF2 AND ITS INTERACTING PARTNERS IN ZEBRAFISH (*DANIO RERIO*) BRAIN

Melek Umay Tüz Şaşik

PhD in Neuroscience

Advisor: Michelle Marie Adams

September, 2020

Aging is a natural process that is ultimate combination of numerous intrinsic and extrinsic changes in an organism. Contrary the common belief, brain aging is not a loss of neurons while it has been shown that subtle cellular and synaptic alterations have contribution to brain aging. Therefore, the molecular and cellular alterations may give more insight into the brain aging process. There are some hallmarks of aging that are common features in different organisms including genomic instability, telomere attrition, cellular senescence. There are some common factors with the ability to regulate more than one of the hallmarks of aging such as Smurf2. HECT-domain E3 ubiquitin ligase Smurf2 has several roles in the cellular processes for example, telomere attrition and cellular senescence. Moreover, its gene expression is higher in the aged brain. Although there are several publications about Smurf2, most of them focused on its role in cancer. We believed that Smurf2 levels should be

examined in terms of brain aging. The first aim of the study was to examine the levels of Smurf2 and its interacting partners across lifespan. Although the Smurf2 protein level was not increased significantly in the whole zebrafish brain, its protein level was upregulated significantly in telencephalon and cerebellum. Also, subcellular protein fractionation demonstrated an enriched Smurf2 level in the cytosolic part. In the case of gene expression levels, *smurf2* level was significantly higher in aged whole brain although its expression was downregulated during aging in telencephalon and cerebellum. In addition, the levels of *mdm2*, *ep300a* and *sirt*1 were lower in the aged telencephalon. According to multivariate analysis there is a potential balance between Smurf2-mediated ubiquitination, ep300a-mediated acetylation and Sirt1-mediated deacetylation but with advancing age, this balance may disrupt and other regulatory genes should also take a role to sustain cellular stability. The second aim was to investigate the roles of Smurf2 on brain aging with the help of genetic interventions including inducible knockin, stable knockout or transient knockdown. Since stable knockin and knockout models should be genotyped before further investigations, the genotyping and phenotyping methods were employed to find an efficient and reliable way. Also, transient knockdown via Vivo-morpholino was applied to adult brain and efficient post injection times of two different morpholinos were identified in order to examine the effects of Smurf2 knockdown in both young and old zebrafish. Lastly, it was aimed to examine the effects of non-genetic interventions including dietary regimens and pharmacological compounds on the gene expression of *smurf2* and its interacting partners and the levels of the neuronal proteins and proliferation/senescence proteins. The opposing short-term dietary regimens, overfeeding and caloric restriction, were altered the levels of neuronal

proteins, HuC and DCAMKL1, and their relation with proliferation and senescence proteins during aging. Also, the gene expression levels of *smurf2* and interacting partners except *tp53* was not influenced by dietary regimens and aging in terms of whole brain. Also, multivariate analysis indicated that the correlations among *smurf2, mdm2, ep300a* and *sirt1* were conserved in both young and old ages independent to dietary regimen which may imply that the balance between ubiquitination, acetylation and deacetylation is maintained in order to provide cellular stability during aging. Heclin, an inhibitor of HECT E3 ligases, were employed to inhibit Smurf2 activity. Before using in adult zebrafish, heclin was applied to embryos to see its effects. The higher dose of heclin decreased the survival ratio and altered the gene expression levels of downstream gene drastically. So, moderate dose of heclin should be applied to the adult brain and neuronal markers should be examined to observe target effects rather than off-target, unspecific impacts. Taken together, Smurf2 has potential roles during aging and it could be a promising target to delay the brain aging process and probably the onset of age-related cognitive decline.

Keywords: zebrafish, aging, brain, smurf2, caloric restriction, overfeeding, genetic interventions, heclin, neuronal proteins

ÖZET

ZEBRABALIĞI (DANIO RERIO) BEYNİNDE YAŞLANMA, DİYET VE OLASI GENETİK MÜDAHALELERİN SMURF2 VE ETKİLEŞİM ORTAKLARININ İFADESİNE ETKİLERİ

Melek Umay Tüz Şaşik

Nörobilim Lisansüstü Programı, Doktora

Tez Danışmanı: Michelle Marie Adams

Eylül, 2020

Yaşlanma, bir organizmadaki çok sayıda içsel ve dışsal değişikliğin nihai birleşimi olan doğal bir süreçtir. Yaygın inancın aksine, beyin yaşlanmasının nöron kaybı olmadığı, küçük hücresel ve sinaptik değişikliklerin beyin yaşlanmasına katkıda bulunduğu gösterilmiştir. Bu nedenle moleküler ve hücresel değişiklikler beyin yaşlanma sürecine daha fazla ışık tutabilir. Genomik kararsızlık, telomer yıpranması, hücresel yaşlanma gibi yaşlanmanın bazı ayırt edici özellikleri vardır, bu özellikler farklı organizmalarda gözlenen ortak özelliklerdir. Smurf2 gibi yaşlanmanın ayırt edici özelliklerinden birden fazlasını düzenleme becerisine sahip olan bazı ortak faktörler vardır. HECT-domain E3 ubikuitin ligaz Smurf2, birçok hücresel işlemde, telomer yıpranması ve hücresel yaşlanma gibi, önemli rollere sahiptir. Ayrıca yaşlı beyinde gen ekspresyonu daha yüksektir. Smurf2 hakkında birçok yayın olmasına rağmen, çoğu kanserdeki rolüne odaklanmıştır. Bu sebeplerle Smurf2 seviyelerinin beyin yaşlanması açısından incelenmesi gerektiğine inanıyoruz.

Çalışmanın ilk amacı, Smurf2'nin ve etkileşimde bulunduğu ortaklarının seviyelerini yaşam boyu incelemekti. Smurf2 protein seviyesi tüm zebrabalığı beyninde önemli ölçüde artmamış olsa da, protein seviyesi telensefalon ve beyincikte (serebellum) önemli ölçüde artmıştır. Ayrıca, hücre içi protein fraksiyonasyonu, sitozolik kısımda zenginleştirilmiş bir Smurf2 seviyesi göstermiştir. Gen ekspresyon seviyeleri durumunda, *smurf2* seviyesi yaşlı tüm beyinde önemli ölçüde daha yüksekken, telensefalon ve beyincikte ekspresyonu yaşlanma sırasında azalmıştır. Ayrıca yaşlı telensefalonda *mdm2, ep300a* ve *sirt1* seviyeleri gençlere göre daha düşüktü. Çok değişkenli analize göre, Smurf2 aracılığıyla ubikuitin ekleme, ep300a aracılı asetilasyon ve Sirt1 aracılı deasetilasyon arasında potansiyel bir denge vardır, ancak ilerleyen yaşla birlikte bu denge bozulabilir ve diğer düzenleyici genlerin de hücresel stabiliteyi sürdürmek için rol alması gerekebilir. İkinci amaç, Smurf2'nin beyin yaşlanmasındaki rolünü, indüklenebilir knockin, stabil knockout veya geçici knockdown gibi genetik müdahaleler yardımıyla araştırmaktı. Kararlı knockin ve knockout modellerinin daha detaylı araştırmasından önce genotiplenmesi gerektiğinden, etkili ve güvenilir bir metot bulmak için genotipleme ve fenotipleme yöntemleri kullanıldı. Ayrıca, Vivo-morfolino aracılığıyla geçici knockdown, yetişkin beynine uygulandı ve Smurf2'nin hem genç hem de yaşlı zebra balığı üzerindeki etkilerini incelemek için iki farklı morfolinonun en etkili olduğu enjeksiyon sonrası süreleri belirlendi. Son olarak, diyet rejimleri ve farmakolojik bileşikleri içeren genetik olmayan müdahalelerin, *smurf2* ve etkileşim ortaklarının gen ekspresyonu ve nöronal ve proliferasyon/senesans proteinlerinin seviyeleri üzerindeki etkilerinin incelenmesi amaçlanmıştır. Zıt kısa süreli diyet rejimleri, aşırı besleme ve kalori kısıtlaması, nöronal proteinlerin, HuC ve DCAMKL1, düzeylerini ve bunların

yaşlanma sırasında proliferasyon ve yaşlanma proteinleri ile ilişkisini değiştirdi. Ayrıca, *tp53* dışındaki etkileşimli partnerlerinin ve *smurf2*'nin gen ekspresyon seviyeleri, beslenme rejimlerinden ve yaşlanmadan etkilenmemiştir. Ayrıca, çok değişkenli analiz, *smurf2, mdm2, ep300a* ve *sirt1* arasındaki ilişkinin, diyet rejiminden bağımsız olarak hem genç hem de yaşlılarda korunduğunu göstermiştir; bu, yaşlanma sırasında hücresel stabiliteyi sağlamak için ubikuitin ekleme, asetilasyon ve deasetilasyon arasındaki dengenin korunduğu anlamına gelebilir. Ayrıca, HECT E3 ligazlarının bir inhibitörü olan heclin, Smurf2 aktivitesini inhibe etmek için kullanıldı. Yetişkin zebra balıklarında kullanılmadan önce, etkilerini görmek için embriyolara heclin uygulandı. Heclin dozunun artması hayatta kalma oranını düşürdü ve bazı genlerin ekspresyon seviyelerini büyük ölçüde değiştirdi. Bu nedenle, yetişkin beynine orta doz heclin uygulanmalı ve hedef dışı, spesifik olmayan etkiler yerine hedef etkileri gözlemlemek için nöronal belirteçler incelenmelidir. Birlikte ele alındığında, Smurf2 yaşlanma sırasında potansiyel rollere sahiptir ve beyin yaşlanma sürecini ve muhtemelen yaşa bağlı bilişsel gerilemenin ortaya çıkışını geciktirmek için umut verici bir hedef olabilir.

Anahtar Sözcükler: zebrabalığı, yaşlanma, beyin, smurf2, kalori kısıtlaması, aşırı beslenme, genetik müdahaleler, heclin, nöronal proteinler

To my beloved family…

ACKNOWLEDGEMENTS

I am deeply grateful to my advisor Prof. Dr. Michelle Adams for giving me a great opportunity to work in the field of the neuroscience, for her endless support, guidance and patient throughout this thesis journey.

I am very thankful to Assoc. Prof. Dr. Güneş Özhan Baykan for her patience with my questions, her feedback and support on the project and being a thesis progress committee and a jury member. I would like to thank to Assoc. Prof. Dr. Urartu Özgür Şafak Sezer for his feedback and critical discussion during my thesis progress and being a thesis progress committee and a jury member. I am also thankful to Assoc. Prof. Dr. Özlen Konu and Assoc. Prof. Dr. Çağdaş Devrim Son for evaluating my thesis and being a jury member.

I would like to thank to Assoc. Prof. Dr. Ayça Arslan-Ergül for her patience, support, critical discussion and encouraging me during these years. I am grateful to my colleagues Elif Tuğce Karoglu-Eravşar for her friendship, endless support and advices, Meriç Kınalı for helping with the preparation of graphs, her sisterhood and compassion. I also thank to all former and current members of Adams Lab; Dilan Çelebi-Birand, Begün Erbaba, Füsun Doldur-Ballı, Zeynep Gültekin, Özge Pelin Burhan, Göksemin Fatma Şengül, Naz Şerifoğlu, Bilge Aşkın, Naz Mengi, Esra Şenol, Beyza Özen, Hande Aydoğan, Duygu Macaroğlu, Duygu Mutlu and Narin Ilgım Ardıç. I would like to record my sincere appreciation to Tülay Arayıcı for her endless support and help in the zebrafish facility.

I have special thanks to my beloved friends, Levent Karacasulu, Merve Akkulak, Ceren Ok and Sevtap Songül for their endless support, understanding, compassion and love.

I am deeply grateful to my parents without them I couldn't get to this point. I would like to thank to my mother Ayşe Şahinbay for encouraging me all the time, her unhesitant support, patience and endless love. I am thankful to my father Ümit Tüz to his support, understanding and great love. I would like to thank my little brother Umut Tüz for his patience, moral support and love.

Last but not least, I am very lucky and grateful to have my spouse Reşat Şaşik. I have special thanks to him for encouraging, understanding, balancing, and helping me without hesitation and his compassion and eternal love. Also, I would like to thank to all family members I haven't mentioned yet in this limited page.

I would like to thank to The Scientific and Technological Research Council of Turkey (TÜBİTAK) for financial support as 2211 National Graduate Scholarship Programme (BIDEB). I would like to acknowledge European Molecular Biology Organization (EMBO) Installation Grant to Michelle M. Adams for financially supporting the experiments during my Ph.D.

TABLE OF CONTENTS

LIST OF FIGURES

LIST OF TABLES

CHAPTER 1

INTRODUCTION

1.1 Brain Aging

Aging is a natural process that is the ultimate combination of numerous intrinsic and extrinsic changes in an organism. Normal aging is associated with impairments in cognitive function, including the slowing of information processing, declines in memory and increased failure of executive or strategic control over cognitive operations [1]. During normal aging, there is a measurable but tolerable loss in cognitive ability that does not affect a person's quality of life or ability to function [2].

At first sight, brain aging is thought to be a result of neuronal death. However, studies using multiple model organisms have shown that there is no significant change in the hippocampal neuron number with aging and so neuron loss does not contribute to age-related cognitive decline [3]. In another study, the number of neurons in the hippocampus, parahippocampal region and subregions of parahippocampal region including perirhinal cortex, lateral entorhinal area, postrhinal cortex and medial entorhinal area showed no significant differences between young and aged groups [4]. Brain aging is not a loss of neurons while it is accompanied by specific and relatively subtle synaptic alterations in the hippocampus and prefrontal cortex [5]. Furthermore, until recently it was hypothesized that neurons are not regenerated unlike cells in colon or skin tissues. Recent evidence showed that neurons also regenerate but at a slower rate than most of the other tissues [6].

Neurogenesis, a process of regenerating new neurons from neural progenitors, occurs in restricted brain regions across lifespan in mammals [7]. Also, it was shown that 700 new neurons are generated every day in each hippocampus of adult human brain [8] while its rate declines with aging [6], [8]. Moreover, it has been shown that subtle cellular and synaptic alterations have contribution to brain aging [9]–[12]. Therefore the molecular and cellular alterations may give more insight into the brain aging process.

1.2 Molecular hallmarks of aging

At the molecular level, because of the accumulation of cellular damage throughout the life, a loss of physiological integrity and function increases vulnerability to pathologies, which are the characteristics of aging process [13]. López-Otín et al. have defined nine hallmarks of aging that represent common features of aging in different organisms, which are genomic instability, telomere attrition, epigenetic alterations, loss of proteostasis, deregulated nutrient sensing, mitochondrial dysfunction, cellular senescence, stem cell exhaustion, and altered intercellular communication [13]. These likely contribute to the aging phenotypes in the brain.

1.2.1 Genomic stability

Genomic instability increases with age because of the accumulation of exogenous and endogenous factors such as mutations and reactive oxygen species [14]. During DNA replication, polymerases can do some errors, however, the other enzymes in the nucleus can proof-read and correct these errors. Also, the external

mutagens such as chemicals and ultraviolet radiation in sunlight cause mutations in the genome. If the errors cannot be compensated by several repair mechanisms, which deal with most of the damages of nuclear DNA, the mutations in the genome are accumulated in the cells [15]. Thus, tumor progression and premature aging diseases, such as Werner syndrome and Bloom syndrome, are the consequence of increased DNA damage accumulation [15], [16]. Because of the important role in the center of cell, genomic instability is a primary hallmark of aging.

1.2.2 Telomere attrition

Telomere attrition is another primary hallmark of aging. During replication, DNA polymerases cannot replicate completely the terminal ends of linear DNA molecules called end-replication problem [17] unless telomerase, a specialized DNA polymerase, is not expressed in the cell. Thus, the progressive and cumulative loss of telomere-protective sequences from chromosome ends occurs and finally telomere attrition is a normal process during aging. Recently, it was demonstrated that post-mitotic neurons display the characteristics of senescence due to telomere attrition [18]. Moreover, telomere shortening leads to apoptosis and replicative senescence [13], [14].

1.2.3 Proteostasis

Proteostasis involves the multiple mechanisms including protein synthesis, protein folding, the stabilization of correctly folded proteins, trafficking, aggregation, disaggregation and degradation of misfolded/unfolded proteins by the proteasome or the lysosome [19]. It was shown that the quality control mechanisms of proteostasis are altered with aging [20]. Moreover, aging and age-related pathologies including

Alzheimer's disease and Parkinson's disease are associated with impaired proteostasis or impaired proteasomal degradation mechanism [19].

1.2.4 Deregulated nutrient sensing

The somatotrophic axis consist the growth hormone (GH) and its secondary mediator, insulin-like growth factor 1 (IGF1). The intracellular signaling pathway driven by IGF1 informs cells about glucose presence like insulin. Thus, insulin and IGF1 signaling (IIS) pathway is the most conserved aging-controlling pathway [13]. Genetic changes or non-genetic interventions that alter the functions of GH, IGF1 receptor, insulin receptor, or downstream intracellular effectors have been linked to longevity both in humans and in model organisms [21], [22]. Also, the sirtuin family regulates the lifespan together with metabolism [23]. For example, the high fat diet in mice caused to downregulation of SIRT1 protein levels in hippocampus [24] while caloric restriction (CR) diet increased *sirt1* gene expression in the prefrontal cortex and hippocampus [25] and SIRT1 protein expression in hippocampus [26].

1.2.5 Cellular senescence

As implied by its name, senescence derives from senex, a Latin word meaning old man or old age. This senescence is an antagonistic hallmark of aging and sometimes termed cellular aging or replicative senescence [27]. The term "senescence" means deteriorative processes following development and maturation. Cellular senescence is a compensatory response that operates by removing damaged and potentially oncogenic cells. In aged organisms, this system may become inefficient and leads to the accumulation of senescent cells that may contribute to aging [13]. The *p16* gene is an important regulator of senescence and used to identify

senescent cells [28]. The other marker to be used for the specific identification of senescent cells is the senescence-associated β-galactosidase (SA-β-gal) [29]. Although the senescence term comes from a word meaning old age, actually it is an important compensatory mechanism to protect organisms from the accumulation of damaged cells and so has an antagonistic effect on aging [13].

1.3 Smurf2 and its interacting partners

SMAD specific E3 ubiquitin protein ligase 2 (Smurf2) has several roles in diverse cellular processes and works coordinately with some interacting partners to regulate downstream genes and proteins [30]. It may a common factor with the ability to regulate most of the hallmarks of aging mentioned previous sections. For example, the ectopic expression of Smurf2 is enough to induce telomere attrition-dependent cellular senescence [31]–[33] and it controls the genomic stability through RNF20 [34]. Moreover, its expression increased in hematopoietic stem cells (HSCs) during aging [35]. In the light of these evidences, Smurf2 and its interacting partners (Figure 1.1) should be investigated in terms of aging in detail.

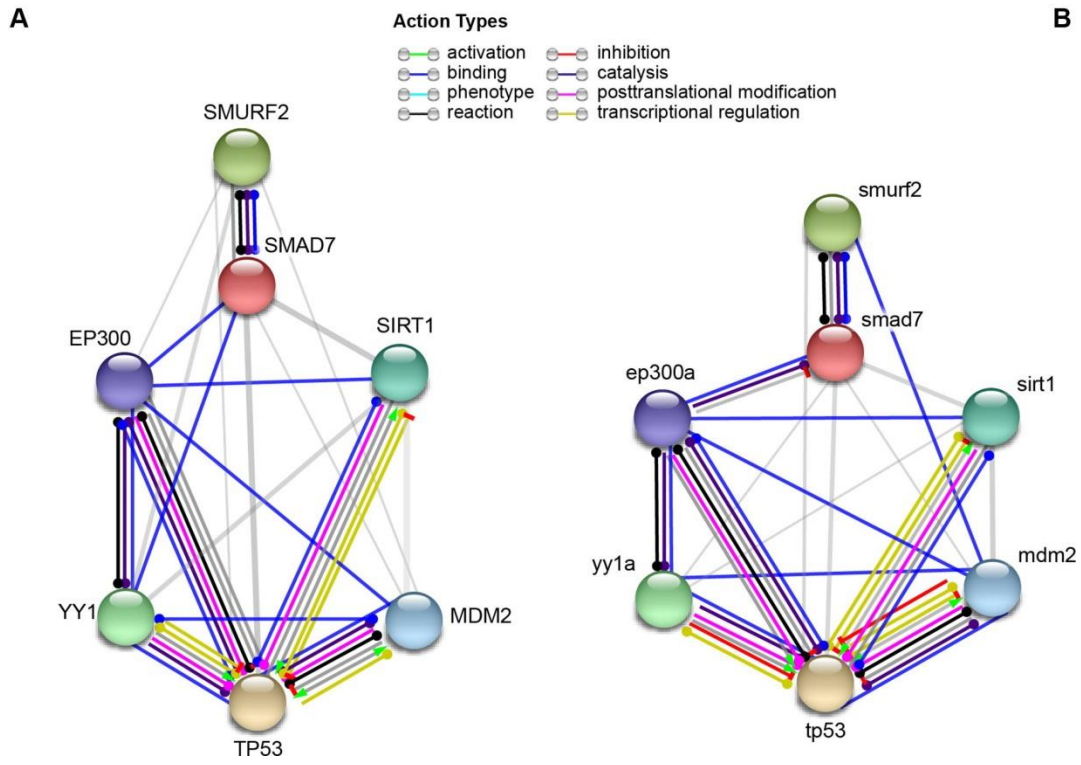

Figure 1.1 STRING analysis of 7 proteins in (A) human; (B) zebrafish. Color nodes represent the proteins and color lines represent interaction type between nodes. Green line: activation, red line: inhibition, blue line: binding, purple line: catalysis, cyan line: phenotype, magenta line: PTM, black line: reaction, yellow line: transcriptional regulation. (Reprinted from Tuz-Sasik et al., 2020 [36])

1.3.1 Smurf2

Smurf2 is a conserved HECT-domain E3 ubiquitin ligase and belongs to Nedd4 subgroup [37]. Firstly, its negative regulatory role in transforming growth factor β (TGF-β) signaling was defined [38]. Smurf2 interacts with phosphorylated Smads and TGF-β type 1 receptor and leads to their ubiquitination and degradation [30]. Then, its role in other signaling pathways and cellular processes were identified [31]–[35]. For example, telomere attrition causes the increased Smurf2 expression

and its overexpression is enough to induce the senescent phenotype [31]. Furthermore, the expression of Id1 at protein level decreases depending on the upregulation of Smurf2 expression which is the result of telomere shortening [31], [32]. It was suggested that the decline in the protein level of Id1 link Smurf2 with p16 mechanistically. It is already known that the gene expression of *p16* increases in cells during senescence and this leads to the decrease in stem cell self-renewal during aging [35]. Moreover, in a review paper by David et al., Smurf2 was defined as a double edged sword because of both tumor-suppressor and tumor-promoter functions [30]. However, most of the published studies focused on its role in cancer mechanism. A previous research of our group indicated that *smurf2* gene expression increases significantly in the brain of aged zebrafish [39]. It should be further investigated in terms of brain aging because of its significant impacts on the hallmarks of aging.

1.3.2 Tp53

Tumor protein p53 (tp53) is often called as the guardian of the genome [40]. It has key regulatory roles in cell cycle arrest, DNA repair, apoptosis, and cellular senescence as a response to cellular stressors [41], [42]. The activity of tp53 is under tight control of post-translational modifications (PTMs), protein-protein interactions and protein stabilization [41], [43]. For example, the predominant negative regulator of tp53 is an E3 ubiquitin ligase ‘mouse double minute 2’ (MDM2) [41]. Also, a transcription factor, Yin Yang 1 (YY1), is also a negative regulator of tp53 [44], [45]. Smurf2 protein regulates both MDM2, and YY1 and indirectly tp53 levels [46], [47]. Furthermore, E1A Binding Protein P300 (ep300), a transcriptional co-activator,

acetylates tp53 protein [48] which inhibits the ubiqutination of tp53 by MDM2 [42]. However, MDM2 suppresses the acetylation of tp53 by ep300 [48].

1.3.3 Mdm2

E3 ubiquitin ligase ‘mouse double minute 2’ (MDM2) is a negative regulator of tp53 [41]. As a RING-domain E3 ligase, MDM2 ubiquitinates and subsequently degrade tp53 protein [42]. Also, MDM2 activity and stability is regulated by several mechanisms [47]. For example, Smurf2 stabilizes the MDM2 protein to promote tp53 degradation [47]. On the other hand, YY1 interacts with MDM2 to form tp53-MDM2 complex and promote the degradation of tp53 [44], [45]. Furthermore, it was shown that dysregulation in the MDM2-tp53 balance leads to premature aging [43], [49].

1.3.4 Ep300a

Ep300, a transcriptional co-activator and histone and lysysl acetyltransferase, acetylates tp53, YY1 and Smad7 proteins [44], [48], [50]. The ep300-mediated acetylation of Smad7 protects it from ubiquitination-mediated degradation [50]. However, ep300-mediated acetylation of tp53 is inhibited by YY1 [44]. Last but not least, ep300 protein levels decrease in the senescent cells [51]. Taken together, ep300 may have an indirect relation with Smurf2 in the regulation of Smad7 and tp53 and should be investigated in terms of brain aging. Moreover, ep300 could be a master regulator of genes dysregulated in the obesity and normalized by CR and resveratrol [52].

Due to the existence of teleost-specific genome duplication [53], there are two paralogues of ep300 in the zebrafish genome, ep300a and ep300b. A previous study indicated that both *ep300a* and *ep300b* expressed in the adult brain while only ep300a

is catalytically active transferase in the brain [54]. In the present study conducted with zebrafish, *ep300a* gene was considered because of its active function in the brain.

1.3.5 Yy1a

YY1 is a transcription factor and it is a well-known negative regulator of tp53 [44], [45]. YY1 disrupts the interaction between tp53 and ep300 and thus acetylation and stabilization of tp53 [44]. As mentioned in previous section, YY1 is physically interacted with MDM2 and promotes the degradation of tp53 [44]. At that point, Smurf2 relieves the suppression on tp53 protein by ubiquitin-mediated degradation of YY1 [46]. In addition, YY1 regulates the genes associated with neurodegenerative diseases according to a transcriptional meta-analysis [55]. Lastly, it was shown that YY1 is a part of the repressor complex with sirtuin 1 (SIRT1) to suppress microRNA-134 and regulate synaptic plasticity and memory formation [56]. Hence, YY1 could be investigated to determine its role during brain aging.

Similar to ep300, YY1 has two paralogoues in the zebrafish genome, yy1a and yy1b, because of the genome duplication [53]. At 3 days post fertilization (dpf), *yy1a* was expressed in the brain and eye tissues and also *yy1a* knockdown caused to upregulation of tp53 and the developmental brain defects [57]. In the present study conducted with zebrafish, *yy1a* gene was considered because of its potential function in the brain.

1.3.6 Smad7

Smad7 is an inhibitory Smad that acts as a negative regulator of TGF-β signaling pathway [58]. Smad7 exports Smurf2 to the cytosol and recruits it to TGF-β

receptor complex for the ubiquitin-mediated degradation of TGF-β receptors as well as Smurf2 itself and Smad7 [58], [59]. However, ep300-mediated acetylation protects Smad7 against the ubiquitin-mediated degradation by Smurf2 [50], [60]. Moreover, Smad7 is deacetylated by SIRT1 to inhibit TGF-β signaling [58]. It has been shown that PTMs compete with each other to regulate the stability of Smad7 [50], [60]; Smad7 is ubiquitinated by Smurf2, acetylated by ep300 and deacetylated by SIRT1 [50], [58], [59].

1.3.7 Sirt1

SIRT1 is a nicotinamide adenine dinucleotide (NAD)-dependent deacetylase that regulates lifespan in concert with metabolism [23]. For example, its protein level decreases in the high fat-fed mice [24] while CR diet increased the gene and protein expression of SIRT1 [25], [26]. Moreover, SIRT1 regulates cellular senescence by deacetylating target proteins [61]. Specifically, SIRT1 deacetylates Smad7 and so inhibits TGF-β signaling [58]. Furthermore, tp53 is deacetylated by SIRT1 [62], [63]. Lastly, SIRT1 works coordinately with YY1 in a repressor complex to regulate synaptic plasticity and memory [56]. Taken together, all of these genes of interest are interacting with each other and their relations in terms of brain aging should be investigated to unravel the neurobiological underpinnings of aging.

1.4 Zebrafish as a gerontological model

Zebrafish (*Danio rerio*) is a small teleost with several advantages. Firstly, one female may produce several hundred transparent eggs which provide an easy visual observation of developing embryos because embryos develop *ex utero* [64].

Secondly, because of their generation time is about 3–5 months [65], they can be reproduced to large populations easily and also large populations can be maintained at very low cost. Other advantage is that zebrafish genome has been sequenced already and show 70% similarity with human genome and 82% similarity with disease-related genes [66].

In addition to general advantages of zebrafish, it has become popular as a gerontological model because it has an integrated nervous system and shows cognitive decline and behavioral properties such as memory and social behaviors [14], [67]–[69]. They age gradually like humans [65]. Moreover, their major brain regions have been mapped and homologous regions were defined [70], [71]. For instance, the ventral division of the lateral zone of area dorsalis (Dlv) in medial pallium is the zebrafish equivalent of mammalian hippocampus while the medial zone of dorsal telencephalon (Dm) is the putative homolog of mammalian amygdala [70], [72]. Also, several studies indicated that long-term potentiation (LTP), the underlying mechanism of learning and memory, occurs in telencephalon region of zebrafish brain and it is N-methyl-D-aspartate (NMDA) receptor-dependent similar to mammals [73]–[75].

The zebrafish brain has regenerative properties and neurogenesis which is not restricted to the telencephalon but is widespread throughout the entire brain with 16 distinct proliferative zones [76], [77]. Although they possess a high regenerative capacity, their growth rate decreases with aging. Moreover, neurogenesis declines during aging [78], [79]. In parallel to decreasing growth rate and neurogenesis, zebrafish tissues such as skin and brain show increased senescent phenotype with age

[79], [80]. An important biomarker of aging, SA-β-gal, increases in a linear fashion with age in zebrafish [80]. Also, as explained in a review of Van Houcke et al., zebrafish share same hallmarks with mammals during aging [14]. All these features make zebrafish an attractive model organism to study brain aging and age-related changes. Also, it was shown that *smurf2* expression is upregulated with advanced age in the adult zebrafish brain [39].

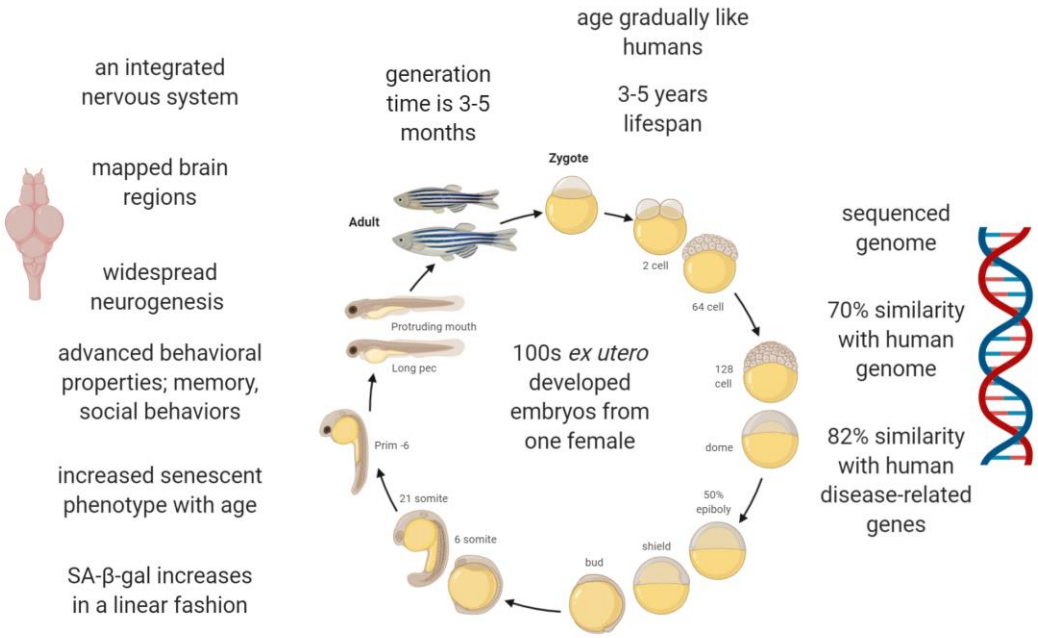

Figure 1.2. Zebrafish developmental time line and its properties as a model organism. The image is created with BioRender.

1.5 Genetic interventions

The forward and reverse genetic approaches are widely applicable on zebrafish to generate mutant or transgenic models. These genetic approaches can be

stable or transient based on their lifelong or short-term effects, respectively. This section covers Tol2 transposase system, CRISPR-Cas9 system and Vivo-morpholino knockdown technology.

1.5.1 Tol2 transposase system

Tol2 transposon system transposases and integrates the gene of interest into zebrafish genome very efficiently. The Tol2 element, the natural transposon in vertebrates, was identified from the genome of the medaka fish (*Oryzias latipes*). Firstly, the plasmid containing a Tol2 vector is produced according to experimental needs. For example, in addition to the gene of interest, a specific promoter that is ubiquitously expressed or expressed by an induction such as heat-shock, and/or a specific tag for easy detection such as EGFP or mCherry fluorescent tags can be integrated into the Tol2 vector [81]. The destination Tol2 vector is co-injected with *in vitro* synthesized Tol2 transposase mRNA into one-cell stage embryos to catalyze the transposition of the Tol2 vector including the gene of interest to the genome in the zebrafish germ lineage [82]. The Tol2 vector and transposase mRNA injected embryos, that are called as F0 generation, are grown to adulthood and crossed with wild-type animals to create stable transgenic fish in the next generations [82]. Moreover, by using the Tol2 transposon system, important genetic methods, such as gene trapping, enhancer trapping, and the Gal4-UAS system were developed to study developmental biology, organogenesis, and neuroscience [83].

1.5.2 CRISPR-Cas9 system

CRISPR/Cas9 can edit the genome of zebrafish with high efficiency [84]. Clustered, regularly interspaced, short palindromic repeats (CRISPR) – CRISPR-associated (Cas) system normally found in bacteria is a defense mechanism to silence foreign nucleic acids [84]. This bacterial defense mechanism has been adapted to create guide RNAs (gRNAs) that direct site-specific DNA cleavage by the Cas9 endonuclease *in vivo*. The site-specific gRNA is designed as 20 bp sequence which is complementary to genomic target sequence adjacent to protospacer adjacent motif (PAM) site of NGG [84]. The mixture of gRNA and Cas9 mRNA/protein is co-injected into one-cell stage embryos to generate gRNA-targeted DNA double strand breaks (DSBs) mediated by Cas9 cleavage enzyme. Then, DSBs are repaired via homology-directed repair (HDR) or non-homologous end-joining (NHEJ) and this repair mechanism generally results in insertions or deletions (indels) of variable length and thus frame shift or non-sense mutations [84], [85]. If these mutations are found in the germ lines, then they are transmitted to next generations and so stable mutant lines are generated.

1.5.3 Vivo-morpholino knockdown technology

Morpholino technology is a widely-used knockdown system in the zebrafish organism [86]. There are two main types of morpholinos; splice-blocking and translational-blocking morpholinos. Splice-blocking morpholinos are designed to target intron-exon junctions and inhibit the pre-mRNA processing [86]–[88]. However, translational-blocking morpholinos are designed to target against the

initiation codon of target mRNA to inhibit the translation of protein [86]–[88]. Vivo-morpholinos are designed to deliver into tissues rather than the embryos [89]. In order to deliver Vivo-morpholino to adult brain, cerebroventricular microinjection (CVMI) method has been developed [90], [91]. After a skull incision under anesthesia, Vivo-morpholino solution including cell tracker dye is injected by using a glass injection capillary at the incision site [91]. Then zebrafish recover in fresh water. At least 30 min later, the fluorescence signal is controlled under anesthesia [91]. The effect of morpholino is transient and lasts for at most 5 days [86], [87], [91].

1.6 Non-genetic interventions

Non-genetic interventions may also be utilized to investigate the cellular and molecular alterations during brain aging. One of the widely used non-genetic intervention is dietary ones including caloric restriction (CR) or overfeeding (OF) [79], [92]–[94]. Moreover, drug or inhibitor treatment is using to change molecular and cellular biology of organism [92], [95]–[97].

1.6.1 Dietary interventions

Non-genetic dietary interventions have impacts on the lifespan, healthspan and mindspan. For example, high calorie or high fat diet leads to age-related metabolic deteriorations including type-2 diabetes, cardiovascular diseases, accelerated brain aging and cognitive impairments [98]–[101]. Moreover, high caloric intake change the molecular and cellular mechanisms in the brain that may cause cognitive decline [98], [99], [102], [103]. On the contrary, caloric restriction (CR) is the only non-genetic intervention to extends the lifespan and healthspan

across multiple species [21], [104], [105]. The low caloric intake (CR) reduces the body fat and delays the onset of age-related metabolic diseases such as type-2 diabetes, cardiovascular diseases [106] and attenuates the cognitive decline with the subtle alterations in the synaptic proteins [10], [107], [108].

Importantly, few studies have investigated the impacts of high calorie intake, overfeeding (OF), and low calorie intake (CR) on the brain aging of zebrafish. For example, a publication indicated that 6 week high fat-fed young zebrafish have increased level of *TrkB* while decreased level of *BDNF* gene expression in the central nervous system [109]. Moreover, lifelong high calorie diet decreased the neurogenesis and declined the cognitive performance in 1 year old zebrafish as compared to *ad libitum* (AL)-fed 1 year old and even 3 year old fish [110]. In addition, CR diet has applied to this model organism previously in our laboratory [79], [92]. However, very few publications have applied these opposing dietary regimens, OF and CR, together in the same experimental conditions to unravel their diverse mechanisms with respect to brain aging. Thus, to the best of our knowledge, this present study is one of the few studies examined the impacts OF and CR diets together in terms of the expression of neuronal proteins as well as the gene expression of *smurf2* and its interacting partners across lifespan.

1.6.2 Pharmacological interventions

The other important non-genetic intervention to alter aging profile is the drug/inhibitor treatment. Some of the chemicals mimic CR diet such as resveratrol and rapamycin or induce the apoptosis of senescent cells named as senolytic drugs

and thus these pharmacological compounds have anti-aging effects [111]. For example, resveratrol, an activator of SIRT1 and a CR mimetic, extends the lifespan of yeast [112] while it changes the health parameters and transcription profile in mouse tissues without extending the lifespan [113]. It has been shown that another CR mimetic, rapamycin, extends the lifespan in yeast, worms and mouse models through the activation of autophagy [111]. Moreover, the accumulation of senescent cells in tissues is the hallmark of aging and this negative effect may be reversed by senolytic compounds such as quercetin [111]. Another approach is to suppress the telomere attrition by using telomerase activators [111]. It was shown that a telomerase activator increases the healthspan in mice [114] and another telomerase activator compound has neuroprotective effects in SOD1 transgenic mouse [115]. Taken together, the pharmacological interventions could also be utilized to increase lifespan, healthspan and mindspan.

A HECT E3 ligase inhibitor, heclin, was identified over the past decade to inhibit specifically HECT-domain E3 ubiquitin ligases, Smurf2, Nedd4, and WWP1 [116]. Since the previously published studies indicated that Smurf2 expression increased during aging [35], [36], [39], it may imply that Smurf2 inhibition via heclin in the adult animals could lead to delayed aging profile. Recently, Redondo et al. demonstrated that hippocampal heclin injection improves the short-term memory, consolidation and retrieval based on the administration time [97]. Taken together, heclin administration to adult zebrafish may delay the onset of aging profile and age-related cognitive decline and should be investigated to unveil the roles of Smurf2 during aging.

1.7 Aims and Hypothesis

According to previous studies [35], [39], Smurf2 expression increases with age in brain and bone marrow. Also, Smurf2 upregulation leads to cellular senescence as a consequence of telomere shortening and it controls the genomic stability [31], [34]. Taken together, it is suggested that Smurf2 protein has important roles in the aging process. Although its expression is well-studied in cancer pathways, to the best of our knowledge, the current study is one of the first studies to investigate Smurf2 gene and protein expression with respect to genetic and non-genetic interventions across lifespan.

The first aim of this thesis was to investigate the Smurf2 protein and gene expression levels across lifespan and to analyze the gene expression levels of its interacting partners during aging in both whole brain and specific brain regions. It was hypothesized that Smurf2 protein expression levels would increase with advanced age and its interacting partners would be affected by this increase. The next purpose was to examine the impacts of Smurf2 alterations in response to genetic interventions including inducible knockin, stable knockout or transient knockdown. We hypothesized that upregulation of Smurf2 would accelerate the brain aging processes while its downregulation could delay the aging phenotypes. Lastly, it was aimed to investigate the effects of non-genetic interventions on the gene expression of *smurf2* and its interacting partners and the protein levels of the neuronal and proliferation/senescence proteins. The hypothesis was that the opposing dietary regimens would have diverse impacts on the neuronal markers as well as on the levels

of Smurf2 and its interacting partners while the Smurf2 inhibition with drug treatment could alter the survival of embryos and the levels of its interacting partners.

CHAPTER 2

METHODS

2.1 Subjects

2.1.1 Animals

All fish were raised and maintained in the zebrafish facility in Bilkent University Molecular Biology and Genetics Department, Ankara, Turkey. Zebrafish were kept on a 14-hour light-10-hour dark cycle at 27.5^0C. Fry fish were fed twice a day with fry dry food and once a day with small *Artemia* while adult fish were fed twice a day with dry food flakes and once a day with live food, *Artemia*, which is live food and a predatory source for the animals. The day before breeding, 6-8 pairs of wild-type (WT) fish were put into the breeding tanks in the afternoon as one pair, keeping the male and female separated with a separator. The next day, the separator was removed from the breeding tanks. After the eggs were fertilized, within 20 min, the embryos were collected into a petri dish and raised in E3 medium. All the birth dates were recorded and the fish with the same date of birth were kept together. All fish were maintained in the zebrafish facility.

In Chapter 3, to determine the gene and protein expression of Smurf2 in the adult brain, a total of 56 WT zebrafish were utilized. The distribution of zebrafish was young (6–8 months old) and old (29–35 months old) male and female animals. The age range of old group were determined according to Yu et al. [69] indicating that in zebrafish cognitive decline occurs between 24-36 months. The animal protocol for

this study was approved by the Bilkent University Local Animal Ethics Committee (HADYEK) with approval date Feb 21, 2018 and number 2018/5.

In Chapter 4, after the eggs were fertilized, within 20 min, the embryos were collected into a petri dish and then Tol2 transposase system or CRIPSR-Cas9 system was injected to one-cell stage embryos. The Tol2 transposase injected F0 generation was labeled as *Tg*(*hsp70l:smurf2_EGFP*) and CRISPR-Cas9 injected F0 generation was labeled as *Tg*(*smurf2*_e10). After *Tg*(*hsp70l:smurf2_EGFP*) F0 animals were grown to adulthood, they were bred with WT animals and embryos were collected for heat-shock application and at the end of the heat-shock application, they were examined under fluorescence microscope and then euthanized on ice. When the *Tg*(*smurf2*_e10) F0 animals became sexually mature, they were bred with WT animals to collect F1 embryos. Also, 8 adult *Tg*(*smurf2*_e10) fish were utilized to optimize the PCR-based genotyping methods. The animal protocol for this study was approved by the Bilkent University Local Animal Ethics Committee (HADYEK) with approval date Feb 21, 2018 and number 2018/5.

Also, in Chapter 4, Vivo-morpholino injections were applied to adult zebrafish. A total 54 of adult zebrafish were anesthetized with Tricaine and then injected with Vivo-morpholinos including Smurf2-specific morpholinos and standard control morpholinos by CVMI. After desired post injection time, the animals were euthanized on ice and their brain tissues were extracted for further analyses. The animal protocol for this study was approved by the Bilkent University Local Animal Ethics Committee (HADYEK) with approval date July 24, 2017 and number 2017/9.

In Chapter 5, the non-genetic feeding interventions were performed on a total of 86 zebrafish in both young and old ages. Age-matched male and female zebrafish were randomly assigned to the feeding tanks; *ad-libitum* (AL), overfeeding (OF) and caloric restriction (CR). The feeding interventions were give to 9 months old (young) and 20 months old (old) animals and lasted for 12 weeks. At the end of the 12 weeks of intervention, the experiment was finished and animals were sacrificed to determine the effects of age and diet on the zebrafish brain. Without deprivation from any dietary nutrient, the calorie intake was altered among the diet groups. AL groups were fed with 180 mg dry flake per day and with *Artemia* 3 times per week similar to usual daily feeding. However, OF groups were fed with 360 mg dry flake/day and with *Artemia* 2 times per day. CR groups were fed with *Artemia* once a week and with 90 mg dry flake per two days. The animal protocol for this study was approved by the Bilkent University Local Animal Ethics Committee (HADYEK) with the approval date: Sept 6, 2017, no: 2017/12.

In Chapter 5, a non-genetic drug treatment was applied to embryos starting from 6 hpf to at most 5 dpf. Each inhibitor solution and control solutions were applied to 10-12 embryos in 2 ml E3 medium and the embryos were maintained at 28^{o}C incubator during treatment. The treatment was ended at 5 days of age (120 hpf).

2.1.2 Cell lines

The protein samples of MDA-MB-231, MCF7, and A172 cell lines were used for the validation of antibodies in the current study. The MDA-MB-231 cell line is a positive control for the anti-SMURF2 C-terminal (ab211746) antibody and the MCF7

cell line is a positive control for anti-SMURF2, 200–300 aa, (ab94483) antibody. The A172, a human brain glioblastoma cell line, was used as a brain-specific cell line. The MDA-MB-231 and MCF7 cell lines were kindly provided as pellets from Dr. Ali Gure's laboratory in Bilkent University.

2.2 Dissection of adult zebrafish brain

Adult female and male zebrafish (young and old) were euthanized in the ice water [117], [118]. Under the dissecting microscope, the head was separated from the body with a sharp blade and the eyes and optic nerve were separated carefully from the head. After cleaning of excessive tissues, the brain was removed from the skull as entirely intact. The weight of the brain was measured and recorded. The body weight and length of adult animals utilized in Chapter 5 were measured and recorded. For DNA, and RNA extraction, the whole brain or whole embryo was snap-frozen in liquid nitrogen and kept in -80^{o}C. For protein isolation, the tissues were immediately homogenized in lysis buffer for experiments in Chapter 3. However, protein samples were extracted from snap-frozen brain tissues in Chapter 4 and 5.

For further experiments in Chapter 3, after the dissection of entire brain, three brain regions; telencephalon (Tel), the optic tectum (TeO) and, the cerebellum/medulla/spinal cord (Ce) were separated from each brain as shown in Figure 2.1 and the 3 microdissected pieces from each of the three animals in the same age group were pooled together for region-specific analysis. Tel region is including olfactory bulb and telencephalon while Ce region consists of cerebellum, medulla and spinal cord as an integrative center as defined in Wullimann et al., 1996 [71]. The

tissues were snap-frozen in liquid nitrogen and stored at -80^{0}C for further RNA isolation. To extract the proteins, fresh tissues were immediately homogenized in lysis buffer. For subcellular fractionation, dissected whole brains and three microdissected brain regions; Tel, TeO, and Ce, which were pooled, were lysed immediately.

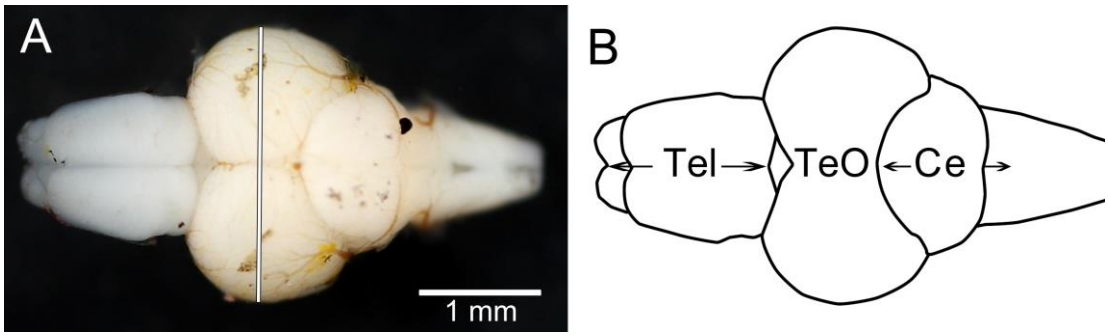

Figure 2.1 Representation of the microdissection procedure. (A) Dorsal photograph of zebrafish brain, (B) schematic representation of brain regions. Tel: telencephalon and olfactory bulb, TeO: the optic tectum, Ce: the cerebellum/medulla/spinal cord. (Adapted from Näslund, 2014 [119])

2.3 Protein Isolation

2.3.1 Total protein isolation

Proteins from individual and pooled brains were homogenized with a 25-gauge, 2-mL syringe in lysis RIPA buffer (50 mM Tris, pH 8.0, 150 mM NaCl, 1% NP40, 0.1% SDS and protease inhibitor [Roche, 5892970001]), for which 60 µL was used per 1 mg of tissue. Homogenates were incubated on ice for 30 min with gentle mixing twice. After centrifuging at 13000 rpm for 20 min at +4^{0}C, supernatants were collected and aliquoted in clean tubes. The protein extraction from the cell lines was

performed in a similar manner for brain tissues as described above. The protein samples were stored at -80^{0}C.

To isolate total protein from the pooled embryos, they were homogenized in lysis RIPA buffer with a sonicator (UP 50H, Hielscher Ultrasonics GmbH, Teltow, Germany) in order to prevent the loss of sample that occurs with the use of a syringe during the protein extraction of pooled embryos. Homogenates were incubated on ice for 30 min with gentle mixing twice. After centrifuging at 13000 rpm for 20 min at +4^{0}C, supernatants were collected in a new tube. The protein samples were stored at -80^{0}C.

2.3.2 Subcellular protein isolation

Subcellular protein fractionation from individual and pooled brains was performed as described in Sezgin et al., (2017) with minor modifications. Whole brain tissues and pooled brain regions were homogenized in 500 µl lysis buffer (50 mM Tris pH 7.5, 150 mM NaCl, 1% Triton X-100, 10 mM NaF and protease inhibitor [Roche, 5892970001]) with Dounce homogenizer. Homogenates were incubated on ice for 10 min and centrifuged at 14000 rpm for 15 min at +4 ^{0}C. Supernatants including cytosolic fraction were collected into a new tube while the pellets including nuclear fraction were dissolved in 150 µl lysis RIPA buffer (50 mM Tris, pH 8.0, 150 mM NaCl, 1% NP40, 0.1% SDS and protease inhibitor [Roche, 5892970001]). Fractions were stored at -80^{0}C.

2.3.3 Bradford assay

To measure the concentration of protein lysates, the Bradford assay (B6916, Sigma) with bovine serum albumin (BSA; Sigma St. Louis, MO, USA) as a standard was performed in the 96-well plate. All standards and samples were loaded in duplicates. Firstly, ddH_2O was added to empty wells as indicated in Table 2.1 for standards. For concentration-unknown protein samples, 4.5 µl ddH_2O was added into each well. Then, protein standards indicated amounts in Table 2.1 and 0.5 µl protein samples were mixed with water.

Table 2.1 Preparation of BSA standards

	BSA (µl) (1mg/ml stock)	ddH_2O (µl)	Final concentration (µg/ml)
Blank	0	5	0
Standard 1	0.5	4.5	2
Standard 2	1	4	4
Standard 3	2	3	8
Standard 4	3	2	12
Standard 5	4	1	16
Standard 6	5	0	20

After 250 µl Bradford reagent was added into the wells, the 96-well plate was mixed in the orbital plate shaker at 300 rpm at room temperature for 2 minutes. The

plate was incubated at room temperature for 10 minutes without shaking before the absorbance value was obtained. The absorbance values were measured at 595 nm wavelength with a multiplate reader (SpectraMax M5, Molecular Devices, Sunnyvale, CA, USA). In the template design, blanks were assigned and utilized to calculate the net absorbance values of standards and unknown proteins. Net absorbance values of standards and the known concentrations were plotted and a linear curve fit was drawn. From the known equation of linear curve fit, the unknown concentrations of samples were calculated with the help of net absorbance values.

2.4 Western Blotting

The protein samples were separated in Sodium dodecyl sulfate polyacrylamide gels (SDS-PAGE) under reducing and denaturing conditions according to their molecular weights. To segregate proteins, 10% resolving gels for total protein lysates and 8% resolving gels for subcellular fractions were prepared. The recipes of resolving gels were shown in Table 2.2. After the resolving gels were polymerized, 5% stacking gels were poured above the resolving gels and 10 or 15-well combs were placed properly. The recipe of stacking gel was shown in Table 2.3.

Table 2.2 10% and 8% Resolving Gel Recipes

Stock solutions	10% Resolving gel (for 10 ml)	8% Resolving gel (for 10 ml)
ddH_2O	4.79 ml	5.29 ml
1.5 M Tris pH 8.8	2.5 ml	2.5 ml
10% SDS	100 µl	100 µl
40% Acrylamide	2.5 ml	2 ml
10% APS	100 µl	100 µl
TEMED	10 µl	10 µl

Table 2.3 5% Stacking Gel Recipe

Stock solutions	5% Stacking gel (for 8 ml)
ddH_2O	4.82 ml
0.5 M Tris pH 6.8	2 ml
10% SDS	80 µl
40% Acrylamide	1 ml
10% APS	80 µl
TEMED	20 µl

For antibody validation, 100 µg of protein lysate from the embryonic zebrafish at 2, 3, and 4 dpf and 40 µg of protein lysates from cell lines were loaded in the gel. For the detection of Smurf2 and β-tubulin proteins, 10 µg of total protein lysate of individual brain or 20 µg of total protein lysate of pooled brain regions was loaded in

the gel. From each subcellular fraction (nuclear and cytosolic), 40 µg of protein lysates were loaded. The required amount of protein and water were mixed to obtain indicated concentrations. Then, equal amount of 2X Loading buffer (Table 2.4) was mixed with each sample. The mixture was incubated in 95^0C for 10 minutes to denature secondary structures of proteins before the samples loaded in the gel. Each sample was loaded at least three times in different gels to obtain technical replicates. A pre-stained protein marker (26616, Thermo Scientific Paisley, UK) was loaded to each gel to determine molecular weights of proteins, 10-180 kDa. Mini-PROTEAN Tetra Cell electrophoresis system (BioRad, CA, USA) was used for the electrophoresis. Firstly, the gels were run at 90 volts (V) for 30 minutes until samples passed to the resolving gel. Then, the gels were run at 120 V for 90 minutes until proteins were separated sufficiently.

Table 2.4 2X Loading Buffer recipe

Stock Solution	2X Loading Buffer (for 10 ml)	Final Concentration
10% SDS	4 ml	4%
100% Glycerol	2 ml	20%
4% Bromophenol blue (BPB)	100 µl	0.04%
0.5 M Tris pH 6.8	2.5 ml	0.125 M
10% DTT is added freshly		

After gel separation was done, the gel was removed from glasses carefully, equilibrated in cold transfer buffer. In a separate container, PVDF membrane was

activated in methanol for 5 seconds and then incubated in cold transfer buffer. The gel and PVDF membrane were placed between cassette and foam pads. The cassette was placed into the tank slots and the tank was filled with cold transfer buffer. The transfer was performed at 100 V for 90-100 min. At the end of transfer, the membrane was removed from cassette cautiously and incubated in a blocking solution (5% milk powder in TBS-T) for 1 hour at room temperature. The membrane was incubated in the primary antibody solution overnight (approximately 16 hours) at $+4^0$C with a moderate shaking. In the following day, the primary antibody was collected back. The membrane was washed with TBS-T for 30 min with 5-min intervals to remove any unbound primary antibody. After washing, the membrane was incubated in the secondary antibody solution for 1 hour at room temperature. To remove any unbound secondary antibody, the membrane was washed with TBS-T for 30 min. The primary and secondary antibodies used in this study were listed in Table 2.5. The protein bands were developed with SuperSignal West Femto Maximum Sensitivity Substrate (34095, ThermoScientific, Rockford, IL, USA) and visualized with ChemiDoc MP Imaging System (BioRad, Hercules, CA, USA).

Table 2.5 Primary and secondary antibodies used in the study.

Antigen	Supplier & Cat. No.	Dilution
SMURF2	Abcam ab94483	1:2000 in 5% milk solution
SMURF2	Abcam ab211746	1:500 in 5% milk solution
LaminB1	Proteintech 66095-1-Ig	1:10000 in 5% milk solution
DCAMKL1	Abcam ab109029	1:1000 in 5% milk solution
HuC	Abcam 78467	1:2000 in 5% milk solution
PCNA	Abcam ab18197	1:1000 in 5% milk solution
β-tubulin	CST 2146S	1:5000 in 5% milk solution
Rabbit-HRP	CST 7074	1:5000 in 5% milk solution
Mouse-HRP	sc-2005	1:2500 in 5% milk solution

The band densities were quantified using the ImageJ program (NIH, Bethesda, MD, USA). Intensity measurements were performed by Elif Tuğçe Karoğlu-Eravşar who was blind to the identity of the group of bands in order to achieve an unbiased quantification. Two subsequent normalization methods were performed. Firstly, within-gel normalization was utilized to reduce exposure time and inter-assay differences between technical replicates run at different gels. Second normalization was tubulin (tub) normalization. The gel-normalized values of proteins of interest were divided to gel-normalized values of the housekeeping control, β-tubulin, and values obtained with this calculation were designated as tub-normalized data.

2.5 RNA isolation

Individual and pooled snap-frozen brain samples were homogenized in TRIzol reagent (15596018, Invitrogen, Carlsbad, CA, USA) according to the manufacturer's instructions. The RNA concentration was measured with NanoDrop 2000 machine (ThermoScientific). RNA samples were stored at -80^{0}C. The TURBO DNA-free kit (AM1907, Invitrogen) was used to remove possible DNA residuals according to the manufacturer's instructions. The DNase-treated RNA concentration was measured with a NanoDrop 2000 machine (ThermoScientific). The DNase-treated RNA samples were stored at -80^{0}C. To clone the *smurf2* coding sequence into the desired plasmid, total RNA was isolated from snap-frozen tissues with QIAGEN RNeasy Mini Kit (74104, Qiagen, Venlo, Netherlands) according to manufacturer's instructions. RNA samples were stored at -80^{0}C.

2.6 cDNA synthesis

cDNAs were synthesized from 500 ng DNase-treated RNA samples by using an iScript cDNA Synthesis Kit (1708891, Biorad, Hercules, CA, USA) according to manufacturer's instructions. cDNA samples were diluted for quantitative PCR depend on the efficiency of primer pairs used.

2.7 Quantitative real time PCR (qRT-PCR)

In order to examine relative gene expression levels of genes of interest, quantitative real-time PCR (qRT-PCR) was utilized. Reactions were performed in a 20 µl final volume. Light cycler 480 SYBR Green I Master mix solution (04887352001, Roche, Mannheim, Germany) was used according to the

manufacturer's instructions. All qPCR experiments were performed in Roche LightCycler 480 System (Roche, Basel, Switzerland). The primer pairs, and final primer concentrations are listed in Table 2.6.

A housekeeping control, *rpl13a*, was used as the reference gene [121]. ΔCt was calculated as Ct (target gene) – Ct (reference gene). ΔΔCt was calculated as the ΔCt of sample – average ΔCt of all samples. In order to express fold changes, 2^(-ΔΔCt) was calculated. Finally, fold change values were $\log_2$ transformed to reduce the variation and get better visualization of the data for further statistical analysis.

Table 2.6 The sequences of primer pairs used in this study.

Gene symbol	Forward Primer 5'--> 3'	Reverse Primer 5'--> 3'	Final conc. in reaction
smurf2	ACTTCCTGCACACACAGACG	GGACCCAACTCCTCACAGTT	0.5 µM
tp53	TTGTCCCATATGAAGCACCACA	CAGCAACTGACCTTCCTGAGTC	0.5 µM
mdm2	GATTCGCGAAACGGTCAC	TCGTTGTCAACCTTGCTGAT	0.5 µM
smad7	CCCCTATGGGGTTTTCAGAT	GTGCCCTGAGGTAGGTCGTA	1 µM
yy1a	TGACAGGCAAGAAACTGCCA	TTGTGCAACCTTTGTGTGGG	1 µM
ep300a	GGCTTATGTGCCTATCTCCGA	GCCAAAATCGTTTCCATCGCT	1 µM
sirt1	TTCAGTGCCACGGGTCTTTT	GGACACCTGGGACAATGAGG	1 µM
rpl13a	TCTGGAGGACTGTAAGAGGTATGC	AGACGCACAATCTTGAGAGCAG	0.5 µM

2.8 DNA isolation and plasmid isolation

DNA was extracted from embryos and tissues with DNA lysis buffer (100 mM Tris pH 8.2, 10 mM EDTA, 200 mM NaCl, 0.5% SDS and 1X proteinase K) at 55^0C overnight in a shaker. The next day, samples were heated to 95^0C to inactivate proteinase K and the DNA was precipitated with isopropanol and the suspended DNA was stored at $+4^0$C.

Plasmid isolations were performed with NucleoSpin Plasmid, Mini kit for plasmid DNA (740588, Macherey-Nagel, Düren, Germany) according to manufacturer's instructions. The isolated plasmids were stored at $+4^0$C for short period and -20^0C for longer period.

2.9 Conventional PCR

To amplify the gene of interest, conventional PCR was utilized.

2.9.1 PCR amplification to obtain Smurf2 CDS flanked with *attB* sites

Total cDNA sample was amplified with primers in Table 2.7. Phusion Hot Start Flex 2X Master Mix (M0536, NEB, Ipswich, MA, USA) was used because Phusion DNA Polymerase possesses 5′→ 3′ polymerase activity, 3′→ 5′ exonuclease activity thus it is one of the most accurate thermostable polymerases. It is suitable for cloning and long amplification. Two-step PCR setup will be used to amplify 2298 bp length coding sequence of *smurf2*. Smurf2tg-f1 and –r1 primers are specific to gene of interest and Smurf2tg-f2 and –r2 primers add *attB* sites which are necessary for recombination with pDONR221 vector.

Table 2.7 Primer sequences for PCR to add *attB* (recombination sites) to Smurf2 coding sequence.

Primer name	Sequence 5'--> 3'
smurf2tg-f1	AAAAAGCAGGCTTAGCCTGGATAAGGGTCAAGG
smurf2tg-r1	AGAAAGCTGGGTTACATCATTCCACAGCGAAGC
smurf2tg-f2	GGGGACAAGTTTGTACAAAAAAGCAGGCT
smurf2tg-r2	GGGGACCACTTTGTACAAGAAAGCTGGGT

2.9.2 PCR amplication to genotype *Tg(hsp70l:smurf2_EGFP)* F1 embryos

The primer pairs were designed to amplify EGFP and SmuGFP and smurf2 genes in the genome (Table 2.8). These primers were optimized with WT DNA samples and the construct which was injected to embryos to create Tol2 transgenesis. Phusion Hot Start Flex 2X Master Mix was utilized in PCR amplification.

Table 2.8 Primer sequences for genotyping *Tg(hsp70l:smurf2_EGFP)* F1 embryos.

Primer pairs	Primers	Sequence 5'--> 3'	Product length
egfp	egfp-for	GGTGAACTTCAAGATCCGCC	229 bp
	egfp-rev	CTTGTACAGCTCGTCCATGC	
smugfp	smugfp-for	TACCCAAAGCACACACTTGCT	206 bp
	smugfp-rev	CTCGACCAGGATGGGCACC	
smurf2	Smurf2-right	GGACCCAACTCCTCACAGTT	1459 bp
	Smurf2-left	ACTTCCTGCACACACAGACG	

2.9.3 PCR-based methods to genotype *Tg*(*smurf2*_e10)

A simple and efficient method to screen CRISPR-Cas9 induced mutants were established by Hua et al. [122]. In their method, they used the critical annealing temperature because an optimal annealing temperature suppresses mismatched annealing and reduces the generation of non-specific products. According to this, they developed ACT-PCR to detect CRISPR/Cas9-induced mutants. This method includes the design of primers, the detection of the critical annealing temperature by gradient PCR and the screening of mutants. The most important part of their method is the design of the target specific primers because the forward primer flanks the double strand break (DSB) site with its 3' end containing a 1-4 bp overhang relative to the DSB site to ensure specificity and sensitivity for WT gene binding and PCR amplification; the reverse primer is located outside the DSB site and has a higher melting temperature (Tm) value than the forward primer to ensure DNA template

binding at the critical annealing temperature. Accordingly, the 3 diverse reverse primer flanks the DSB site with its 3’ end containing a 1-4 bp overhang relative to the DSB site and the forward primer located outside the DSB site with a higher melting temperature (Tm) value than reverse primer were designed (Table 2.9). The gradient PCR were applied to find the critical annealing temperature.

Table 2.9 Primer pairs for ACT-PCR.

	Primer name	Sequence 5'--> 3'
Primer pair 1	g3.2_geno_for	CGTCCTATGCCTGCTCTGTA
	smurf2_geno_dsrev1	GTTCCTTATCTCCCAGCC
Primer pair 2	smurf2_geno_for	CGTCCTATGCCTGCTCTGTACCA
	smurf2_geno_dsrev2	TGTTCCTTATCTCCCAGCCC
Primer pair 3	smurf2_geno_for	CGTCCTATGCCTGCTCTGTACCA
	smurf2_geno_dsrev3	GTTCCTTATCTCCCAGCCCG

Also, 8 adults of F0 were euthanized and DNA samples were extracted from their tails and gonads for genotyping. To genotype F0 animals, following PCR, the products were used in T7E1 assay to detect the mismatch [123] or in RFLP (Restriction Fragment Length Polymorphism) method [124] to check any mutation in the expected DSBs. The co-injection of guide RNA and cas9 RNA cause the cleavage of target DNA sequence and then the repair at this site may cause mutations. T7E1

assay performed for detecting the mismatch at target site and cleaved the PCR products at that mismatch site [123]. However, RFLP method utilized a restriction enzyme after PCR amplification. Because there is a *SmaI* restriction site at the expected mutation site, this restriction site allows genotyping by RFLP. In WT fish, *SmaI* restriction enzyme cut PCR product at one site leading 399 bp and 544 bp fragments. However, if there is a mutation at that site, the restriction enzyme may not cut PCR product. RFLP was applied to PCR product of tail and gonads of adults.

2.10 Tol2 transposase system

The Tol2kit was a gift from Kristen M. Kwan [81], Utah University, with a permission from Dr. Koichi Kawakami. Tol2kit includes 6 different types of vectors; 5' entry clones (promoters), middle entry clones, 3' entry clones (reporter and polyA), destination vectors, donor vectors and transposase vector. According to the study's requirements, the scientists are flexible to choose different vectors. The Gateway cloning is based on a recombination reaction of *att* sites between at least 2 vectors. The BP recombination reaction is used to create a middle entry clone from an *attB*-flanked PCR product and pDONR221 backbone. The LR recombination reaction transfers the desired gene from an entry clone to destination vector. According to Gateway cloning system, three entry clones (5', 3' and middle) are combined in one destination vector.

In the present study, p5E-*hsp70l* entry clone was chosen for heat-shock induction in the adult brain, p3E-EGFPpA for the expression of EGFP reporter. Furthermore, to increase the efficiency of transposition *in vivo*, capped transposase

mRNA was synthesized from pCS2FA-transposase plasmid via *in vitro* transcription by using Ambion mMessage mMachine SP6 Transcription Kit (AM1340, Thermo Fisher Scientific, Waltham, MA, USA).

The coding sequence of Smurf2 will be amplified as defined in previous section. The amplicon was cloned into pDONR221 donor vector to create middle entry clone via BP reaction (Gateway BP Clonase II Enzyme mix, 11789100, Invitrogen, Carlsbad, CA, USA). After successful BP recombination reaction and transformation, isolated entry clones (pDONR221+Smurf2) was sequenced with the primers in Table 2.8 to confirm the correct recombination. Then, a middle entry vector (pDONR221+Smurf2), which have the correct sequence, was combined with desired 5' entry (p5E-*hsp70l*) and 3'entry (p3E-EGFPpA) vectors in a destination vector (pDestTol2CG2) via LR recombination reaction (Gateway LR Clonase II Enzyme mix, 11791100, Invitrogen, Carlsbad, CA, USA).

Table 2.10 M13 Sequencing primers.

Primer name	Sequence 5'--> 3'
M13F	GTAAAACGACGGCCAG
M13R	CAGGAAACAGCTATGAC

2.11 CRISPR-Cas9 knockout system

pDR274, a gift from Keith Joung (Addgene plasmid # 42250) [84], is a guide RNA (gRNA) expression vector used to create a gRNA to a specific sequence and uses T7 promoter for *in vitro* transcription by using the MEGAshortscript T7 Kit

(AM1354, Thermo Fisher Scientific, Waltham, MA, USA). pT3TS-nCas9n, a gift from Wenbiao Chen (Addgene plasmid # 46757) [125], is used to transcribe *Cas9* mRNA by using Ambion mMESSAGE mMACHINE T3 Transcription Kit (AM1348, Thermo Fisher Scientific, Waltham, MA, USA).

Three different gRNAs which target different domains of Smurf2 were designed via online bioinformatics tools with the help of Marion Gradl and Vanessa Gerbe (Table 2.9). The oligo pairs were annealed together to obtain gRNAs. The guide RNAs, which have *BsaI* cut sites was cloned into pDR274 backbone, which is also digested with *BsaI*, by using restriction digestion-ligation methods. These plasmids containing gRNAs was sequenced with M13F primer (Table 2.8) to confirm the presence of gRNA. Then, *Cas9* mRNA was *in vitro* transcribed from pT3TS-nCas9n vector.

Table 2.11 Oligo sequences to anneal guide RNAs.

	Oligo name	Sequence 5'--> 3'
Oligo pair 1-e1 (guide RNA 1)	smurf2e1g1o1	TAGGAGTCACGGTCCTGTGGCC
	smurf2e1g1o2	AAACGGCCACAGGACCGTGACT
Oligo pair-e10 (guide RNA 3)	smurf2e10g3o1	TAGGGTCCATTGCCCCCGGGCT
	smurf2e10g3o2	AAACAGCCCGGGGGCAATGGAC
Oligo pair-e15 (guide RNA 4)	smurf2e15g4o1	TAGGGCATCGAGGCTCAGTTCC
	smurf2e15g4o2	AAACGGAACTGAGCCTCGATGC

2.12 Microinjection into one-cell stage embryos

The injection solution of Tol2 or CRISPR-Cas9 was prepared; for Tol2 knockin, 25 pg DNA (pDest+Smurf2 plasmid), 25 pg transposase mRNA and 1X phenol red (P0290, Sigma, St. Louis, MO, USA), which is used as an indicator of injection, was mixed in 10 µl solution just before injection whereas for CRISPR-Cas9 knockout, 20 ng/µl gRNA, 75 ng/µl *cas9* mRNA and 1X phenol red was prepared fresh in 10 µl solution just before injection.

The injection needle was prepared and back-filled with the injection solution. With RNase-free forceps, the tip of the needle was cut carefully. The calibration of needle was done by adjusting the microinjector pressure and time setting. By using micrometric slide, the volume of a droplet was measured. In these experiments, about 2 nl of injection mix was injected to embryos.

Collected embryos in one-cell stage were aligned into a petri dish and the injection mix was applied into yolk of one-cell stage embryos. In each experiment, uninjected embryos were separated in a petri dish to check their viability. Also, for the CRISPR-Cas9 injection, only *cas9* mRNA solution was injected as an injection control.

2.13 Heat-shock treatment

When F0 injected animals became mature, these potential founders were bred with WT animals. At 24 hpf, the F1 embryos were divided randomly into two groups; heat-shock treated (hs) and no heat-shock treated (no hs). The embryos in hs group were treated with heat-shock at 37^{o}C for 1 hour to induce the Smurf2-EGFP

expression and replaced back to a 28^{o}C incubator whereas no hs group kept at 28^{o}C during this time. After 4 hour, the embryos checked for EGFP signal under the fluorescence microscope and their survival rates were recorded. At 48 hpf, the heat-shock treatment was repeated to hs group to increase the amount of inducible protein at 37^{o}C for 1 hour and the animals were put back into a 28^{o}C incubator while embryos in no hs group was kept at 28^{o}C. The last heat-shock applied at 72 hpf and EGFP signal was imaged under the fluorescence microscope. For further analyses, embryos were collected and stored at -80^{o}C. Alternatively, heat-shock was applied at 5 dpf (120 hpf) for 1 hour, and then embryos were euthanized and collected after 2 hours for further analysis.

2.14 Vivo-morpholino injection

Vivo-morpholinos are designed to knock-down a gene of interest in living organism such as adult zebrafish. According to protocol of Kizil and Brand [90], Vivo-morpholino were injected via cerebroventricular microinjection (CVMI) into the adult zebrafish brain. The experiment was performed as defined in Kizil et al. [91]. By using CVMI, Vivo-morpholinos was administered into the cerebroventricular fluid and distributed along the rostrocaudal axis of the brain [91]. To estimate the dispersion and the uptake of the morpholino, Smurf2-specific Vivo-morpholinos were co-injected with a cell tracker dye (CellTracker Red CMTPX Dye, C34552, Invitrogen, Carlsbad, CA, USA) which is a non-fluorescent cell-permeant molecule [90]. When it is internalized by the cells, is converted by Gluthatione-S-transferase to a red fluorescent compound [126]. Therefore, the fluorescence signal is an indication of the cells that take up the injected morpholino. At least 30 minutes

after microinjection, injected fish were anesthesized again to check red fluorescence signal (Figure 2.2).

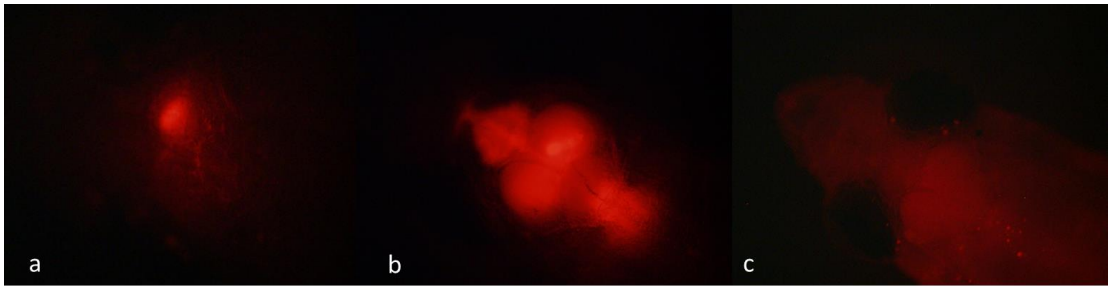

Figure 2.2 (a) Fluorescent signal at the injection site, the dispersion of injection solution is weak. (b) A good injection with homogenous dispersion of fluorescence signal. (c) Uninjected control, long exposure than injected ones.

2.15 Heclin treatment

Heclin (SML1396, Sigma, St. Louis, MO, USA) was dissolved in DMSO (A3672, Applichem, Darmstadt, Germany) to obtain 5 mg/ml stock solution. Stock solution was aliquoted and stored at -20^{o}C. The molecular weight of heclin is 283.32 g/mol and so the molarity of stock solution is 17.65 mM. The stock solution was diluted with DMSO to obtain the concentrations of 2.5 mM, 3.4 mM, 4.5 mM and 6 mM. Then each solution was diluted in E3 medium to obtain working solutions of 5 μM, 6.8 μM, 9 μM and 12 μM heclin. Thus, each working solution contained the same concentration of DMSO (0.2% v/v) when embryos were exposed to these solutions. Also, there was a blank control which is only E3 medium without DMSO and heclin. To eliminate DMSO effect, there was also DMSO control which is including 0.2% DMSO (v/v) in E3 medium.

At 6 hpf, embryos were randomly divided into 24 well-plates. Each well contained 10-12 embryos and 2 ml E3 medium. Each solution was replaced with 2 ml experimental solution and embryos were kept at 28^{o}C until 24 hpf. At 24 hpf, the dead embryos were discarded and the numbers were recorded. After the experimental solutions were changed with fresh solutions, the embryos were incubated at 28^{o}C. Experimental solutions were renewed every 24 hours and the dead embryos were removed and recorded. According to experimental requirements, the treatment was applied for 72 hours or 120 hours. At the end of the treatments, the embryos were euthanized on ice and then were washed with E3 medium twice. The pooled embryos were snap-frozen and stored at -80^{o}C until the further experiments.

2.16 STRING analysis for interacting partners of Smurf2 protein

STRING database was utilized to prepare a protein network map of Smurf2 and its interacting partners for both humans and zebrafish [127]. In the human interaction map, SMURF2, TP53, MDM2, YY1, EP300, SMAD7, and SIRT1 proteins were identified. However, because of the existence of teleost-specific gene duplication [53], there are two paralogues of ep300 and yy1 in the zebrafish genome. According to previous publications [54], [57], only functional paralogues, *ep300a* and *yy1a* were investigated in the current analysis. Thus, smurf2, tp53, mdm2, yy1a, ep300a, smad7, and sirt1 proteins were defined in the zebrafish map. The minimum required interaction score was set to low confidence (0.150).

2.17 Statistical Analysis

The SPSS program (IBM, Armonk, NY, USA) was employed to perform statistical analysis of the gene and protein expression levels in Chapters 3, 4 and 5. The assumptions of a normal distribution and homogeneity of variance were checked with the Shapiro-Wilk and Levene tests, respectively. If these assumptions were violated, non-parametric tests including Kruskal-Wallis test and Mann-Whitney U test, were applied. When the cases fulfilled the assumptions, parametric tests were applied.

Specifically, in Chapter 3 whole brain protein expression of both total lysates and subcellular fractions were analyzed with an unpaired t-test with the factor of age with the significance levels of $p<0.05$. In the analysis of region-specific protein expression of total lysates, non-parametric Kruskal-Wallis test was conducted between age and region followed by pairwise comparisons which was corrected with Bonferroni method. Thus, a new significance level of $p<0.0167$ was used due to three pairwise comparisons (Tel young vs. old, TeO young vs. old, Ce young vs. old). On the other hand, a two-way ANOVA with factors of age and region was employed in subcellular fractions of region-specific protein expression levels. The gene expression levels in whole brain tissues were analyzed with a Mann-Whitney U test or an unpaired t-test. However, for all genes of interest, a two-way ANOVA was utilized in the brain region-specific gene expression. The gene expression levels were further investigated with Principal component analysis (PCA) and Pearson correlation analysis in the case of both the whole brain and the brain-specific regions by using both the R (Free Software Foundation) and SPSS programs.

In Chapter 4, a two-way ANOVA was used to analyze *smurf2* gene expression levels with the factors of heat-shock and genotype (WT and Tol2). The protein level of Smurf2 after CVMI was analyzed with a one-way ANOVA for exon-skipping Vivo-morpholino injected or two-way ANOVA for translational blocking Vivo-morpholino injected animals.

In Chapter 5, Kruskal-Wallis test was conducted for the body weight, body-mass index (BMI) and Fulton K factor analysis in terms of feeding regimens. However, for body length a two-way ANOVA was employed with factors of age and diet. The protein and gene expression levels following dietary regimen were analyzed with a two-way ANOVA. The further analysis was done with Pearson correlation. However, after heclin treatment, survival analysis was performed with Log-Rank (Mantel-Cox) test while the gene and protein levels were investigated with Kruskal-Wallis test or two-way ANOVA.

The graphic representations of both the gene and protein expression levels were generated using the SPSS program or Graphpad Prism (San Diego, CA, USA). The PCA plots in Chapter 3 were drawn with the prcomp method and the fviz_pca_biplot package in R by Meriç Kınalı. The some color-coded correlation coefficient tables were drawn in R program by Meriç Kınalı and some of them were drawn in GraphPad Prism software.

CHAPTER 3

THE LEVELS OF BRAIN-SPECIFIC EXPRESSION OF SMURF2 AND ITS INTERACTING PARTNERS WERE ALTERED ACROSS LIFESPAN

3.1 Two commercially available Smurf2 antibody were validated in zebrafish brain

Previous research indicated that *smurf2* gene expression increased during aging [35], [39]. To understand whether this up-regulation of *smurf2* gene expression is evident also in the protein expression levels, the western blot analysis was conducted. Since Smurf2 antibodies had not been used in zebrafish tissues previously, two commercially available Smurf2 antibodies were validated. The anti-SMURF2, 200-300 aa. antibody is directed against the 200-300 amino acid residues of the human SMURF2 protein while anti-SMURF2 C-terminal antibody recognizes the C-terminal region of human SMURF2 protein. The MCF7 cell line is indicated as a positive control for the anti-SMURF2, 200-300 aa antibody in the manufacturer's datasheet. Also, the MDA-MB-231 cell line is used as a positive control for anti-SMURF2 C-terminal antibody. As expected, the anti-SMURF2, 200-300 aa antibody yielded an 86 kDa band in all samples of zebrafish embryos, cell lines and zebrafish brain lysates (Figure 3.1). However, the anti-SMURF2 C-terminal antibody yielded a slightly heavier band (app. 100 kDa) in zebrafish embryos and a heavier band (app. 250 kDa) in zebrafish brain lysates (Figure 3.1). Also, the anti-LaminB1 antibody was utilized as nuclear marker in nuclear and cytosolic fractions of MDA-MB-231 cell line and zebrafish brain lysates to confirm the subcellular fractionation. As

expected, anti-LaminB1 was enriched in nuclear fractions while anti-β-tubulin was enriched in cytosolic fractions (Figure 3.1). Interestingly, the bigger band than the expected band (app. 250 kDa) was observed in both total lysates and cytosolic lysates extracted from adult brain. In addition, a slight increase in embryo lysates might indicate a regulatory mechanism such as post-translational mechanisms and complex formation on the Smurf2 protein across lifespan.

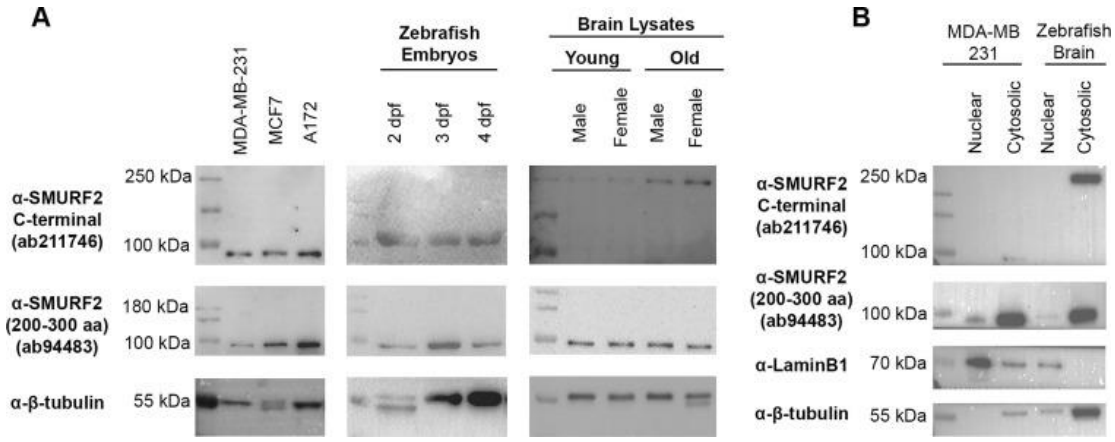

Figure 3.1 Antibody validation of anti-SMURF2 antibodies, the anti-SMURF2, 200–300 aa, and anti-SMURF2 C-terminal antibody. (A) Protein lysates from the MDA-MB-231 cell line, the MCF7 cell line, and the A172 cell line, protein lysates of zebrafish embryos and protein lysates of zebrafish brain. (B) Subcellular fractionation was validated with a nuclear marker, LaminB1 and a cytosolic marker, β-tubulin. (Reprinted from Tuz-Sasik et al., 2020 [36])

3.2 Smurf2 protein expression was altered during brain aging

Our primary hypothesis was that the increasing trend in *smurf2* gene expression can be followed by Smurf2 protein expression during brain aging. In order to test this hypothesis, whole brain lysates and region-specific lysates were analyzed

in terms of age (Figure 3.2). The whole brain was separated to three integrative centers as telencephalon (Tel), the optic tectum (TeO) and the cerebellum/medulla/spinal cord (Ce) as defined in [71]. All young and old samples were loaded on the gels as cohorts and each cohort was run at least three times. According to t-test, there was no significant main effect of age ($t(18)=1.059$, $p=0.304$, Figure 3.3A) on the whole brain lysates blotted with anti-SMURF2, 200-300 aa. On the other hand, brain region-specific analysis showed that Smurf2 protein levels detected with anti-SMURF2, 200-300 aa, altered significantly ($\chi^2(5)=11.990$, $p=0.035$, Figure 3.3A) by age and region interaction. According to pairwise comparisons, Smurf2 protein levels increased significantly during aging in Tel ($p=0.003$) but not in TeO ($p=0.726$) and Ce ($p=0.121$) areas. Same protein samples were blotted with anti-SMURF2 C-terminal antibody and similar pattern was observed. Whole brain analysis indicated no significant effect of age on Smurf2 protein levels ($t(18)=-1.046$, $p=0.309$, Figure 3.3B). Moreover, there was an interaction effect between age and region ($\chi^2(5)=17.275$, $p=0.004$) in the brain region-specific analysis. The significant increase with advancing age was evident in the Tel ($p=0.002$) and Ce ($p=0.008$) but not in the TeO ($p=0.703$) areas (Figure 3.3B). While there was no obvious increase in whole brain, Smurf2 protein levels altered in a region-specific manner during aging. It may implicate that up-regulation of *smurf2* gene expression does not cause the global alteration in the protein expression. In addition to heavier molecular weight of protein detected with anti-SMURF2 C-terminal antibody, Smurf2 protein expression was significantly higher in aged Ce region than in young Ce when it was detected with anti-SMURF2 C-terminal antibody. These may imply that there is a regulation on Smurf2 regulation such as

post-translational modifications or complex formation and should be further investigated.

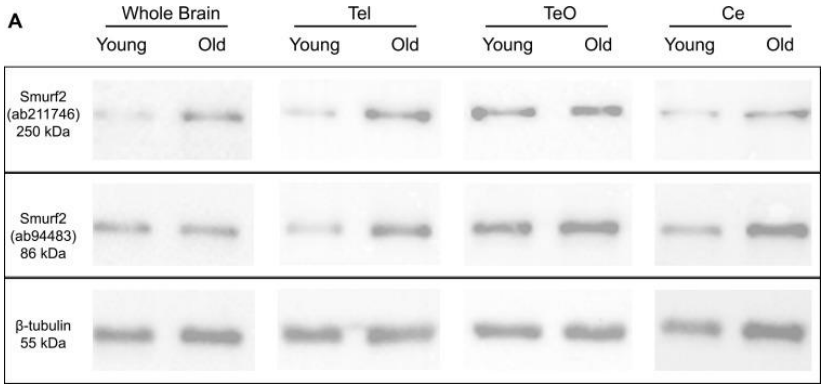

Figure 3.2 Representative Western images for Smurf2 antibodies and the housekeeping, β-tubulin, in whole brain lysates and region-specific lysates including telencephalon (Tel), the optic tectum (TeO) and the cerebellum/medulla/spinal cord (Ce) areas. (Reprinted from Tuz-Sasik et al., 2020 [36])

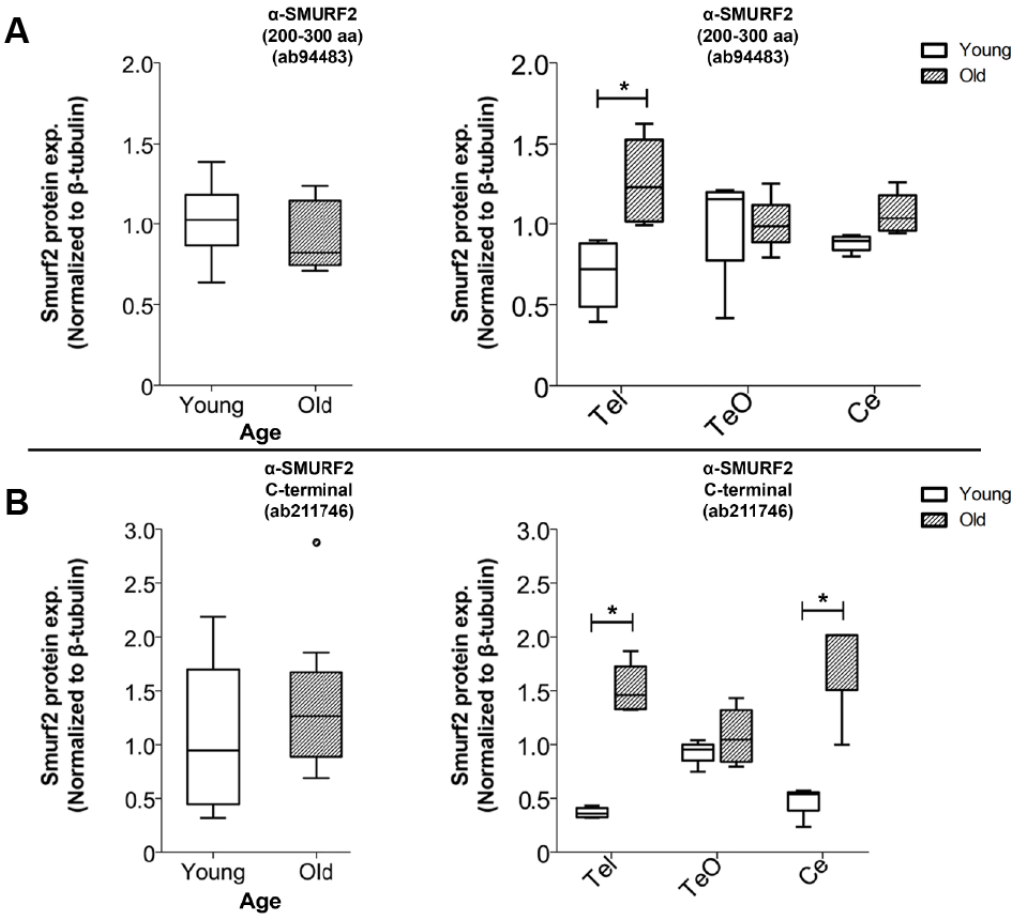

Figure 3.3 (A) Smurf2 protein expression levels detected with the anti-SMURF2 (200–300 aa) antibody. (B) Smurf2 protein expression levels detected with the anti-SMURF2 C-terminal antibody. Tub-normalized values are indicated in (A) and (B). * indicates $p<0.0167$. (Reprinted from Tuz-Sasik et al., 2020 [36])

3.3 Smurf2 protein was localized mostly in cytosolic fraction

Previous research indicated that Smurf2 protein forms a complex with Smad7 and this complex degrades TGF-β receptor complex via the ubiquitin-mediated proteosomal degradation in the cytosol or ubiquitinate the nuclear targets in the nucleus [59], [128]. Smad7 interaction cause the activation and export of Smurf2

from nucleus to cytosol [58], [59], [128]. In order to observe the age effect on the subcellular localization of Smurf2 in the zebrafish brain, the subcellular fractionation was utilized to obtain nuclear and cytosolic fractions from the whole brain and specific brain regions; Tel, TeO, Ce. As shown in Figure 3.1, the subcellular fractionation was confirmed with enriched LaminB1 in the nuclear fraction and enriched β-tubulin in the cytosolic fraction. Both fractions of each sample were loaded on the gel at least three times and blotted with anti-SMURF2, 200-300 aa, and anti-SMURF2 C-terminal antibody in addition to anti-LaminB1 and anti-β-tubulin. Both in young and old samples, Smurf2 protein was enriched in the cytosolic fraction regardless of SMURF2 antibody and brain regions (Figure 3.4). Also, the molecular weight of Smurf2 protein detected with anti-SMURF2 C-terminal antibody was bigger than the expected weight in the cytosolic fraction. It may imply that this antibody recognized the complex of Smurf2 in the cytosol and show bigger band in the immunoblots. On the other hand, anti-SMURF2, 200-300 aa, is directed against a different domain of Smurf2 protein and may detect the unbound, free Smurf2 protein in the cytosol which had the expected molecular weight in the immunoblots. In order to determine the exact mechanism and complex structure of Smurf2, further experiments including co-immunoprecipitation and mass spectrometry should be performed.

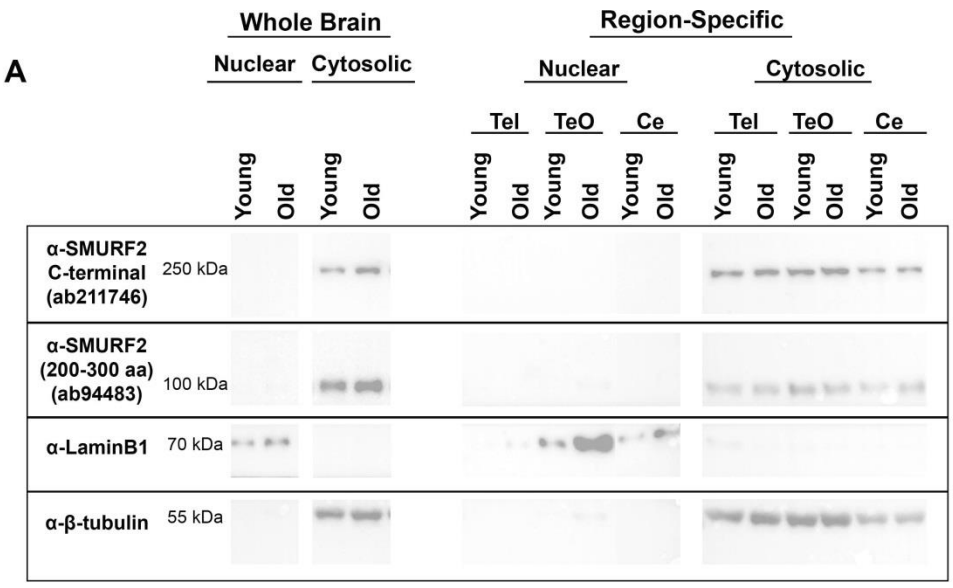

Figure 3.4 Representative Western blots for subcellular fractions. Smurf2 protein was enriched in the cytosolic fraction of the zebrafish brain. (Reprinted from Tuz-Sasik et al., 2020 [36])

In the current study, the expression in subcellular fractions was analyzed across lifespan. In the whole brain analysis, the expression of Smurf2 in the cytosolic fraction was similar to the expression in the total lysates (Figure 3.3); Smurf2 protein expression increased during aging but was not significant for both anti-SMURF2, 200-300 aa, and anti-SMURF2 C-terminal antibodies ($t(4)=-0.470$, $p=0.663$ and $t(4)=-0.632$, $p=0.562$, respectively; Figure 3.5). However, the brain region-specific analysis with anti-SMURF2 C-terminal antibody indicated that the main effect of age and main effect of region were close to being statistically significant ($F(1,24)=3.977$, $p=0.058$ and $F(2,24)=3.356$, $p=0.052$, respectively; Figure 3.6A) without an interaction effect ($F(2,24)=0.718$, $p=0.498$, Figure 3.6B) on the cytosolic protein

level of Smurf2. Also, Smurf2 protein detected with anti-SMURF2, 200-300 aa, antibody was analyzed in the cytosolic fractions. There was a significant main effect of region ($F(2,22)=7.512$, $p=0.003$) without a main effect of age and an interaction effect between age and region ($F(1,22)=1.714$, $p=0.204$ and $F(2,22)=0.276$, $p=0.761$, respectively; Figure 3.6C). The similar patterns in Smurf2 protein levels across lifespan using total lysates and subcellular cytosolic lysates and also the enriched amount of Smurf2 protein in cytosol rather than nuclear fraction may indicate that the changes in the total lysates was driven by the alteration of cytosolic expression of Smurf2.

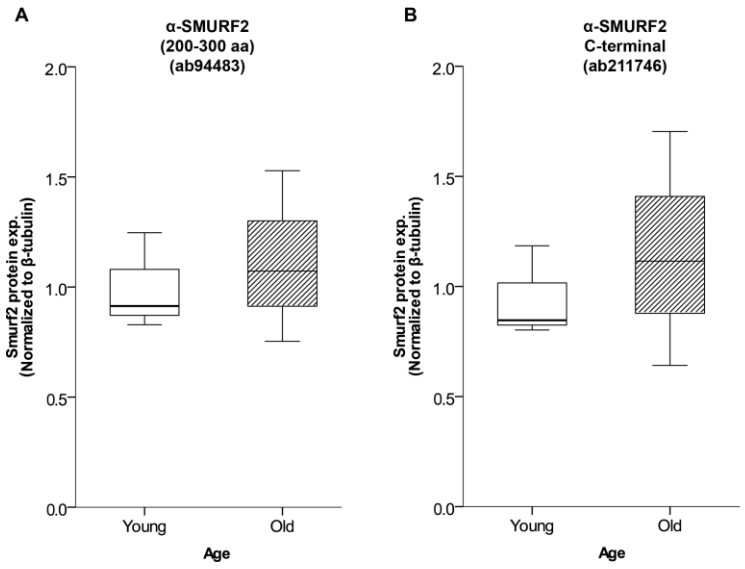

Figure 3.5 Smurf2 protein was enriched in the cytosolic fraction of the zebrafish brain. (A) Smurf2 protein expression levels detected with the anti-SMURF2 (200–300 aa) antibody. (B) Smurf2 protein expression levels detected with the anti-SMURF2 C-terminal antibody. Tub-normalized values are indicated in (A) and (B).

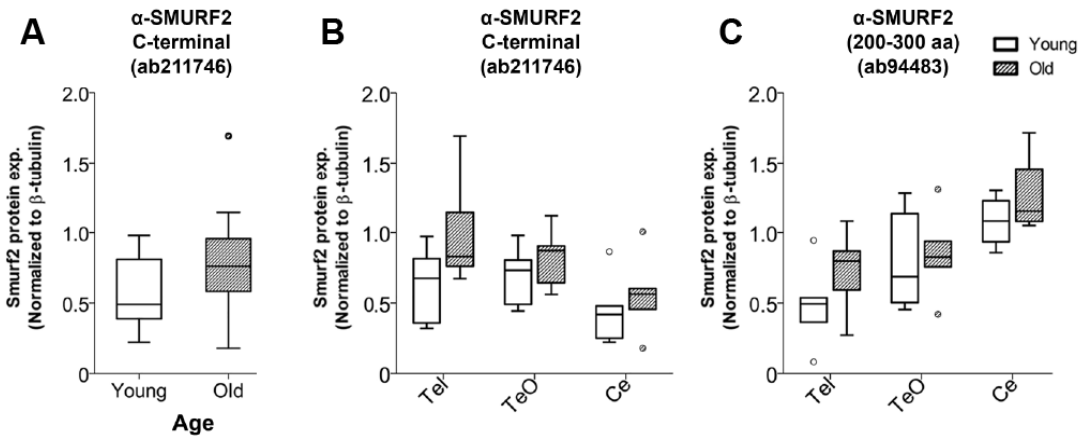

Figure 3.6 Smurf2 protein was enriched in the cytosolic fraction of the zebrafish brain. (A)(B) Smurf2 protein expression levels detected with the anti-SMURF2 C-terminal antibody in the cytosolic fraction of the zebrafish brain. (C) Smurf2 protein expression levels detected with the anti-SMURF2, 200–300 aa, antibody in the cytosolic fraction of the zebrafish brain. Tub-normalized values are indicated in (A), (B), and (C). (Reprinted from Tuz-Sasik et al., 2020 [36])

3.4 The expression levels of *smurf2* and its interacting partners were changed in the whole brain and brain regions across lifespan

The gene expression patterns of *tp53, mdm2, ep300a, yy1a, smad7,* and *sirt1* in addition to *smurf2* were analyzed with qRT-PCR in the whole brain and the specific brain regions (Figure 3.7). The gene expression levels of *smurf2* were upregulated in the aged whole brain (U=5.00, z=-2.082, p=0.037; Figure 3.7A). In the whole brain analysis, the interacting partners were not changed significantly in terms of age although there were numerical increases in *mdm2* and *yy1a* levels during aging (U=8.00, z=-1.061, p=0.109 and U=11.00, z=-1.121, p=0.262, respectively). Similarly, there were slight increases in the expression of *ep300a* and *sirt1* in the old

ages (t(10)=-1.561, p=0.149 and U=10.00, z=-1.281, p=0.200, respectively). On the other hand, *tp53* and *smad7* levels were remained at comparable levels during brain aging (t(10)=-0.447, p=0.665 and t(10)=-0.138, p=0.893, respectively). Since previous research indicated that post-translational modifications can compete with each other or prevent further modification to regulate the stability of common targets including tp53 and Smad7 [41], [42], [50], [60], the stable expression of *tp53* and *smad7* during brain aging could be under tight control of several factors.

Similar to the comparable level of Smurf2 protein in the whole brain, the gene expression of interacting partners was not altered significantly in the whole brain. However, brain region-specific Smurf2 expression indicated a significant alteration in Tel and Ce region. Thus, we hypothesized that the gene expression of interacting partners are also changed in a brain region-specific manner. In order to test this hypothesis, whole brain was divided into three integrative centers; Tel, TeO and Ce and these regions were subjected to qRT-PCR analysis. Firstly, *smurf2* expression showed a main effect of age and region (F(1,18)=54.251, p<0.0005 and F(2,18)=6.072, p=0.010, respectively) with an interaction effect (F(2,18)=34.059, p<0.0005; Figure 3.7B). Post hoc analysis demonstrated a significant effect of age in both Tel (p<0.0005) and Ce (p=0.013) regions and also a significant effect of region in both young (Tel vs. TeO p<0.0005, Tel vs. Ce p=0.014 and TeO vs. Ce p=0.002) and old (Tel vs. TeO p=0.002, Tel vs. Ce p=0.001) groups. Similar to whole brain gene expression pattern, the brain-specific gene expression of *tp53* was not changed significantly in terms of age (F(1,18)=1.297, p=0.270) and region (F(2,18)=0.131, p=0.878) as well as age by region interaction (F(2,18)=1.328, p=0.290; Figure 3.7C).

On the other hand, there were a significant main effect of age (F(1,12)=21.003, p=0.001) on *mdm2* levels while a main effect of region was not statistically significant (F(2,12)=1.166, p=0.344). Also, there was a significant interaction effect between age and region on *mdm2* expression levels (F(2,12)=13.953, p=0.001; Figure 3.7D). According to pairwise comparisons, there was a significant effect of age in Tel (p<0.0005) and a significant effect of region in the young group (Tel vs. TeO p=0.003 and Tel vs. Ce p=0.007). While there was no significant main effect of region (F(2,18)=1.072, p=0.362) on *ep300a* levels, there was a significant effect of age (F(1,18)=5.419, p=0.032) with an interaction effect between age and region (F(2,18)=6.092, p=0.010; Figure 3.7E). Post hoc analysis indicated that a significant main effect of age was evident in the Tel (p=0.001) and a significant effect of region was apparent in the young group (Tel vs. TeO p=0.012) on *ep300a* expression levels. However, there was neither significant age effect nor region effect on *yy1a* (F(1,18)=0.012, p=0.914 and F(2,18)=2.035, p=0.160, respectively) and *smad7* (F(1,18)=1.235, p=0.281 and F(2,18)=2.720, p=0.093, respectively) levels. Not surprisingly, age by region interaction was not significant on *yy1a* (F(2,18)=1.328, p=0.290; Figure 3.7F) and *smad7* (F(2,18)=0.657, p=0.530; Figure 3.7G) levels. Finally, *sirt1* level was altered significantly with respect to factor of age (F(1,12)=12.305, p=0.004). Although there was no significant effect of region (F(2,12)=2.323, p=0.140) on *sirt1* expression levels, age by region interaction was significant (F(2,12)=9.299, p=0.004; Figure 3.7H); the interaction was evident during aging in the Tel (p<0.0005) and also in young animals, between Tel and TeO (p=0.003) and between Tel and Ce (p=0.015). To understand the potential interactions between genes of interest, further analysis should be conducted.

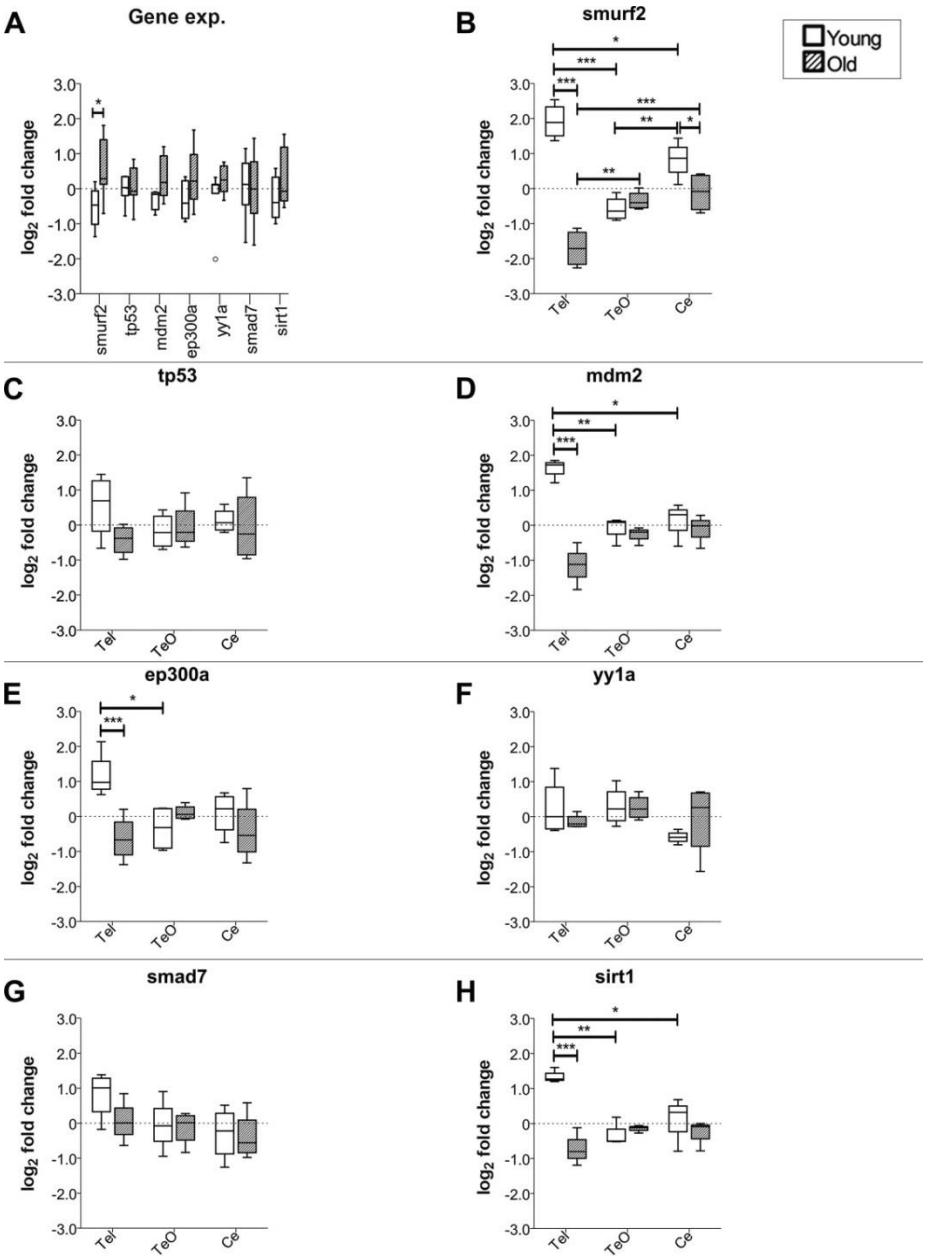

Figure 3.7 The relative gene expression levels of *smurf2* and its interacting partners. (A) The relative expression levels of the target genes of interest in whole zebrafish brain during aging. The brain region-specific expression levels of (B) *smurf2*, (C) *tp53*, (D) *mdm2*, (E) *ep300a*, (F) *yy1a*, (G) *smad7* and (H) *sirt1* during aging. * indicates $p<0.05$, ** indicates $p<0.01$, *** indicates $p<0.001$. (Reprinted from Tuz-Sasik et al., 2020 [36])

3.5 There was a potential balance between ubiquitination, acetylation, and deacetylation regulatory genes during brain aging according to multivariate analysis

To reveal the relationship between the genes of interest, Principal Component Analysis (PCA) and Pearson correlation analysis was conducted. Two principal components were extracted independent to the factor of age in the whole brain expression dataset which was including ΔCt values of seven genes of interest. First component (PC1) explained 75.3% of the variance in the dataset whereas second component (PC2) contributed 11.2% of total variance (Figure 3.8). PC1 was driven by seven genes of interest; their loading values were greater than 0.5 (Table 3.1). However, PC2 was affected by only *yy1a* and marginally by *mdm2* (Table 3.1). Moreover, the conducted correlation analysis did not indicate any correlation between *yy1a* and *mdm2* (Figure 3.9). It was apparent also in the loading plot (Figure 3.8); *yy1a* and *mdm2* had inverse contribution to the covariance. As seen in the loading plot (Figure 3.8) and the correlation matrix, *smad7* was not correlated with *tp53* or *mdm2* similar to no correlation between *yy1a* and *tp53/mdm2* in the whole brain. On the other hand, the contribution of *smurf2*, *ep300a* and *sirt1* were very similar to the variance and also they were highly correlated with each other. Since their proteins regulate same target proteins such as tp53 and smad7 via different post-translational mechanisms; ubiquitination, acetylation and deacetylation, their similar contribution in the gene expression levels could be predictable and also may explain the comparable levels of *tp53* and *smad7* during brain aging (Figure 3.7). The scatterplot (Figure 3.8) indicate that the age had a different effect on the variance. Second

component did not contribute the covariance in the old group; it implied that *yy1a* and *mdm2* contribution to PC2 was driven by young group. Moreover, the correlation analysis conducted in young group indicated that only associated genes with each other were *smurf2*, *ep300a* and *sirt1* (Figure 3.10A). The other genes had inverse contribution to variance (*tp53*-*mdm2*) did not have correlation in the young group. Yet, in the old group, almost all genes were correlated with each other (Figure 3.10B). It might imply that the balance among PTMs controlled by Smurf2, ep300a and Sirt1, is enough to control the stability in the adult brain; however, in the aged adult, there is a shift in their balance and other factors have to take a role to maintain the stability of target proteins and cellular processes in the brain.

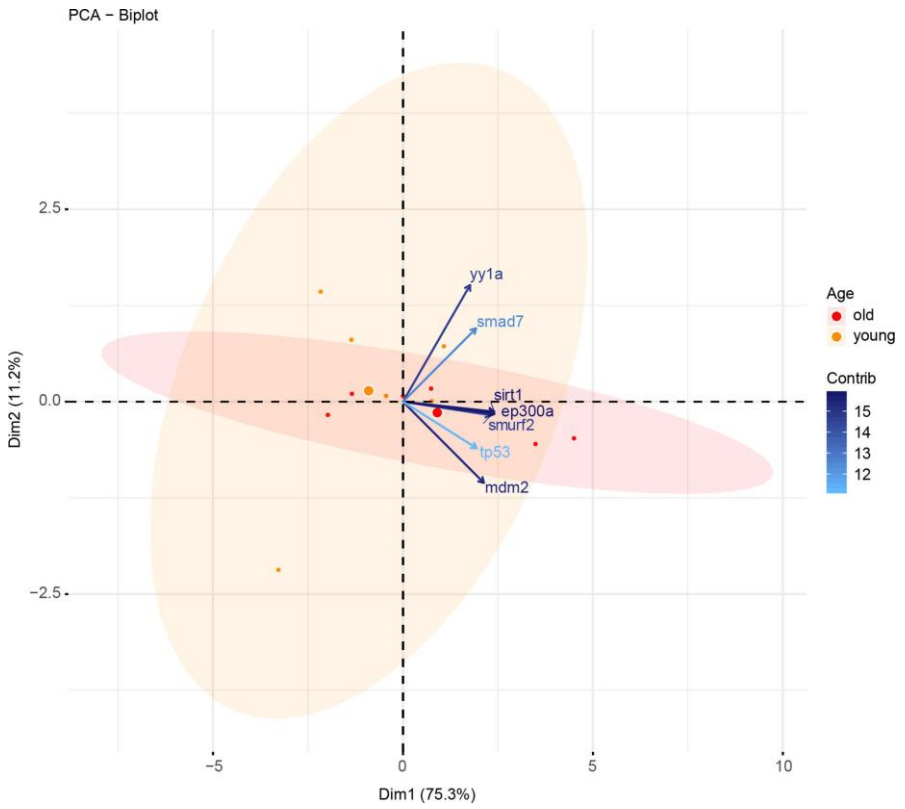

Figure 3.8 Loading plot and scatterplot of the first and second principal component scores arranged by the factor of age in whole zebrafish brain. Old=red, young=orange. The loading plot was generated by Meriç Kınalı. (Reprinted from Tuz-Sasik et al., 2020 [36])

Table 3.1 Component loading scores of PC1 and PC2 in terms of whole brain gene expression.

	Component loading scores	
Component	PC1 (75.3%)	PC2 (11.2%)
smurf2	0.938	-0.071
tp53	0.786	-0.245
mdm2	0.863	-0.427
ep300a	0.977	-0.064
yy1a	0.716	0.615
smad7	0.780	0.386
sirt1	0.975	-0.053

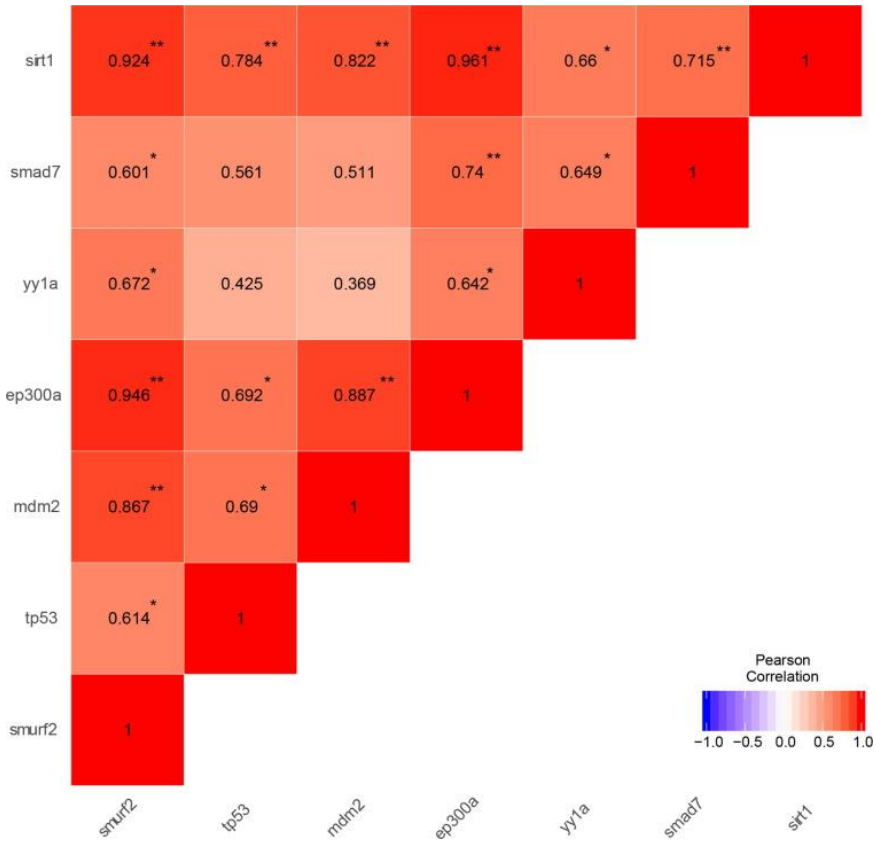

Figure 3.9 Pearson correlation matrix of genes of interest in whole zebrafish brain. *p<0.05, **p<0.01. The correlation matrix was generated by Meriç Kınalı. (Reprinted from Tuz-Sasik et al., 2020 [36])

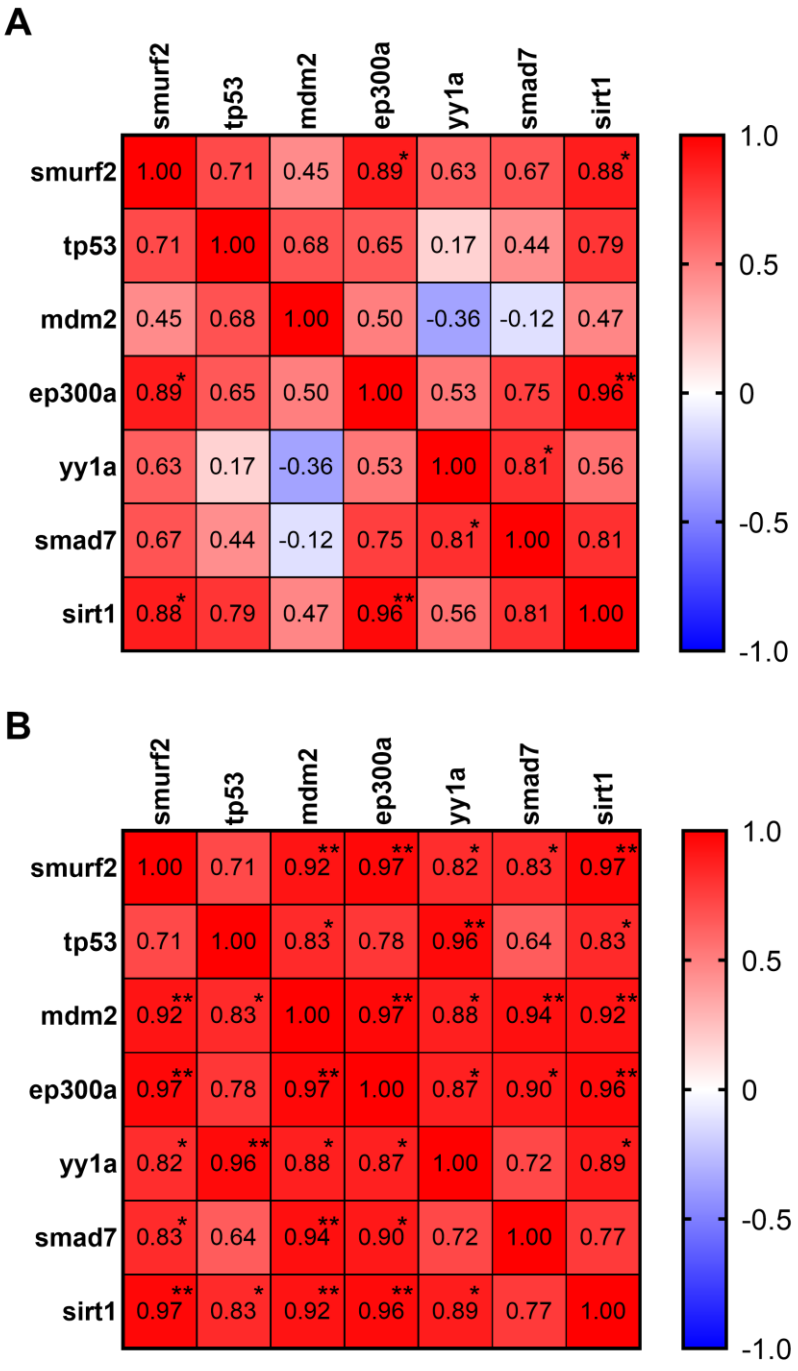

Figure 3.10 Pearson correlation matrices of genes of interest in (A) young and (B) old whole zebrafish brain. *$p < 0.05$, **$p < 0.01$.

In addition to whole brain data, the region-specific data was analyzed with PCA and Pearson correlation analysis. Again, the region-specific dataset included the ΔCt values of seven genes of interest. Individual PCAs were conducted for three brain regions (Tel, TeO and Ce) independent of the factor of age. In each brain region, two components were extracted. The percentage contribution of PC1 and PC2 to overall variance in each brain region was indicated in Table 3.2 and Figure 3.11. PC1 of Tel, TeO and Ce were driven by all seven genes although PC2 was impacted by diverse genes in each brain region (Figure 3.11). In Tel region, only *yy1a* influenced PC2. In the case of TeO region, PC2 was driven by *smurf2, smad7* and *sirt1* as well as *yy1a*. On the other hand, PC2 component of Ce region was driven by *yy1a* and marginally by *tp53* and *sirt1*. Furthermore, the correlation analysis demonstrated that each brain region had different pattern (Figure 3.12). Surprisingly, with respect to TeO region, there was a distinct correlation between *yy1a* and *mdm2* whereas in the case of whole brain, Tel and Ce regions, there was no significant correlation between these genes (Figure 3.12). It was observed that *smurf2, ep300a* and *sirt1* impacted variance similarly in the whole brain gene expression (Figure 3.8); however, the loading plots of brain regions (Figure 3.11) had distinct patterns. For instance, in the case of TeO and Ce regions, *smurf2* and *sirt1* contributed to dataset similarly while *ep300a* had similar contribution with *tp53* in TeO region and with *smad7* in terms of Ce region (Figure 3.11B and C). With respect to Tel region, in addition to *smurf2* and *ep300a, mdm2* had also similar impact on the variance (Figure 3.11A). Altogether, it may imply that the expression and interaction of *smurf2* and its partners have different patterns in age- and brain region-specific manner in order to balance PTMs including ubiquitination, acetylation, and deacetylation.

Table 3.2 Component loading scores of PC1 and PC2 in terms of brain regions; Tel, TeO and Ce.

	Component loading scores					
Region	Tel		TeO		Ce	
Component	PC1 (79.5%)	PC2 (11.2%)	PC1 (58.9%)	PC2 (30.6%)	PC1 (78.8%)	PC2 (16.1%)
smurf2	0.941	-0.327	0.7	-0.692	0.863	-0.378
tp53	0.937	0.315	0.901	-0.123	0.903	0.428
mdm2	0.973	-0.185	0.92	0.322	0.957	-0.253
ep300a	0.913	-0.268	0.894	-0.113	0.941	0.041
yy1a	0.679	0.653	0.755	0.599	0.639	0.733
smad7	0.797	0.164	0.501	0.78	0.982	0.066
sirt1	0.961	-0.142	0.592	-0.75	0.886	-0.44

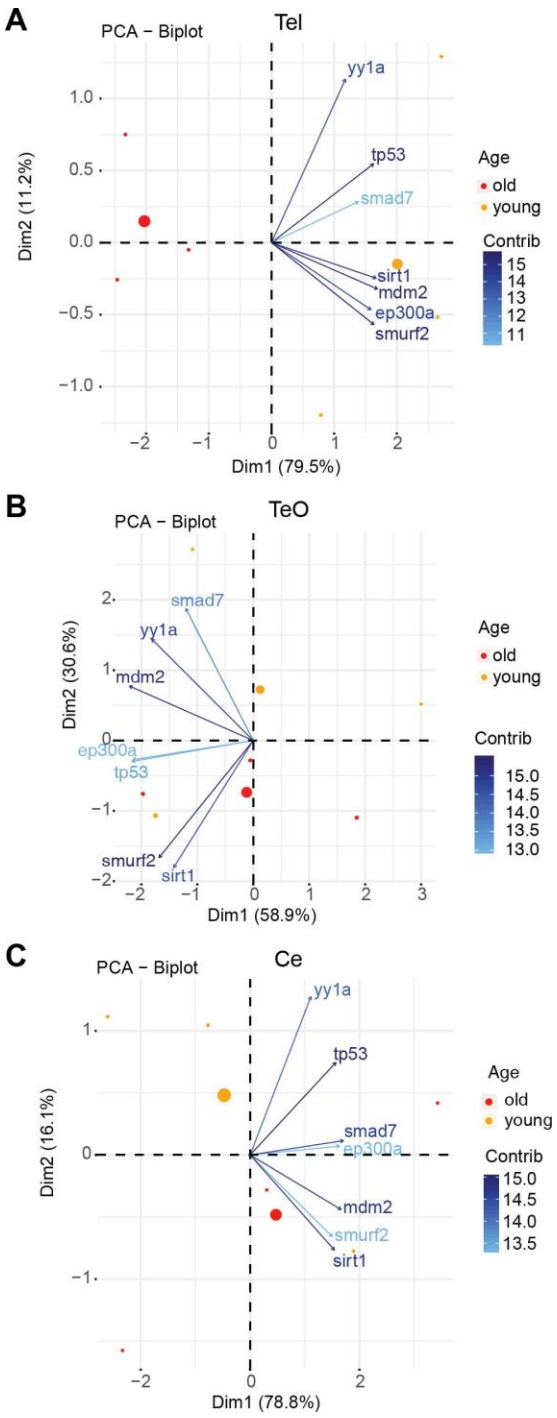

Figure 3.11 Loading plots the scatterplots of the first and second principal component scores arranged by the factor of age in specific zebrafish brain regions; (A) Tel, (B) TeO, (C) Ce. Old=red, young=orange. The loading plots were generated by Meriç Kınalı. (Reprinted from Tuz-Sasik et al., 2020 [36])

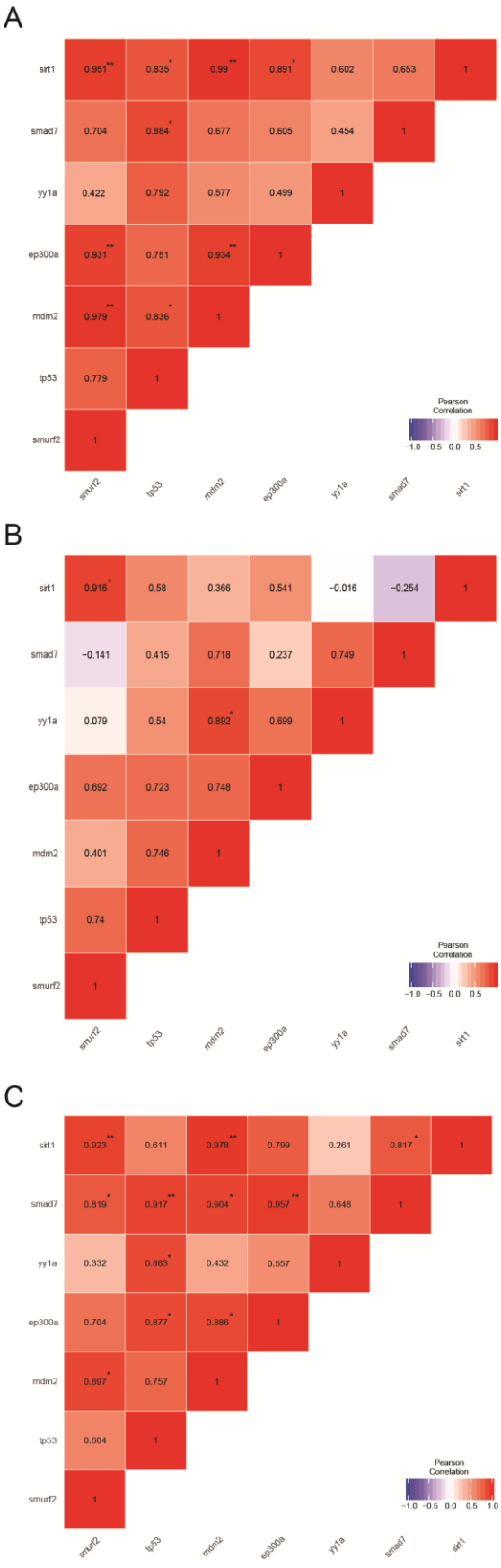
A
sirt1
smad7
yy1a
ep300a
mdm2
tp53
smurf2
0.951**
0.835*
0.99**
0.891*
0.602
0.653
1
0.704
0.884*
0.677
0.605
0.454
0.422
0.792
0.577
0.499
0.931**
0.751
0.934**
0.979**
0.836*
0.779
Pearson Correlation
−1.0 −0.5 0.0 0.5
smurf2 tp53 mdm2 ep300a yy1a smad7 sirt1
B
sirt1
smad7
yy1a
ep300a
mdm2
tp53
smurf2
0.916*
0.58
0.366
0.541
−0.016
−0.254
1
−0.141
0.415
0.718
0.237
0.749
0.079
0.54
0.892*
0.699
0.692
0.723
0.748
0.401
0.746
0.74
Pearson Correlation
−1.0 −0.5 0.0 0.5
smurf2 tp53 mdm2 ep300a yy1a smad7 sirt1
C
sirt1
smad7
yy1a
ep300a
mdm2
tp53
smurf2
0.923**
0.611
0.978**
0.799
0.261
0.817*
1
0.819*
0.917**
0.904*
0.957**
0.648
0.332
0.883*
0.432
0.557
0.704
0.877*
0.886*
0.897*
0.757
0.604
Pearson Correlation
−1.0 −0.5 0.0 0.5 1.0
smurf2 tp53 mdm2 ep300a yy1a smad7 sirt1

Figure 3.12 Correlation matrices of target genes of interest in zebrafish (A) Tel, (B) TeO and (C) Ce. Significance of correlation coefficients (2-tailed): *p < 0.05, **p< 0.01. The correlation matrices were generated by Meriç Kınalı. (Reprinted from Tuz-Sasik et al., 2020 [36]**)**

3.6 Discussion and Conclusions

This part of the current study focused on the Smurf2 expression levels across lifespan and its relationship with interacting partners during aging. Previous research has shown that *smurf2* gene expression levels increased in the aged brain and HSCs [35], [39]. In the present study, firstly Smurf2 protein expression was analyzed with two commercially available antibodies in order to demonstrate whether the protein levels have similar pattern with mRNA levels during aging. Although the Smurf2 level was not increased significantly in the whole zebrafish brain, in the case of specific brain regions, Smurf2 protein levels increased significantly in Tel and Ce. Moreover, subcellular protein fractionation indicated enriched Smurf2 levels in the cytosol. Secondly, the interacting partners and substrates of Smurf2 were analyzed in terms of gene expression levels. With respect to whole brain, only *smurf2* levels increased significantly in aged brain while *tp53* and *smad7* were stable during aging. However, region-specific analysis indicated that the expression levels of *smurf2* and other genes of interest were changed in a region-specific manner during aging. In addition, multivariate analysis with PCA and correlation demonstrated that *smurf2, ep300a* and *sirt1* influence the data similarly in the whole brain. The correlation of 7 genes of interest were diverse in the young and old brain; in terms of young brain, only *smurf2, ep300a* and *sirt1* were highly correlated while almost all genes had

correlation with each other in the aged brain. This might imply that there is a balance between the regulatory genes controlling ubiquitination, acetylation and deacetylation but with advancing age, this balance may disrupt and other regulatory genes should also take a role to sustain cellular stability.

In order to detect the protein band of Smurf2 in zebrafish tissues, we had two commercially available antibodies, anti-SMURF2, 200-300 aa, and anti-SMURF2 C-terminal. These two antibodies have not been validated in the zebrafish tissues so they were validated at the beginning of the current study. Anti-SMURF2, 200-300 aa, yielded expected 86 kDa band in both cell lines and zebrafish embryos and brain. However, interestingly anti-SMURF2 C-terminal antibody recognized a band whose molecular weight was heavier than the expected 86 kDa in the zebrafish embryos (app. 100 kDa) and brain (app. 250 kDa). Since there was a gradual increase between the embryos and adult brain, we asked about the potential regulatory mechanisms of Smurf2 across lifespan. There were a brain-specific PTMs or a complex formation on this protein. Other possibility was the one antibody was not enough to detect the protein because of the PTMs of it. For example, as observed in the study of Li et al. [42], acetylation of lysine residues on tp53 protein prevented the recognition of tp53 protein with PAb421, C-terminal antibody because the recognition sites of antibody was occupied by acetyl residues. Smurf2 protein also was controlled by PTMs, it would be reasonable to observe different bands with two antibodies. For example, Smurf2 were methylated at arginine residues (R234 and R239 of human SMURF2) by protein arginine methyltransferase 1 (PRMT1) [129] and these methylation sites would be overlapped with anti-SMURF2, 200-300 aa, antibody. Thus, it would be

possible that anti-SMURF2, 200-300 aa, recognizes unmethylated Smurf2 while anti-SMURF2 C-terminal, whose recognition sites were independent from methylation sites, may recognize the methylated version of Smurf2. Moreover, Smurf2 protein levels and activity is regulated by other modifications such as sumoylation and autoubiquitination [128], [130]. On the other hand, the complex formation of the Smurf2 protein with Smad7 [128] would be the cause of the higher molecular weight yielded with anti-SMURF2 C-terminal antibody. Surprisingly, neither anti-SMURF2, 200-300 aa nor anti-SMURF2 C-terminal antibody were cross detecting the other band, 250 kDa or 86 kDa, respectively. There might be more complex interaction what we thought and thus mutagenesis experiments could be performed to mutate the potential PTM sites altering the binding of antibodies to Smurf2 protein and thus underlying reason behind the different band sizes in different antibodies might be unveiled by using Western blotting and co-immunoprecipitation. Furthermore, in order to understand the exact mechanism on Smurf2 protein across lifespan, immunoprecipitation or mass spectrometric analysis should be further conducted in the brain tissue.

In the case of whole brain, Smurf2 protein levels did not alter significantly during aging. However, microdissected brain regions, Tel, TeO and Ce, indicated a region-specific increase in the aged brain in terms of Smurf2 protein levels. These upregulation was robust in Tel region detected with both antibodies. Previous research has shown that Smurf2 has a role in cellular senescence [31] and its expression levels increased during aging [35], [39]. Moreover, a recent study demonstrated that SA-β-gal levels, an important senescence marker, in Tel region of

aged zebrafish upregulated as compared to young [79]. The accumulation of Smurf2 protein in Tel region during aging might be a protective mechanism against the senescence or be a consequence of the senescence. Furthermore, since Smurf2 has a role in stem cell exhaustion and aging in HSCs [35], it may also be a critical in stem cell niches of zebrafish brain which are located in entire brain compared to restricted regions in mammalian brain [76], [77] and thus Smurf2 protein was upregulated in aged brain. Moreover, the homologues structure of hippocampus and amygdala were found in the zebrafish Tel and this region has diverse roles in the sensory, motor and cognitive functions including learning and memory [70]. Thus, zebrafish Tel is a vulnerable region in terms of cognitive functions. It might also imply that age-dependent alteration of Smurf2 in the case of Tel region might indicate its role during aging and in age-related cognitive declines. To understand the role of Tel and Smurf2 gene and protein levels better in this region during aging, only Tel can be separated from whole brain and analyzed and compared with remaining of the brain in terms of gene and protein expression. Also, immunochemistry may help to localize Smurf2 protein in specific brain regions and colocalize it with neuronal and glial markers to assign the global or cell-specific expression of Smurf2. On the other hand, the cytosolic fraction was enriched in terms of Smurf2 protein. Although its expression pattern was similar to whole lysate's pattern, the effect of age and region was marginally significant. The reason behind this discrepancy could be undetectable protein level of Smurf2 in the nuclear fraction. The loading amount of proteins could be increased to overcome this under detection of Smurf2 protein in nuclear fraction. Moreover, the commercial kits may be utilized to increase the efficiency of fractionation especially in small tissues like Tel. Also, it is critical to show this

cytosolic enrichment in tissues by utilizing immunochemical staining on brain sections. Unfortunately, up to now the antibodies used in the current study did not work in immunohistochemical sections of zebrafish brain; however, further development of new antibodies could lead to detailed anatomical analysis of Smurf2 in the aged brain.

In order to relate the upregulation of Smurf2 with its interacting partners, the gene expression of six interacting partners as well as *smurf2* was analyzed in the current study. *Smurf2* level was higher in the aged brain as compared to young brain in the case of whole brain. However, its gene expression decreased in terms of Tel and Ce regions in aged brain. The accumulation of Smurf2 protein in Tel region during aging could cause the downregulation in gene expression. Since Smurf2 protein accumulated in Tel and may interfere with cognitive functions or lead to stem cell exhaustion at that region, there might be a feedback mechanism to decrease the protein accumulation. In order to understand the antagonistic expression of Smurf2 in Tel, it should be further investigated and in situ hybridization and immunohistochemistry experiments can be conducted on brain sections.

Furthermore, other genes of interest did not change significantly in the whole brain during aging. Even, the levels of *tp53* and *smad7* were almost stable during aging in the case of whole brain. Moreover, the expression of *mdm2, ep300a* and *sirt1* as well as *smurf2* was altered in a region-specific manner although *tp53* and *smad7* levels were not changed significantly with respect to age and brain region. Then, multivariate analysis was conducted to understand the relations among the genes of interest. The expression levels of *smurf2, ep300a* and *sirt1* in the whole

brain had similar contributions to the variance and their expressions were highly correlated with each other. Since their proteins are regulating the diverse PTMs, ubiquitination, acetylation and deacetylation, on same targets [41], [42], [60], their similar contribution in terms of gene expression might also be conceivable. The crosstalk and competition among diverse PTMs could be likely contributed to cellular aging in the brain. Moreover, brain region-specific analysis indicated diverse contributions by genes of interest in each brain region. Most noticeable difference was *yy1a* contribution and correlation in TeO. For example, *yy1a* had different influence in terms of whole brain and it was not correlated with *mdm2* neither in the whole brain nor brain regions, Tel and Ce. However, there was a correlation between *yy1a* and *mdm2* in the case of TeO. Both MDM2 and YY1 proteins are the negative regulators of tp53 [45], [47] and they have physical interaction [45], [131], thus there might be a potential competition or compensation mechanism between them during aging. The stability and activity of tp53 is under tight control of PTMs including ubiquitination by MDM2, inhibition by YY1, acetylation by ep300, indirect control by MDM2 and YY1 ubiquitination via SMURF2 [44]–[48]. According to our results and previous findings, it might be implied that there is region-specific needs for diverse PTMs during aging. Although the current study demonstrated potential relations among the genes of interest, their protein levels and protein-protein interactions in the brain will be further studied to unravel their roles in terms of brain aging.

As a conclusion, this part of thesis work demonstrated the levels of Smurf2 and its interacting partners with respect to age and brain regions. In order to

understand the role of Smuf2 in brain aging in detail, the upregulation or downregulation of Smurf2 in the zebrafish model organism should be analyzed. Therefore, some genetic and non-genetic interventions will be analyzed in the next sections.

CHAPTER 4

THE STABLE AND TRANSIENT GENETIC INTERVENTIONS CHANGED THE SMURF2 LEVELS IN THE ADULT ZEBRAFISH BRAIN

4.1 The heat-inducible Tol2 transposase system was utilized to obtain an inducible Smurf2 overexpression model

4.1.1 The prepared destination vector and Tol2 transposase mRNA were co-injected into one-cell stage embryos which grew in the adulthood

To obtain heat-inducible Smurf2 over-expression line, Tol2 transposase system was utilized. The primers were designed for the cloning of Smurf2 coding sequence into pDONR221 donor vector via recombination reaction. The alignment of plasmids with expected plasmid sequence and with NM_001114426.1 (*Danio rerio SMAD specific E3 ubiquitin protein ligase 2* (*smurf2*), mRNA) identified with sequencing. After LR reaction, the destination vector was 11 kb length and thus, it was not easy to be sequenced the plasmid. With the help of online tools, I determined the expected sequence and restriction cut sites in it. Several restriction digestion experiments were performed to show the presence of *hsp70l* sequence, *smurf2* CDS and EGFP sequence. Also, the integrity of *in vitro* transcribed capped Tol2 transposase mRNA from pCS2FA-transposase was examined by agarose gel electrophoresis (Figure 4.1). Finally, 25 pg DNA (pDest+Smurf2 plasmid) and 25 pg Tol2 transposase mRNA were injected to one-cell stage embryos by microinjection. The survival rates of Tol2-injected and uninjected groups were followed for 3 days

and let them grow as founder fish named as *Tg*(*hsp70l:smurf2_EGFP*) with the date of birth, 15.02.17.

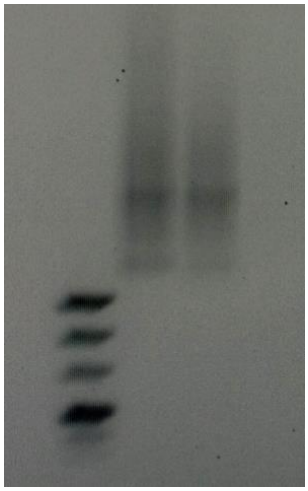

Figure 4.1 Agarose gel to confirm transposase mRNA integrity. Lane 1: DNA marker, Lane 2, 3: *in vitro* transcribed transposase mRNA.

4.1.2 Heat-shock application and PCR experiments was used to confirm the founder animals and their F1 generation

The embryos were raised to sexual maturity and then they were bred with WT animals to identify the founder fish. The F1 embryos from potential F0 founders were induced by heat-shock because of the *hsp70l* promoter and thus Smurf2 protein should be tagged with EGFP. After the breeding of potential founders with wt animals, at 24 hpf, the F1 embryos were divided randomly into two groups; heat-shock treated (hs) and no heat-shock treated (no hs). The embryos in hs group were treated with heat-shock at 37^{o}C for 1 hour to induce the Smurf2-EGFP expression and replaced back to a 28^{o}C incubator whereas no hs group kept at 28^{o}C during this time. After 4 hour, the embryos checked for EGFP signal under the fluorescence

microscope and their survival rates were recorded. At 48 hpf, the heat-shock treatment was repeated to hs group to increase the amount of inducible protein at 37^{o}C for 1 hour and the animals were put back into a 28^{o}C incubator while embryos in no hs group was kept at 28^{o}C. The last heat-shock applied at 72 hpf and EGFP signal was imaged under the fluorescence microscope. The dsRed fluorescence signal used to check autofluorescence. Two potential F0 founder fish was identified (Figure 4.2). In addition, the WT animals used as control and they divided into hs and no hs group.

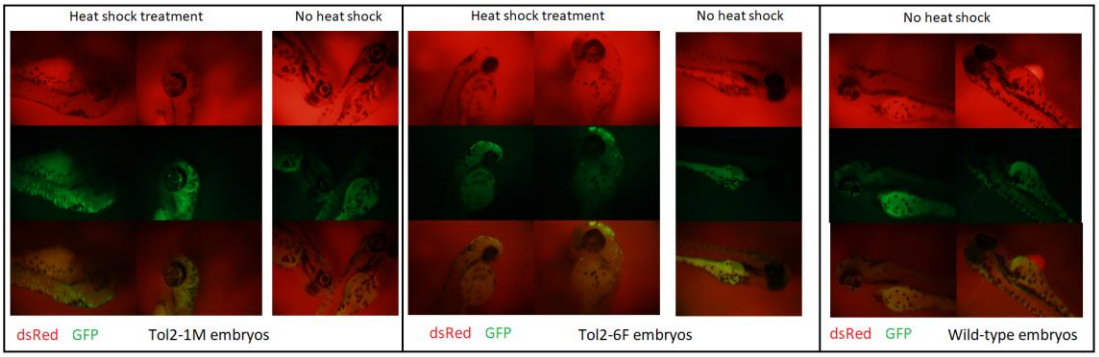

Figure 4.2 Fluorescence microscope images of *Tg(hsp70l:smurf2_EGFP)* F1 (Tol2-1M, Tol2-6F) and WT embryos.

In order to confirm the transposition and integration of the genes of interest into zebrafish genome, the gene amplification was performed with conventional PCR and with 3 primer pairs; EGFP and SmuGFP and Smurf2. I tried to optimize these primers with WT DNA samples and the construct which was injected to embryos to create Tol2 transgenesis. Smurf2 primers worked with both DNA samples from WT and embryos of potential founders (Figure 4.3). It was expected that EGFP primers work with the Tol2 construct while not with WT DNA samples (Figure 4.4).

However, PCR product of EGFP in neither Tol2 embryos nor WT embryos were detected whereas a housekeeping gene, β-Actin, primers amplify DNA in all samples (Figure 4.5).

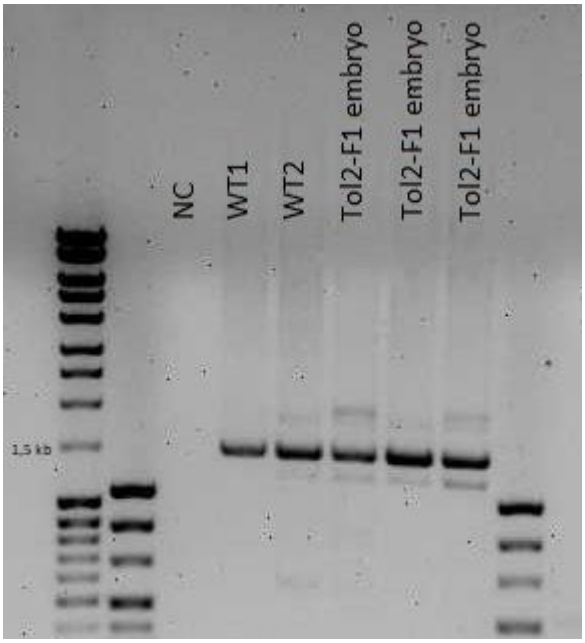

Figure 4.3 PCR products of Smurf2 primers.

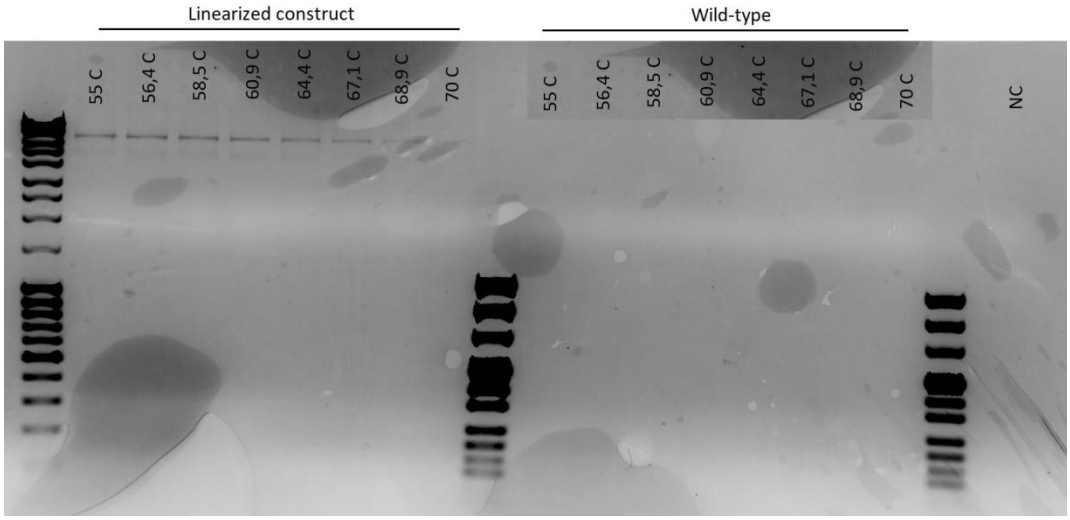

Figure 4.4 Gradient PCR products of EGFP primers. 61^{o}C was chosen for the next PCR experiments with this primer pair.

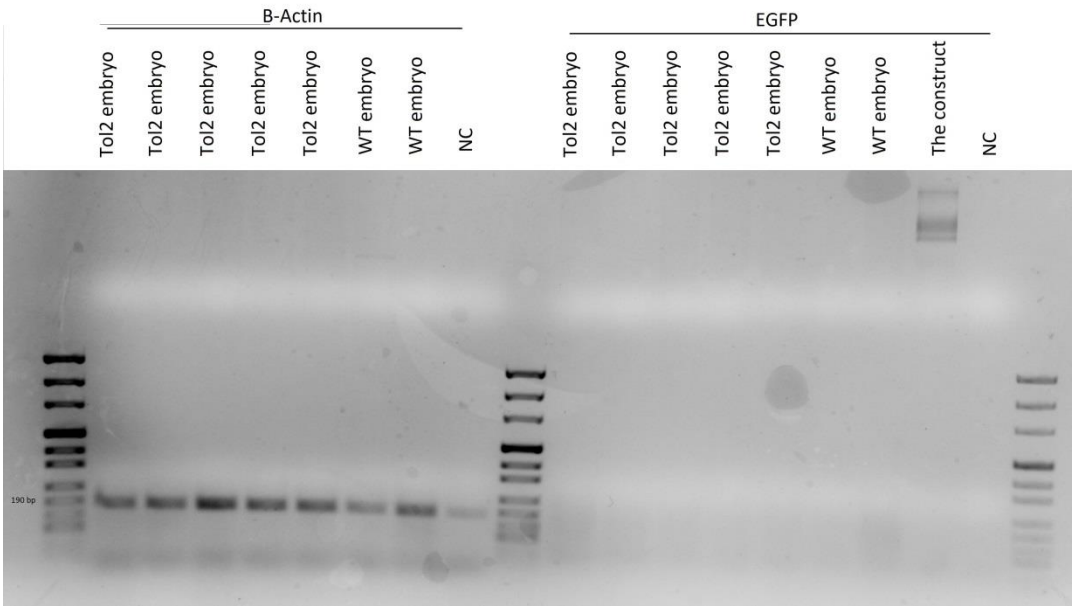

Figure 4.5 PCR products of β-Actin and EGFP primers.

At the same time, the potential founders named as Tol2-6F and Tol2-1M according to fluorescence signals of their progenitors, were bred with WT animals again and their embryos were collected (DOB: 28.12.17) and they were grown as F1 generation. After, they became mature and they were bred them with WT animals and check EGFP signal on their embryos after heat-shock treatment because F1 generation has more stable transgenesis and their embryos (F2) should have more stable EGFP signal after heat-shock treatment.

Moreover, I applied heat-shock at 5 dpf (120 hpf) for 1 hour, and then embryos were euthanized after 2 hours. RNA samples were extracted from pooled embryos. According to qRT-PCR results, *smurf2* gene expression levels were altered with a main effect of genotype (2 factors, WT and *Tg*(*hsp70l:smurf2_EGFP*) (Tol2) F1; $F(1,28)=5.621$, $p=0.025$; Figure 4.6). However, there were no main effect of heat-shock and no interaction effect ($F(1,28)=0.843$, $p=0.366$ and $F(1,28)=0.366$, $p=0.550$,

respectively). The genotype effect was robust between heat-shock treated WT and heat-shock treated Tol2 embryos (p=0.042). Since *hsp70l* promoter was a leaky promoter [132], we also observe increased gene expression of *smurf2* in no heat-shock treated Tol2 embryos as compared to no heat-shock WT but this was not statistically significant (p=0.229).

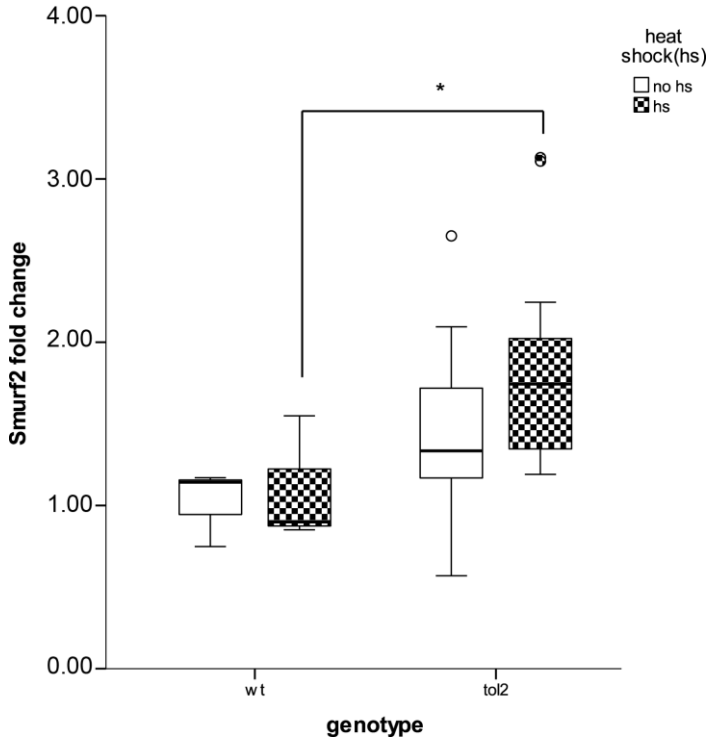

Figure 4.6 Gene expression levels of *smurf2* was increased with Tol2 genotype in heat-shock treated group as compared to WT heat-shock treated embryos. *: p<0.05.

4.1.3 Discussion and Conclusions

The main aim of this part was to obtain an inducible Smurf2 transgenic animal by utilizing Tol2 transposase system. The inducible system gives us to overexpress the gene of interest at the desirable time across lifespan rather than the overexpression throughout the life. Also, the overexpression is a powerful method to see the function and potency of the gene of interest. After we obtain a stable generation, we may induce the overexpression of Smurf2 in the adulthood by heat-shock, especially in the young ages in order to accelerate the aging process and compare them with their age-matched counterparts and older animals. For these purposes, we generated the desired vectors and injected them to one-cell stage embryos which were defined as F0 generation. After they became sexually mature, they were crossed with WT animals to obtain F1 generation which were exposed to heat-shock for three consecutive days in order to induce the expression of Smurf2, and EGFP. Few animals were defined as founders according to EGFP signal in their offspring; however, the gene amplification did not confirm the integrated copies of EGFP in their genome. As an alternative way, heat-shock was applied at 5 dpf for 1 hour and the mRNA expression levels of Smurf2 indicated an upregulation in the F1 embryos of *Tg*(*hsp70l:smurf2_EGFP*) with heat-shock. However, because of the time limitations, the desired stable generation could not be obtained and thus the potential accelerated aging model could not be tested during this thesis work. The further crossing and testing of the generations should be completed in order to obtain a stable transgenic line.

Generally, F0 generation has mosaic expression [82] thus, it was not expected to observe ubiquitous expression of EGFP in adult F0 animals. However, the important point is the germ-line transmission of Tol2 insertion to create a stable line. Germ cells of the injected fish also are mosaic, and, by crossing founder F0 fish with WT fish, non-transgenic fish and heterozygous transgenic fish can be obtained [82]. Unfortunately, the frequency of germline transmission of the injected DNA is very low i.e. about 5% of the injected fish can produce transgenic offspring [82]. More F0 generation should be bred and so more offspring could be investigated after heat shock. Furthermore, in the current study the heat shock were started at 24 hpf and repeated for three consecutive days or applied at 5 dpf for once. In LaBonty and colleagues' article [133], they started to heat-shock treatment at 5 hpf. This approach could be considered to induce the earlier expression and more robust fluorescence signal.

The inducible system gives the opportunity to overexpress the gene of interest at the desirable time rather than the overexpression throughout the life. After we obtain a stable generation, we may induce the overexpression of Smurf2 in the adulthood by heat-shock, especially in the young ages in order to accelerate the aging process and compare them with their age-matched counterparts and older animals. For example, if the overexpression of Smurf2 leads to an accelerated brain aging phenotype, it is expected to see an increased senescent phenotype which can be measured with increased level of SA-β-gal and *p16* gene expression in the brain [28], [79], [80]. Moreover, the proliferation rate could be affected and so the levels of global proliferation marker, proliferating cell nuclear antigen (PCNA), and an

astrocyte and astrogliosis marker, glial fibrillary acidic protein (GFAP), could be changed because of the early-onset of aging phenotype [78], [134]–[138]. Similarly, neuronal marker, embryonic lethal, abnormal vision (ELAV; Drosophila) like 3 (HuC), could be downregulated because its protein level decreases during aging [78], [139]. After the heat-shock treatment is applied to young transgenic animals, the brain tissues can be sectioned and immunohistochemical staining can be conducted to colocalize Smurf2 protein, which is tagged with EGFP, with neuronal proteins, proliferation markers and SA-β-gal signal. Since the three different Smurf2 antibodies could not work in the immunosections during the current study, EGFP tag might be a better way to label Smurf2 protein and so colocalize Smurf2 with other proteins.

As shown in Chapter 3, *smurf2* gene expression level decreases during aging in a region-specific manner, especially in Tel and Ce,[36] but these could be the consequences of the protein accumulation in these specific regions which has been also shown in Chapter 3 [36]. Similar to these results, overexpression of Smurf2 in the young ages may mimic the older Smurf2 protein level and cause to decrease in the gene expression level due to the accumulation of Smurf2 protein. Furthermore, it has been known that Smurf2 can play a critical role in inflammation by controlling the degradation of tumor necrosis factor receptor 2 (TNF-R2) and so promoting the activation of c-Jun N-terminal Kinase (JNK) [30], [140]. Also, increased activation of nuclear factor κB (NF-κB), which is highly correlated with chronic inflammation during normal aging, induces the upregulation of *smurf2* gene expression in aged mesenchymal stem cells and enhances the ubiquitin-mediated degradation of β-

catenin similar to TNF-induced Smurf2 expression does in mesenchymal stem cells [141], [142]. Since the roles of Smurf2 in inflammation and potentially in inflammaging, the overexpression model can be utilized to understand the inflammatory/anti-inflammatory effects of Smurf2 in the brain. Although our treatment is heat-inducible, it should be overexpressed in the all somatic and germ cells after heat-shock treatment. Thus, our treatment can lead to systemic alterations and should be investigated to understand the aging profile among multiple organs.

To conclude, because of the limitations including time and inducible systems, the desired stable transgenic line and potential inducible accelerated aging model could not be generated and tested for the neuronal impacts of Smurf2 overexpression. The phenotyping and genotyping could be done with more F0 animals. If it is necessary, new injections can be performed easily with the same vectors which have already generated and found in the laboratory. Moreover, since we have complete Tol2kit, the new constructs could be generated for the different inducible systems or ubiquitous expression throughout the life.

4.2 The gene knockout of Smurf2 across lifespan were obtained by utilizing CRISPR-Cas9 system

To achieve a knockout model of Smurf2, the CRISPR-Cas9 system was employed. Firstly, three different gRNAs which target different domains of Smurf2 were designed with the help of Marion Gradl and Vanessa Gerber in Karlsruhe Institute of Technology. The gRNA targeting exon10 of Smurf2 corresponding WW

domains, was cloned and transcribed with T7 polymerase. pT3TS-nCas9n plasmid was used to transcribe capped *cas9* mRNA with T3 polymerase. The alignment of expected plasmid sequence of pDR274+guide3 with prepared plasmid compared with sequencing. Finally, gRNA and *cas9* mRNA were injected to one-cell stage embryos by microinjection. The survival rates of co-injected, only *cas9* injected and uninjected groups were followed for 4 days. The injected embryos were named as *Tg*(*smurf2*_e10) with the date of birth, 20.01.17.

4.2.1 Several PCR-based methods were employed for genotyping the founder fish and F1 generation embryos

After they reached the sexual maturity, adults in F0 generation were bred with WT zebrafish to identify the founders. The DNA was extracted from collected embryos and was subjected to PCR reactions. Hua et al. [122] established a simple and efficient method to screen CRISPR-Cas9 induced mutants called as ACT-PCR. In the current study, the temperature of 64.8^{o}C was chosen as the critical annealing temperature for genotyping pair #1. This method should be confirmed with F0 generation and F1 embryos.

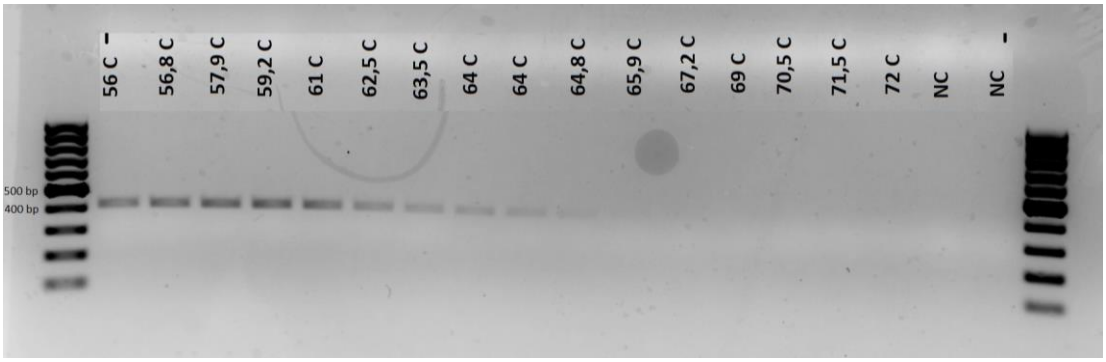

Figure 4.7 Gradient PCR for genotyping pair #1 to utilize in ACT-PCR.

Four pairs of potential founders (F0) were inbred and then their embryos were collected to check their phenotypes. After breeding, these 8 adult fish were euthanized and DNA samples were extracted from their tails and gonads for genotyping. To genotype F0 animals, PCR products were used in T7E1 assay to detect the mismatch [123] and in Restriction Fragment Length Polymorphism (RFLP) method [124] to check any mutation in the expected DSB site. After T7E1 assay, the samples were run on the agarose gel (Figure 4.8). It was expected that if guide RNA injection caused to mutation, T7E1 enzyme recognize the mismatch and produced cleaved fragments which is detectable in the gel. However, the results were not reliable because both control *cas9* injected and gRNA injected male gonads have cleaved products while female gonads have only uncleaved PCR products. This method should be optimized with control *cas9* injected embryos/tissues or naïve emrbyos/tissues and then applied to *Tg*(*smurf2*_e10) F0 adults or F1 embryos.

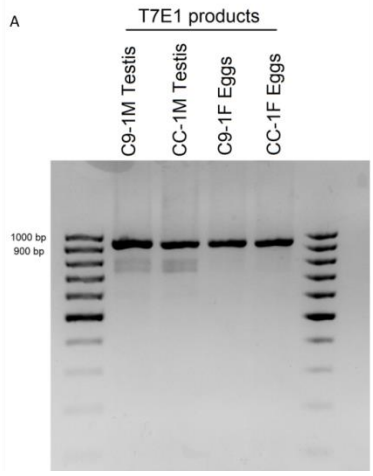

Figure 4.8 Representative image of T7E1 assay. C9: only *cas9* injected F0, CC: gRNA and *cas9* injected F0.

Lastly, RFLP method was performed with a *SmaI* restriction enzyme. Since there is a *SmaI* restriction site at the expected mutation site, this restriction site allows genotyping by RFLP. In WT fish, *SmaI* restriction enzyme cut PCR product at one site leading 399 bp and 544 bp fragments. However, if there is a mutation at that site, the restriction enzyme may not cut PCR product. I applied RFLP to PCR product of tail and gonads of adults and ran the restriction products on the gel (Figure 4.9). Unfortunately, all PCR products were cut by *SmaI* enzyme; all *Tg*(*smurf2*_e10) F0 adult tissues were same at the restriction site in *smurf2* gene. The experimental conditions should be optimized more to identify the knockout animals.

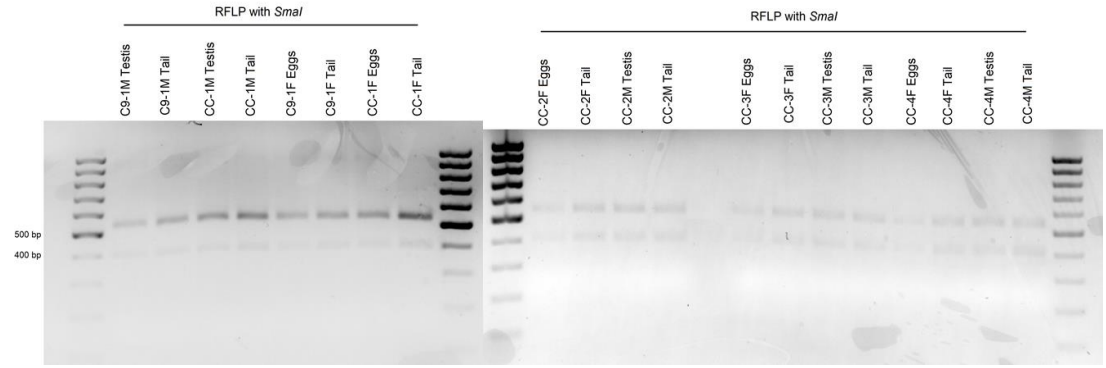

Figure 4.9 Representative RFLP results. C9: only *cas9* injected F0, CC: gRNA and *cas9* injected F0.

4.2.2 Discussion and Conclusions

In order to achieve a knockout model of Smurf2 across lifespan, the CRISPR-Cas9 system was utilized. After generation of gRNAs and *cas9* mRNA, they were co-injected into one-cell stage embryos and were grown to maturity. The F0 adult tissues and F1 embryos were used in the several PCR-based genotyping methods. Unfortunately, they were not optimized in the time of thesis work. They will be

optimized and if it is needed, new injections will be performed with already prepared gRNA and *cas9* mRNA. Also, rather than the *in vitro* transcribed *cas9* mRNA, Cas9 protein can be co-injected with gRNAs to increase the efficiency [143]. Moreover, the solutions can be injected to cell rather than the yolk of one-cell stage embryos to increase the efficiency [144], [145]. Besides, qRT-PCR method will be performed with genotyping primers that were designed for ACT-PCR to screen mutants because if there is a mutation at the reverse primer target site, the threshold cycle value may be higher than the normal threshold cycle values because the primer pairs cannot amplify the mutated DNA samples. After optimize a genotyping procedure, the generation of Smurf2 knockout will be a beneficial model to study brain aging.

4.3 Vivo Morpholino

In the current work, the last genetic intervention to alter Smurf2 expression was Vivo-morpholino treatment. To deliver Vivo-morpholino solutions to zebrafish brain, cerebroventricular microinjection (CVMI) technique [90] was utilized. The effect of Vivo-morpholino technology is transient that is time- and dose-dependent [90]. The purpose was the knockdown of Smurf2 expression during adulthood for a short time at most 5-7 days rather than a lifelong knockout model. For this purpose, two different Vivo-morpholinos were designed and applied to adult brain; exon-skipping which targets to exon15-intron15 junction of *smurf2* gene and translational blocking.

4.3.1 Exon-skipping Vivo-morpholino decreased the protein intensity in a non-significant manner

Firstly, exon-skipping Vivo-morpholino was applied and it was expected that the morpholino injection on the adult brain cause a deletion of exon 15 during splicing and so a truncated protein. Also, exon 15 and consecutive exons translates HECT domain of Smurf2. This domain is the catalytic domain for E3 ubiquitin ligase activity. So, the truncated protein was expected to be a non-functional and affect the roles of Smurf2 on brain aging. Since anti-SMURF2 antibody (anti-SMURF2 C-terminal; ab211746) recognizes Smurf2 protein between 507-765 aminoacid residues, after the deletion of exon 15 this antibody could not bind to protein. Thus, the intensity of the band should be less than untreated groups according to the knockdown efficiency.

After zebrafish were CVMI-injected, they were incubated in a tank which was oxygenated and was kept at 28^{o} C until euthanization. For each time point, at least 3 animals were euthanized and their protein were extracted and applied to Western blot analysis. Anti-SMURF2 C-terminal and β-tubulin antibody were used in Western blot (Figure 4.10). Each sample was loaded on the gel at least TWO times. The protein level of Smurf2 was not altered significantly with time post injection ($F(7,24)=1.108$, $p=0.405$; Figure 4.11). However, according to relative protein expression levels of Smurf2 after Vivo-morpholino injection, at 1 days post injection (dpi), there was about 41% decrease in terms of Smurf2 protein expression level. This time point could be utilized for further analysis to determine neuronal alterations as a response to possible non-functional truncated Smurf2 protein.

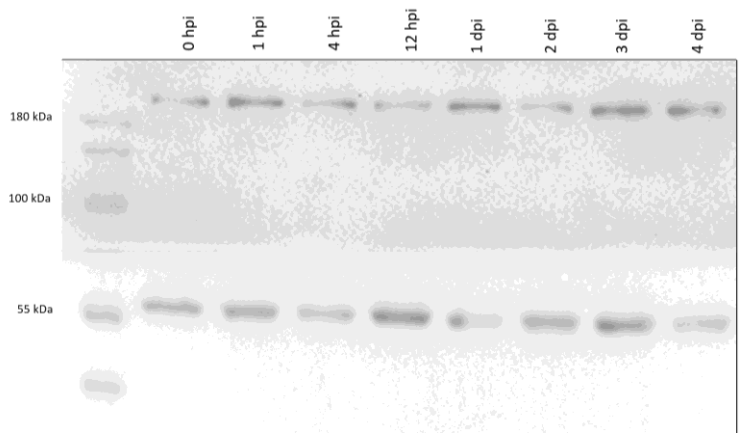

Figure 4.10 Representative Western image for Anti-SMURF2 C-terminal (~200 kDa) and β-tubulin (55 kDa) antibodies after exon-skipping Vivo-morpholino injection.

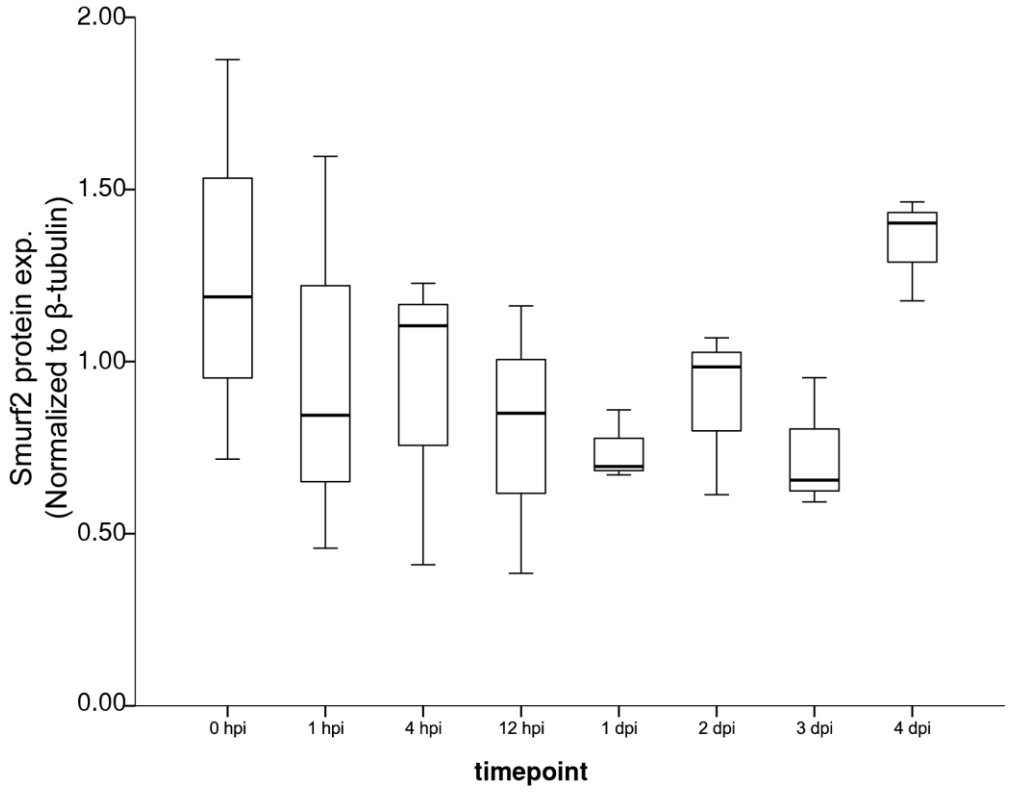

Figure 4.11 Protein expression level of Smurf2 was not altered with respect to post injection time. Tub-normalized values are indicated.

4.3.2 Translational Vivo-morpholino also decreased the protein levels of Smurf2 but the level of downregulation did not reach statistically significant level with observed timepoints

As an alternative, translational blocking Vivo-morpholino of Smurf2 was injected to adult zebrafish brain via CVMI. Since translational blocking MOs bind complementary mRNA sequences near the translational start site to hinder ribosome assembly and thus inhibit the translation of protein [86], it was expected to decrease in Smurf2 protein level. In this experiment, 5 time points including uninjected (0 hpi), 12 hpi, 1, 3, 5 dpi for both Smurf2_tr Vivo-morpholino and standard control Vivo-morpholino, a negative control MO that targets a human beta-globin intron mutation, were investigated. After injection of Vivo-morpholinos, zebrafish kept in a tank which was oxygenated and was kept at 28^{o} C until desired time points. Proteins were loaded on the gel as 3 cohorts and at least 3 times (Figure 4.12). Surprisingly, in standard control Vivo-morpholino injected protein lysates had numerically less amount of Smurf2 than translational Vivo-morpholino injected ones' (Figure 4.13) but there was no significant main effect of treatment ($F(1,20)=0.333$, $p=0.571$) or time point ($F(4,20)=1.651$, $p=0.201$). The decrease in standard control injected animals can be caused by the stress or off-target effects. Also, in this experiment uninjected group was just anesthetized and then recover in fresh fish water; any incision or injection was not applied to them.

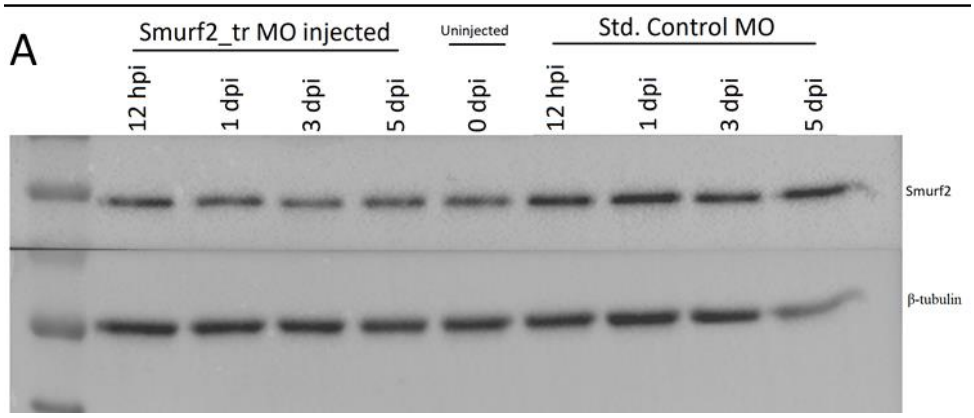

Figure 4.12 Representative Western image after translational blocking Vivo-morpholino injection.

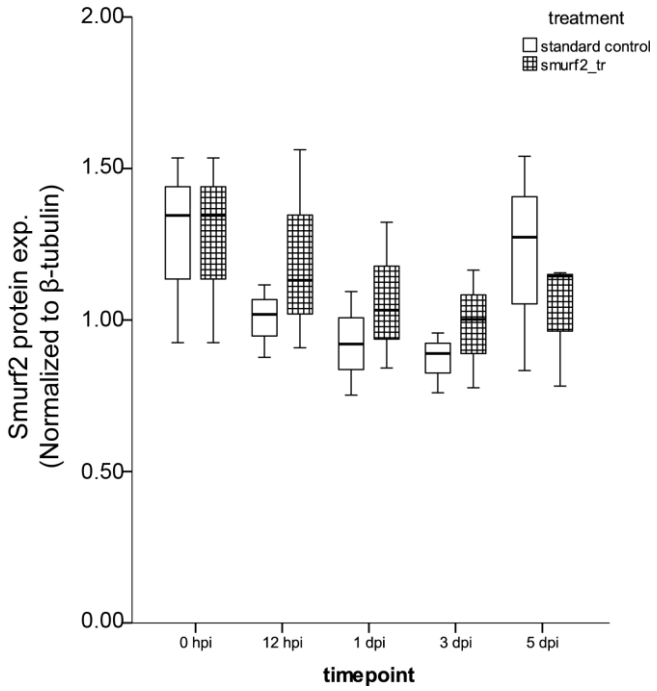

Figure 4.13 Protein expression level of Smurf2 was not altered with respect to treatment and post injection time. Tub-normalized values are indicated.

To eliminate the confounding stress effect induced by incision to skull which was necessary for injecting the morpholino solution to cerebroventricular region, uninjected group (0 hpi) was anesthesized and only incision was applied to their skull. Then, the animals were recovered in the fresh water and then added the analysis. The cohorts were run on the gel as duplicate. The main effect of treatment and main effect of timepoint were not statistically significant ($F(1,20)=0.005$, $p=0.942$ and $F(4,20)=0.442$, $p=0.777$, respectively; Figure 4.14) and also there was no interaction effect between treatment and timepoint ($F(4,20)=0.363$, $p=0.832$). Since Smurf2 protein expression level decreased at 1 dpi while restored at 3 dpi, timepoint of 2 dpi could be used to investigate the consequences of Smurf2 downregulation with translational blocking Vivo-morpholino.

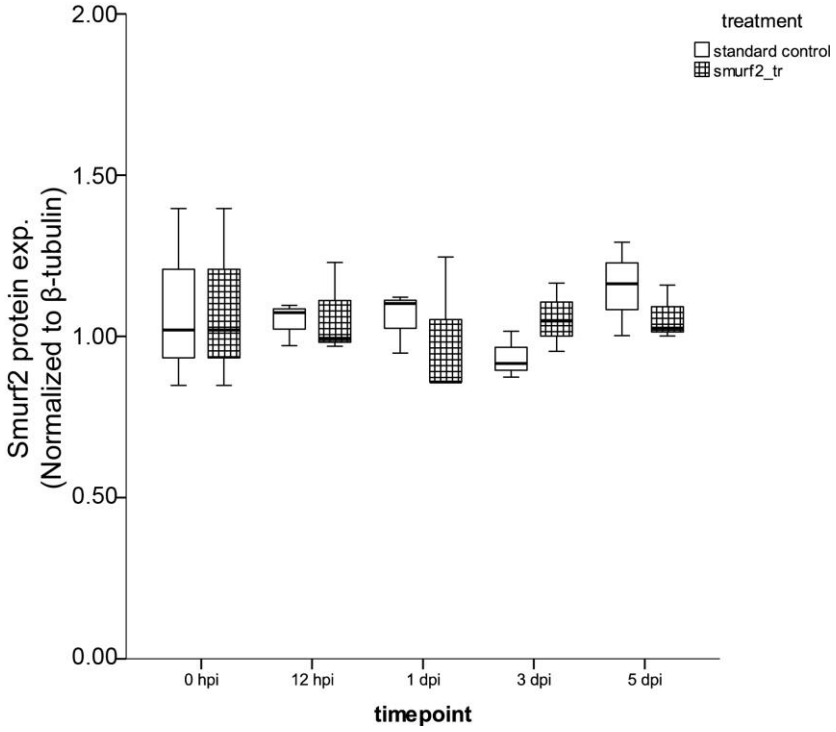

Figure 4.14 Protein expression level of Smurf2 was not altered with respect to treatment and post injection time when uninjected animals were also incised with syringe under anesthesization. Tub-normalized values are indicated.

4.3.3 Discussion and Conclusions

Vivo-morpholinos are designed to knockdown a gene of interest *in vivo* such as adult zebrafish. Generally, Vivo-morpholino is delivered systemically by intravenous or intraperitoneal injections. Also, Kizil and Brand established CVMI method to deliver Vivo-morpholino into the adult zebrafish brain [90]. CVMI of Vivo-morpholinos blocks protein production efficiently approximately up to a week and lead to functional consequences [90], [91]. In the current study, two Vivo-morpholinos were employed and injected to adult brain.

Firstly, exon-skipping Vivo-morpholino which targets to exon15-intron15 junction was investigated. This Vivo-morpholino injection may cause a deletion of exon15 during splicing and so producing a truncated protein. Since one of SMURF2 antibodies, anti-SMURF2 C-terminal recognizes Smurf2 protein between 507-765 aminoacid residues that are expressed from exon15-exon19, after Vivo-morpholino treatment, this antibody could not bind to truncated protein. However, the protein level of Smurf2 was not altered significantly with time post injection. On the other hand, after Vivo-morpholino injection, at 1 dpi, there was about 41% decrease in terms of Smurf2 protein expression level. This time point could be utilized for further analysis and also a control injection including standard control Vivo-morpholino or mismatch control Vivo-morpholino could be beneficial to compare the levels of knockdown.

Moreover, a translational blocking Vivo-morpholino was investigated in terms of Smurf2 protein level. Translational blocking morpholinos bind to complementary mRNA sequences near the translational start site and so hinder ribosome assembly following inhibition of the translation [56]. Thus, it was expected to decrease in Smurf2 protein level but the treatment including Smurf2_tr Vivo-morpholino and standard control Vivo-morpholino, and the post injection timepoints did not altered Smurf2 level significantly. Besides, Smurf2 protein expression level decreased numerically at 1 dpi while restored at 3 dpi, timepoint of 1 dpi and/or 2 dpi could be further investigated to demonstrate the impacts of Smurf2 downregulation in the case of adult brain.

To conclude, Vivo-morpholino gives an opportunity to knockdown the gene of interest at any time during lifespan however, its effect was transient. Moreover, the knockdown level of each gene is different because its level is dependent on the expression level of endogenous proteins and on the efficiency of the morpholino [91]. Thus, each Vivo-morpholino solution was demonstrated with the factor of post injection timepoints to determine the 50% efficiency in the current study. The future investigations should be performed in terms of Smurf2 protein levels during post injection times with immunostaining as well as Western blotting before performing further experiments to observe neuronal impacts of Smurf2 knockdown with Vivo-morpholino. Moreover, as mentioned in the next chapter, non-genetic drug treatment could be utilized to demonstrate the inhibition of Smurf2 activity and its consequences.

CHAPTER 5

THE NON-GENETIC INTERVENTIONS INCLUDING DIET AND INHIBITOR TREATMENT ALTERED THE EXPRESSION OF INTERACTING PARTNERS OF SMURF2 AND NEURONAL MARKERS

5.1 Dietary interventions, overfeeding and caloric restriction, altered the body parameters and neuronal markers while they did not affect the expression of Smurf2 and its interacting partners in the brain

5.1.1 The dietary regimens changed the primary and secondary body parameters

At the end of 12 week dietary interventions, the primary body parameters, body weight and length, of each fish were measured and recorded. Then, the secondary parameters, BMI and Fulton K factor, were calculated. In terms of body weight (Figure 5.1), there was a main effect of age ($\chi^2(1)=10.952$, $p=0.001$) and diet ($\chi^2(2)=44.850$, $p<0.0005$). Pairwise comparisons indicated that the main effect of age was evident in AL ($p=0.012$) and CR ($p=0.019$) fish. Moreover, the body weight was significantly different between OF and CR fed fish in both young and old ages ($p<0.0005$ and $p=0.0004$, respectively) and between AL and CR in both young and old fish ($p=0.0006$ and $p=0.001$, respectively). It was obvious that CR regimen leads to weight loss in both young and old fish while fish fed with OF diet gain weight which was not significant in both ages. Since zebrafish continue to grow even in advanced age [146], [147], previous research indicated that aged animals had higher in weight and length [79], [92]. Thus, the body length was analyzed in the current

study; both the main effect of age and diet were significant ($F(1,80)=50.626$, $p<0.0005$ and $F(2,80)=40.305$, $p<0.0005$, respectively) with an interaction effect ($F(2,80)=5.588$, $p=0.005$, Figure 5.2). The main effect of diet was significant between AL and CR-fed fish ($p<0.0005$) and between OF and CR fish ($p<0.0005$). According to pairwise comparisons, the age effect was evident in AL and CR groups ($p<0.0005$ and $p<0.0005$, respectively) but not in terms of OF ($p=0.176$). The effect of diet was evident in young (AL vs. OF, $p=0.005$; AL vs. CR, $p<0.0005$; OF vs. CR, $p<0.0005$) and old (AL vs. CR, $p<0.0005$; OF vs. CR, $p=0.001$) in the case of body length. The current study revealed that body weight and length increase during aging because zebrafish have continuous growth. It might imply that the dietary regimens have an impact on the body weight and length.

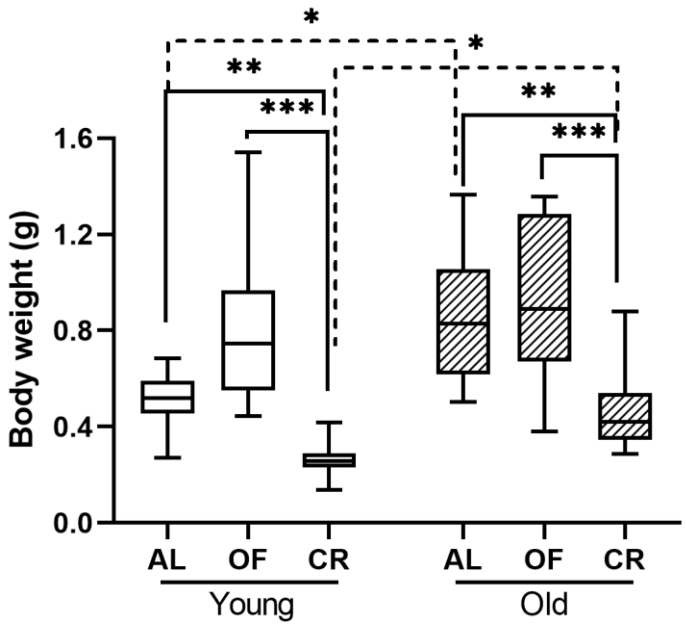

Figure 5.1 Body weight was altered with respect to aging and dietary regimens. Corrected *p*-values, *: $p<0.025$, **: $p<0.005$, ***: $p<0.0005$.

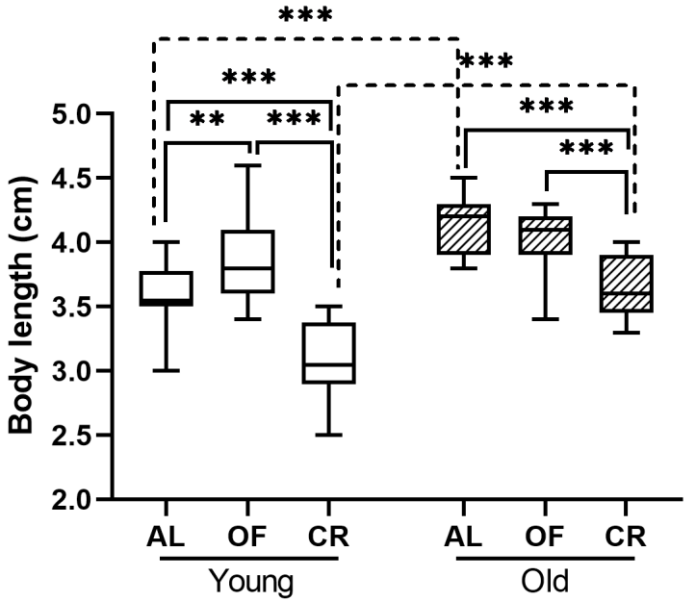

Figure 5.2 Body length of zebrafish was altered in terms of age and diet. *: $p<0.05$, **: $p<0.01$, ***: $p<0.001$.

The secondary body parameters including BMI and Fulton K factor were calculated since body weight and length were changed with respect to age and diet and only weight is not enough to define the status of overweight/obesity or well-being of fish. BMI and Fulton K factor was used in previous zebrafish research [92]–[94], [148], [149]. In terms of BMI, the main effect of age was significant ($\chi^2(1)=5.264$, $p=0.022$). There was a main effect of diet ($\chi^2(2)=45.400$, $p<0.0005$); this effect was evident in both young and old fish between OF and CR ($p<0.0005$ and $p<0.0005$, respectively) and between AL and CR ($p<0.0005$ and $p=0.002$, respectively) in the case of BMI. While Fulton K factor was not altered during aging ($\chi^2(1)=0.658$, $p=0.417$), the diet effect was significant ($\chi^2(2)=36.347$, $p<0.0005$). Similar to BMI result, the diet effect was apparent between OF and CR in both young

and old (p<0.0005 and p<0.0005, respectively) and between AL and CR (p=0.002 and p=0.006, respectively). The present results demonstrated that our CR regimen was effective to decrease body weight and BMI values of zebrafish. However, OF regimen did not increase the body parameters significantly as compared to age-matched AL-fed fish except the body length of young OF group. A previous study conducted by Ran et al. revealed that their 8 week OF diet was increased Fulton K factor by 13.9% in young adults while 8 week CR diet decreased Fulton K factor by 8.5% [149]. Our present 12 week OF diet increased Fulton K factor by 16.2% and 13.0% in young and old fish, respectively. Also, Fulton K factor decreased with CR diet by 20.2% and 22.6% in young and old group. We may imply that our non-genetic interventions including OF and CR was effective to change body parameters and probably the gene and protein expression profile in the brain which will be explained in next section.

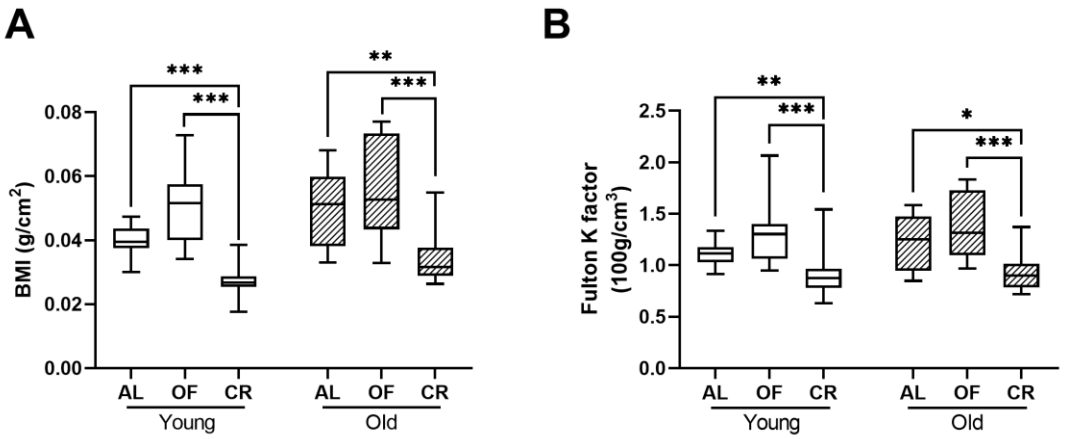

Figure 5.3 Secondary body parameters, (A) BMI and (B) Fulton K factor, were changed by dietary regimens. Corrected *p*-values, *: $p<0.025$, **: $p<0.005$, ***: $p<0.0005$.

5.1.2 The neuronal markers, HuC and DCAMKL1, were altered by aging and dietary regimens

In order to observe the neuronal alterations of age and diet, the early-differentiated neuronal marker, HuC, and the post-mitotic neuronal markers, DCAMKL1, were analyzed. Prior to the current study, anti-HuC antibody and anti-DCAMKL1 antibody were not validated in zebrafish tissues. Thus, firstly these antibodies were validated with positive controls and zebrafish brain tissue (Figure 5.4A). The molecular weight of detected bands was at the expected size; HuC was approximately at 40 kDa and DCAMKL1 was approximately at 82 kDa. After validation, each sample was run as cohorts at least 3 times on the gel (Figure 5.4B).

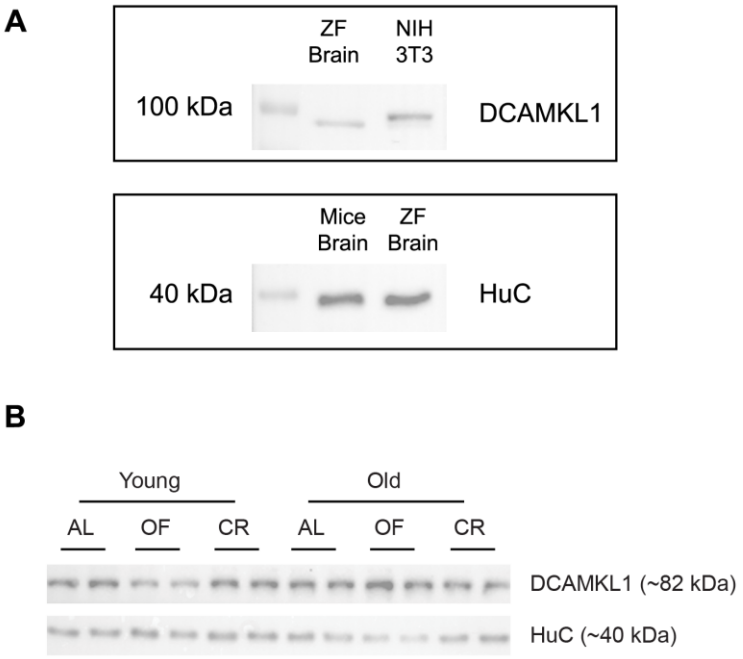

Figure 5.4 HuC and DCAMKL1 antibodies were validated in zebrafish brain. (A) Antibody validation with positive controls; NIH3T3 and mice brain lysate. (B) Representative Western blots for HuC and DCAMKL1 across age and diet groups.

The early-differentiated neuronal protein, HuC, levels were decreased significantly during aging ($F(1, 30)=9.706$, $p=0.004$) whereas neither the main effect of diet nor the interaction effect was statistically significant ($F(2, 30)=0.020$, $p=0.980$ and $F(2, 30)=2.235$, $p=0.124$, respectively). Based on pairwise comparisons, the main effect of age was apparent in OF and CR groups ($p=0.023$ and $p=0.007$, respectively; Figure 5.5A). HuC is an early-differentiated neuronal marker [150], while DCAMKL1 has persistent expression in the post-mitotic neurons [151]. Thus, DCAMKL1 was also investigated in the current study. There was a significant

interaction effect between age and diet ($F(2, 30)=3.903$, $p=0.031$) without a main effect of age ($F(1, 30)=0.005$, $p=0.945$) and a main effect of diet ($F(2, 30)=2.337$, $p=0.114$) in the case of DCAMKL1 protein levels. The interaction effect between age and diet was evident between young OF and old OF fish ($p=0.046$; Figure 5.5B). Moreover, DCAMKL1 protein levels were marginally significant between young AL and young OF group ($p=0.056$). While early differentiated neuronal protein, HuC, level decreased during aging especially in OF and CR fish, the level of post-mitotic neuronal protein, DCAMKL1, had higher in aged OF fish as compared to young OF. This might imply that the different steps of neurogenesis could be under control of age and diet and the alteration in the neuronal proteins could be the result of decreased proliferation or increased senescence in advanced age [78], [80].

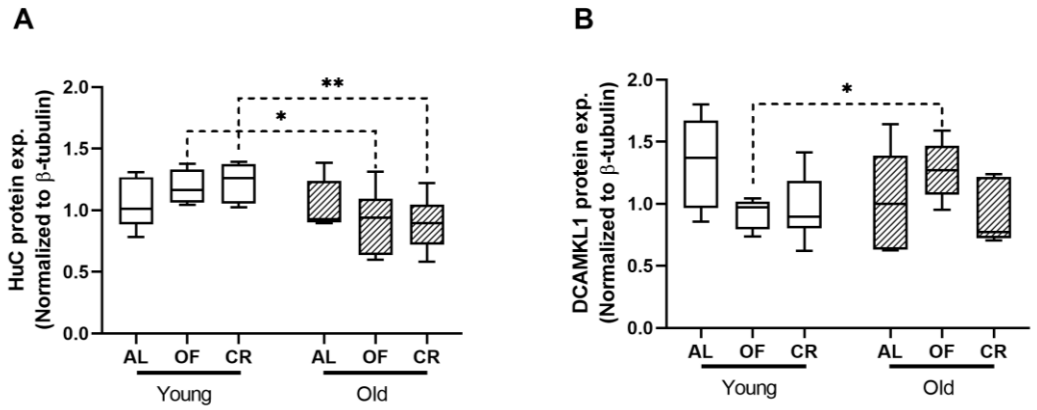

Figure 5.5 Protein expression levels of post-mitotic neuronal markers (A) HuC and (B) DCAMKL1 in terms of age and diet. Tub-normalized values are indicated in (A) and (B). *: $p<0.05$, **: $p<0.01$.

5.1.3 Global proliferation marker, PCNA, and senescence associated protein Smurf2, did not change with age and diet

In order to investigate the role of aging and short-term dietary regimens on the proliferation and senescence, PCNA and Smurf2 protein expression levels were analyzed in the present study. Similar to anti-HuC and anti-DCAMKL1, anti-PCNA antibody should be validated in the zebrafish tissue. The expected protein size, 29 kDa, was detected in the zebrafish brain while HEK293 and NIH3T3 cell lysates, positive controls, gave slightly higher band, 35 kDa, which is also similar to presented image in the antibody datasheet. Anti-SMURF2 antibody was already validated in the zebrafish brain in the Chapter 3 of the current study (Figure 3.1A) [36]. After antibody validation, each sample was run as cohorts at least 3 times on the gel and blotted with anti-PCNA and anti-SMURF2 as well as anti-β-tubulin (Figure 5.6B).

Figure 5.6 PCNA antibody were validated in zebrafish brain. (A) Antibody validation with positive controls; HEK293 and NIH3T3 protein lysates. (B) Representative Western blots for PCNA and Smurf2 across age and diet groups.

The proliferation marker, PCNA, levels did not alter with age (F(1, 30)=0.808, p=0.376) and diet (F(2, 30)=2.836, p=0.074). Furthermore, there was no interaction effect between age and diet (F(2, 30)=1.699, p=0.200; Figure 5.7A). The expression pattern of PCNA across age and diet was similar to the expression pattern of DCAMKL1 across age and diet (Figure 5.5B) although there was no significant effect on PCNA protein levels. For example, the OF and CR diets in young ages decreased both PCNA and DCAMKL1 protein levels while OF diet increased the levels of PCNA and DCAMKL1 in the advanced age as compared to young. Since the current study focused on the global effects of diet and aging on the brain, the whole brain was analyzed. It may lead to hinder the region-specific alterations in terms of PCNA. However, further region-specific analysis such as protein analysis from microdissected brain regions or immunohistochemical staining will unravel the effects of age and diet on the proliferation and neurogenesis and also the relation between them.

Previous research demonstrated that *smurf2* gene expression increased in the whole brain during aging [39] and also Smurf2 protein expression increased in a region-specific manner in the advanced age [36]. Also, it has been shown that ectopic expression of Smurf2 was enough to induce cellular senescence *in vitro* [31]. Therefore, Smurf2 protein levels were investigated across age and diet (Figure 5.7B); there was no significant main effect of age (F(1, 30)=0.833, p=0.369) and diet (F(2, 30)=2.281, p=0.120). Also, the interaction effect was not statistically significant (F(2, 30)=0.129, p=0.880) in the case of Smurf2 protein levels. Since Smurf2 is not a direct marker of senescence, the further analysis would be done with senescence proteins

and SA-β-gal assay in order to relate the neuronal alteration with senescence mechanism.

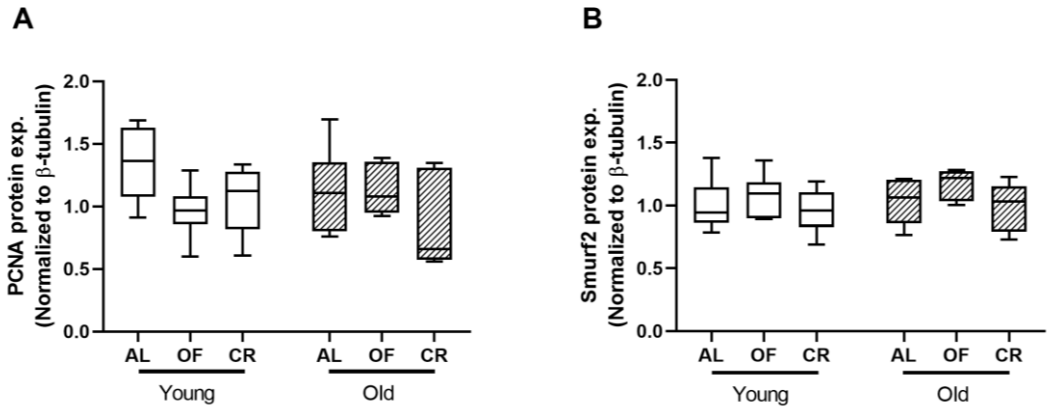

Figure 5.7 Protein expression levels of (A) global proliferation marker, PCNA and (B) senescence-related protein, Smurf2 in terms of age and diet. Tub-normalized values are indicated in (A) and (B).

5.1.4 The neuronal markers, HuC and DCAMKL1, were negatively correlated especially in aged brain while DCAMKL1 and PCNA were highly correlated in both young and aged brain

In order to relate the neuronal markers and proliferation and senescence proteins, correlation analysis was conducted. Independent to age and diet, DCAMKL1 protein levels were negatively correlated with HuC protein levels (r= -0.345, n=36, p=0.039; Figure 5.8). HuC protein is expressed in early-differentiated post-mitotic neurons [150] while DCAMKL1 could be expressed in both mitotic and post-mitotic neurons [151], [152]. Their mostly non-overlapping expression time during neurogenesis could be the reason of negative regulation observed in the

current study. To understand the causative effects behind the negative regulation, further analysis should be performed including immunohistochemistry and coimmunoprecipitation. On the other hand, PCNA proteins label the mitotic neurons [78], [153], [154] and in the present study it was demonstrated that it was highly correlated with DCAMKL1 (r=0.660, n=36, p<0.0005; Figure 5.8). It may imply that the expression of PCNA and DCAMKL1 are correlated and sequentially expressed over time during neurogenesis. Further coexpression/colocalization experiments should be conducted to unravel the exact expression pattern among PCNA, DCAMKL1 and HuC proteins. Also, we tried to understand the role of Smurf2 especially role in senescence in response to aging and non-genetic dietary interventions. However, the dietary interventions did not change the levels of Smurf2 protein (Figure 5.7) and also the correlation analysis has not been shown any relation between Smurf2 and the markers of neurons and proliferation (Figure 5.8).

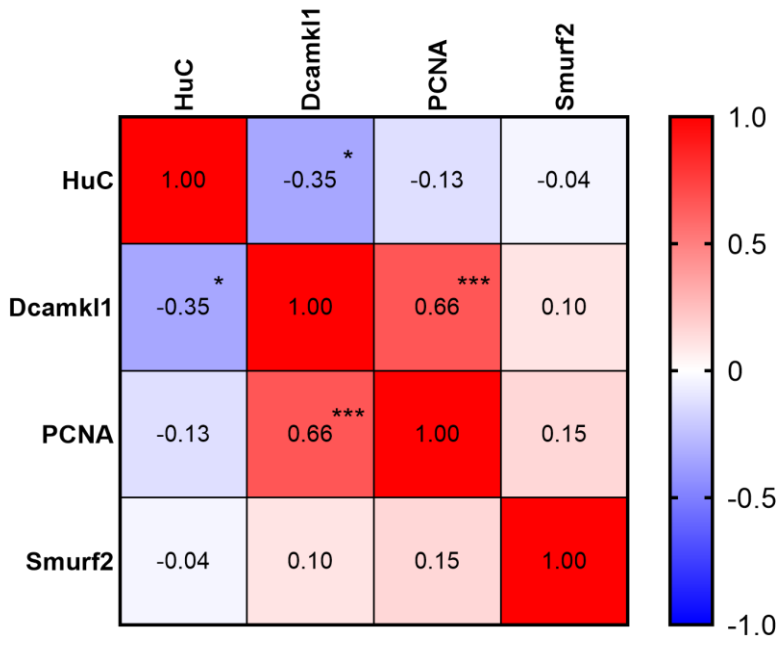

Figure 5.8 Pearson correlation matrix indicated a negative correlation between HuC and DCAMKL1 protein levels and a positive correlation between DCAMKL1 and PCNA protein levels. *: p<0.05, **: p<0.01, ***: p<0.001.

In order to understand the relations among the proteins of interest during aging, the expression levels of young and old were analyzed separately. In both young and old brain, the positive correlation between DCAMKL1 and PCNA was significant (r=0.669, n=18, p=0.002 and r=0.662, n=18, p=0.003, respectively; Figure 5.9). However, the negative correlation between HuC and DCAMKL1 protein levels was not significant (r= -0.257, n=18, p=0.304; Figure 5.9A) in terms of young brain. In the aged brain, the levels of HuC was negatively correlated with DCAMKL1 (r= -0.511, n=18, p=0.030) and also with PCNA (r= -0.473, n=18, p=0.047; Figure 5.9B). Surprisingly, Smurf2 protein levels in the aged brain was positively correlated with DCAMKL1 (r= 0.493, n=18, p=0.037). It may imply that PCNA and DCAMKL1 could be expressed sequentially over time regardless of age. However, the aging

process may affect the dynamics of proliferation and senescence in the neurons; it was evident with the diverse correlation of neuronal markers and PCNA/Smurf2 proteins in the aged brain as compared to young brain (Figure 5.9). This demonstrated that it is essential to perform the immunostaining to colocalize the proteins of interest across lifespan and also create mutant or transgenic model organisms to better understand the aging dynamics of the brain.

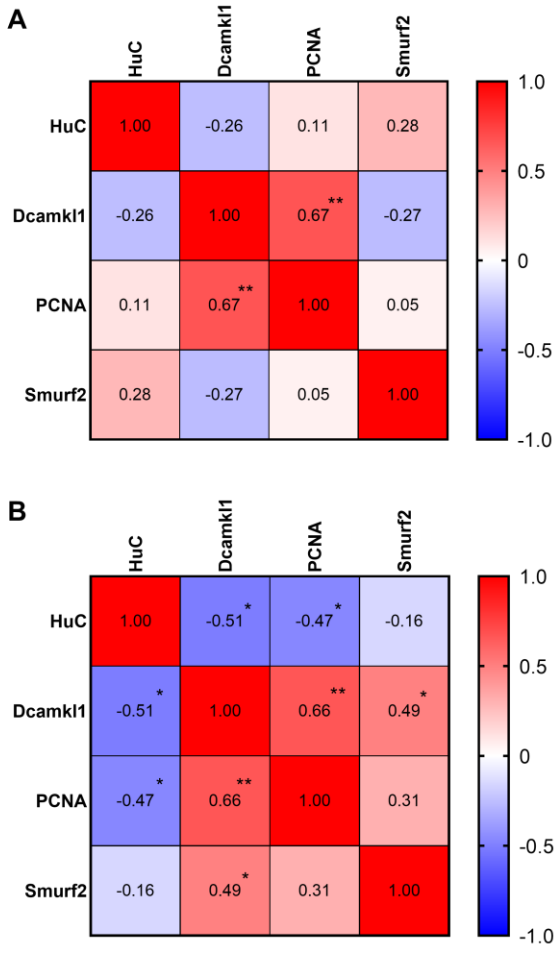

Figure 5.9 Pearson correlation matrices indicated diverse correlations between proteins of interest in (A) young and (B) old brains. *: $p<0.05$, **: $p<0.01$, ***: $p<0.001$.

5.1.5 Age and dietary regimens did not affect the gene expression levels of *smurf2* and interacting partners

One of the aims of the current study was to unravel the effects of non-genetic interventions including OF and CR during aging. Since *smurf2* and its interacting partners altered in a brain region-specific manner during aging (Figure 3.7), we investigated the expression levels of genes of interest in this section across the factor of age and diet. The *smurf2* expression levels did not change significantly with age ($F(1, 30)=0.872$, $p=0.358$) or diet ($F(2, 30)=0.796$, $p=0.460$). Also, the interaction between age and diet was not statistically significant ($F(2, 30)=0.208$, $p=0.813$; Figure 5.10A). Previous studies and our results were shown that *smurf2* expression significantly increased in advanced age in terms of whole brain (Figure 3.7A; [36], [39]). However, the aged fish analyzed in the previous studies [36], [39] was older than the current old OF and CR-fed animals. Possibly, because of the age difference and dietary interventions, the main effect of age was hindered in the case of *smurf2* expression.

On the other hand, *tp53* expression level decreased significantly during aging ($F(1, 30)=16.162$, $p<0.0005$) without a diet effect ($F(2, 30)=0.468$, $p=0.631$) or age by diet interaction effect ($F(2, 30)=1.271$, $p=0.295$). The age effect was evident in CR-fed groups during aging ($p=0.001$; Figure 5.10B) and aged OF fish had lower *tp53* level as compared to young diet-matched group which was marginally significant ($p=0.082$). In consistent with the current result, previous research in mice model demonstrated a significant decrease in the number of tp53 positive cells in CA1 region with respect to high calorie diet [155] and with respect to CR diet [156].

Interestingly, our previous results indicated that neither in the whole brain nor in the specific brain regions, the levels of *tp53* was not changed significantly with age (Figure 3.7; [36]) similar to mice studies which indicated no significant alteration in the *tp53* gene expression levels during aging in the case of whole brain [157] and hippocampus [158]. Thus, it may imply that *tp53* expression in the brain could be more vulnerable against the dietary alterations rather than aging.

In the case of *mdm2* levels, there was not any significant main effect of age or diet ($F(1, 30)=0.889$, $p=0.353$ and $F(2, 30)=1.395$, $p=0.263$, respectively) and age by diet interaction ($F(2, 30)=0.487$, $p=0.619$; Figure 5.10C). Similar to this result, our previous data demonstrated that *mdm2* levels did not change significantly with age in terms of zebrafish whole brain (Figure 3.7D; [36]). Moreover, the recent research with the rodent model revealed that *mdm2* was expressed differentially among adipose tissues in response to high fat diet [159] while the advanced age decreased the mdm2 mRNA and protein levels in hippocampus [158] and both white and brown adipose tissues [160]. This might imply that *mdm2* expression levels are tissue-dependent and even region-dependent because its expression level altered according to the localization of adipose tissue [159] and specific brain regions [36][158].

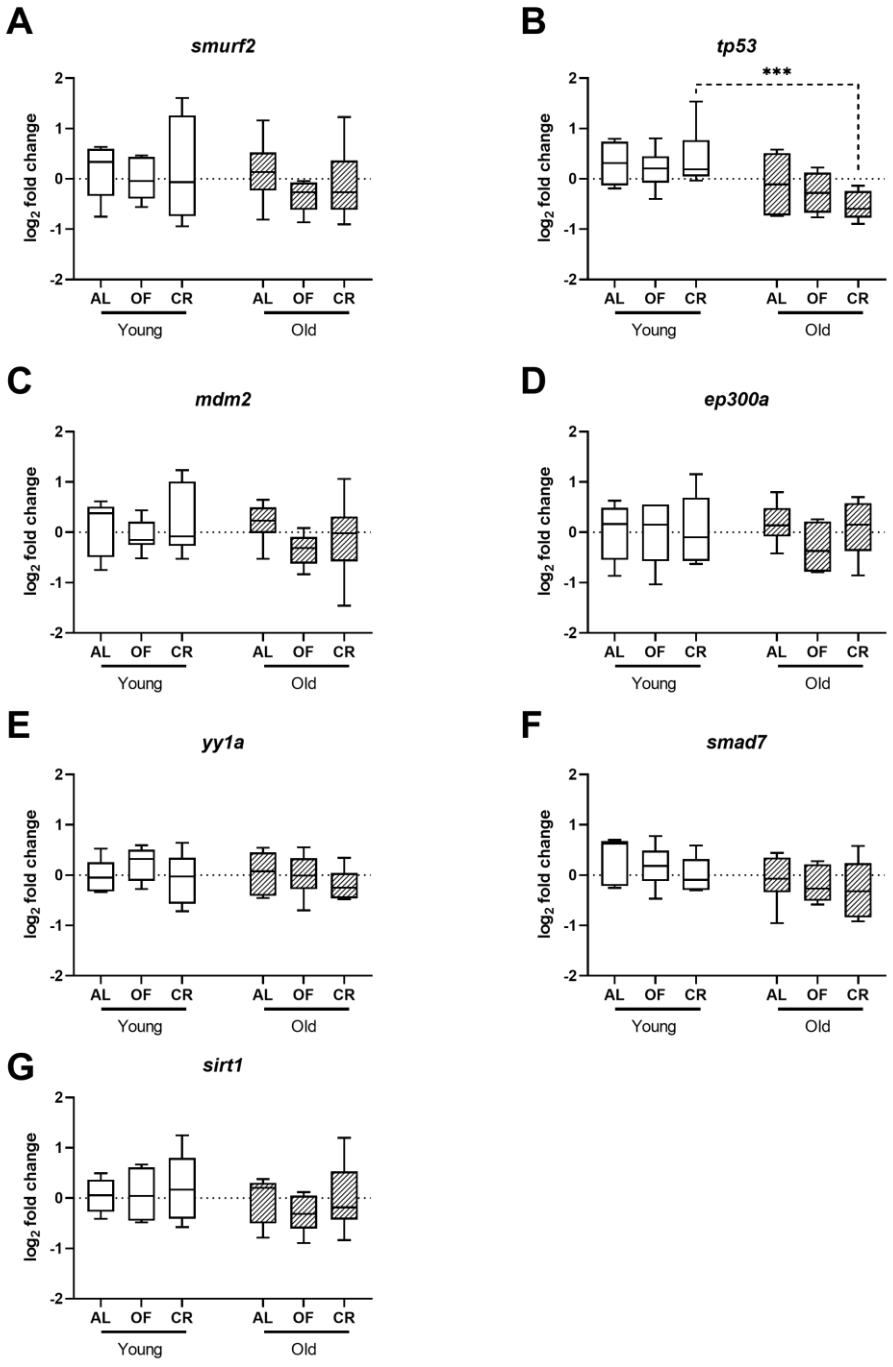

Figure 5.10 The relative gene expression levels of *smurf2* and its interacting partners. (A) *smurf2*, (B) *tp53*, (C) *mdm2*, (D) *ep300a*, (E) *yy1a*, (F) *smad7* and (G) *sirt1* with respect to age and diet. ***: $p<0.001$.

In terms of *ep300a* expression levels, the main effect of age and the main effect of diet were not statistically significant ($F(1, 30)=0.042$, $p=0.839$ and $F(2, 30)=0.742$, $p=0.485$, respectively). Also, the interaction effect was not significant ($F(2, 30)=0.540$, $p=0.589$; Figure 5.10D) in *ep300a* levels. Although a previous research has been shown that EP300 acetyltransferase is a master regulator of genes dysregulated in OF diet in the case of human and zebrafish adipose tissue [52], the present study did not show any alteration with diet in the case of brain *ep300a* levels except a slight decrease in the aged OF group (Figure 5.10D). However, the age effect on the whole brain expression was consistent with our previous result (Figure 3.7E; [36]); the gene expression of *ep300a* was not altered significantly across lifespan in the whole brain homogenates. Since there was a brain region-specific alteration in the level of *ep300a* [36] and the regulatory role in adipose tissue, *ep300a* expression might be tissue- or cell-specific.

Moreover, the gene expression level of *yy1a* was not altered by age or diet ($F(1, 30)=0.591$, $p=0.448$ and $F(2, 30)=1.139$, $p=0.334$, respectively) or age by diet interaction ($F(2, 30)=0.410$, $p=0.668$; Figure 5.10E). The previous analyses with the factor of age and the factor of region indicated no significant alteration in *yy1a* expression levels with respect to age or brain regions (Figure 3.7; [36]). However, a recent study demonstrated that the level of *YY1* mRNA increased in the liver of high fat fed young mice [161]. In the current study, *yy1a* levels of young OF fish was a slightly higher than the levels of young AL in a non-significant manner (Figure 5.10E).

On the other hand, *smad7* gene expression was changed with the factor of age ($F(1, 30)=5.613$, $p=0.024$); the aged brain had less amount of *smad7* transcript. However, there was no main effect of diet ($F(2, 30)=1.088$, $p=0.350$) or interaction effect ($F(2, 30)=0.082$, $p=0.921$; Figure 5.10F) on the levels of *smad7*. Also, pairwise comparisons demonstrated that age effect was not apparent in any diet groups in terms of *smad7*. It was shown previously that the expression level of *smad7* was not age- or brain region-dependent in our recent study (Figure 3.7; [36]). Another recent study revealed that long-term high fat diet downregulate the *smad7* level in mice pancreas [162].

Lastly, in the case of *sirt1* levels, neither main effect of age nor main effect of diet was significant ($F(1, 30)=1.564$, $p=0.221$ and $F(2, 30)=0.565$, $p=0.575$, respectively). Moreover, age by diet interaction was not statistically significant ($F(2, 30)=0.256$, $p=0.776$; Figure 5.10G). There were several studies which represented the gene and protein levels of Sirt1 during aging and in response to dietary regimens because SIRT1, a NAD-dependent deacetylase, regulates the lifespan in accord with the metabolism. It has been shown that in the advanced age, SIRT1 gene and protein expression were decreased in substantia nigra and hippocampus of rodents [26], [163], [164] and in telencephalon region of zebrafish [36]. Also, the high fat diet in mice caused to downregulation of SIRT1 protein levels in hippocampus [24] while CR diet increased *sirt1* gene expression in the prefrontal cortex and hippocampus [25] and SIRT1 protein expression in hippocampus [26]. In the present study, the pattern among old diet groups was similar to previous studies; *sirt1* level was downregulated in OF diet whereas it was upregulated in CR diet but these alterations

were not statistically significant. The age and dietary effect could be underestimated in the whole brain and the region-specific analysis of *sirt1* could be further performed.

5.1.6 The post-translational modifications, ubiquitination, acetylation and deacetylation, controlling genes were in a potential balance during aging

In order to relate the expression levels of genes with each other, Pearson correlation analysis was conducted among the genes of interest. Similar to our previous results (Figure 3.9, Figure 3.12, [36]), the pairwise correlations among *smurf2, mdm2, ep300a* and *sirt1* were observed in this dataset (Figure 5.11). However, the correlation of *tp53* with other genes of interest was changed since *tp53* expression levels could be more prone to the dietary alterations. Moreover, although the genes of interest were correlated differently in young and old brains (Figure 5.12), the correlation among *smurf2, mdm2, ep300a* and *sirt1* were mostly conserved in both young and aged brains. The young and old brains had diverse relations; *yy1a* was correlated with *smurf2, mdm2* and *ep300a* in only young brains (Figure 5.12A). However, *tp53* were related with *mdm2* in only young brain while *tp53* and *smad7* was correlated only in the aged brain (Figure 5.12B). Because of their roles in PTMs, the relation among *smurf2, mdm2, ep300a* and *sirt1* could be conserved to balance between ubiquitination, acetylation and deacetylation during aging.

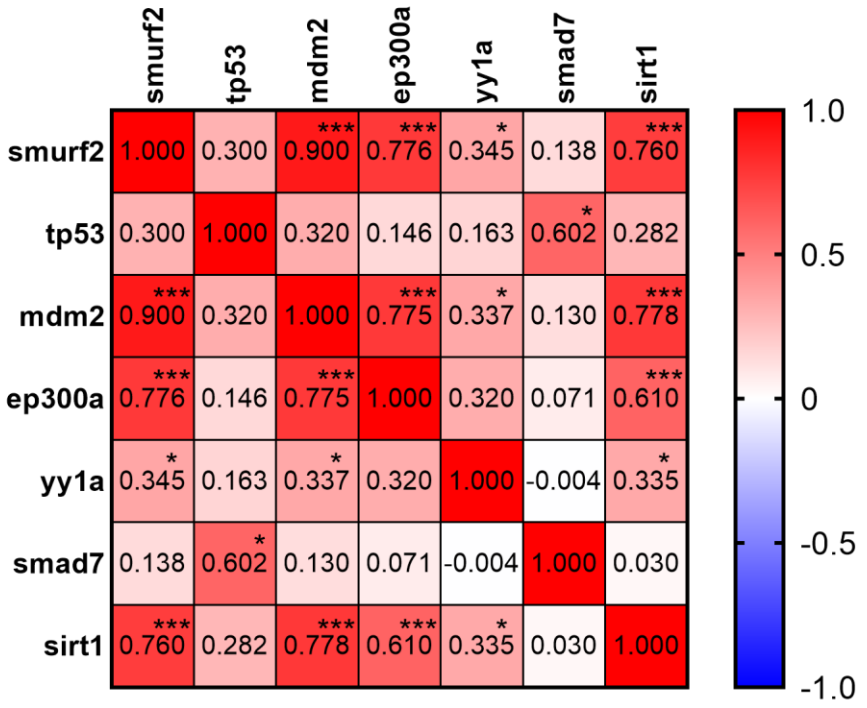

Figure 5.11 Pearson correlation matrix indicated strong correlations among *smurf2, mdm2, ep300a* and *sirt1* expression levels. *: p<0.05, **: p<0.01, ***: p<0.001.

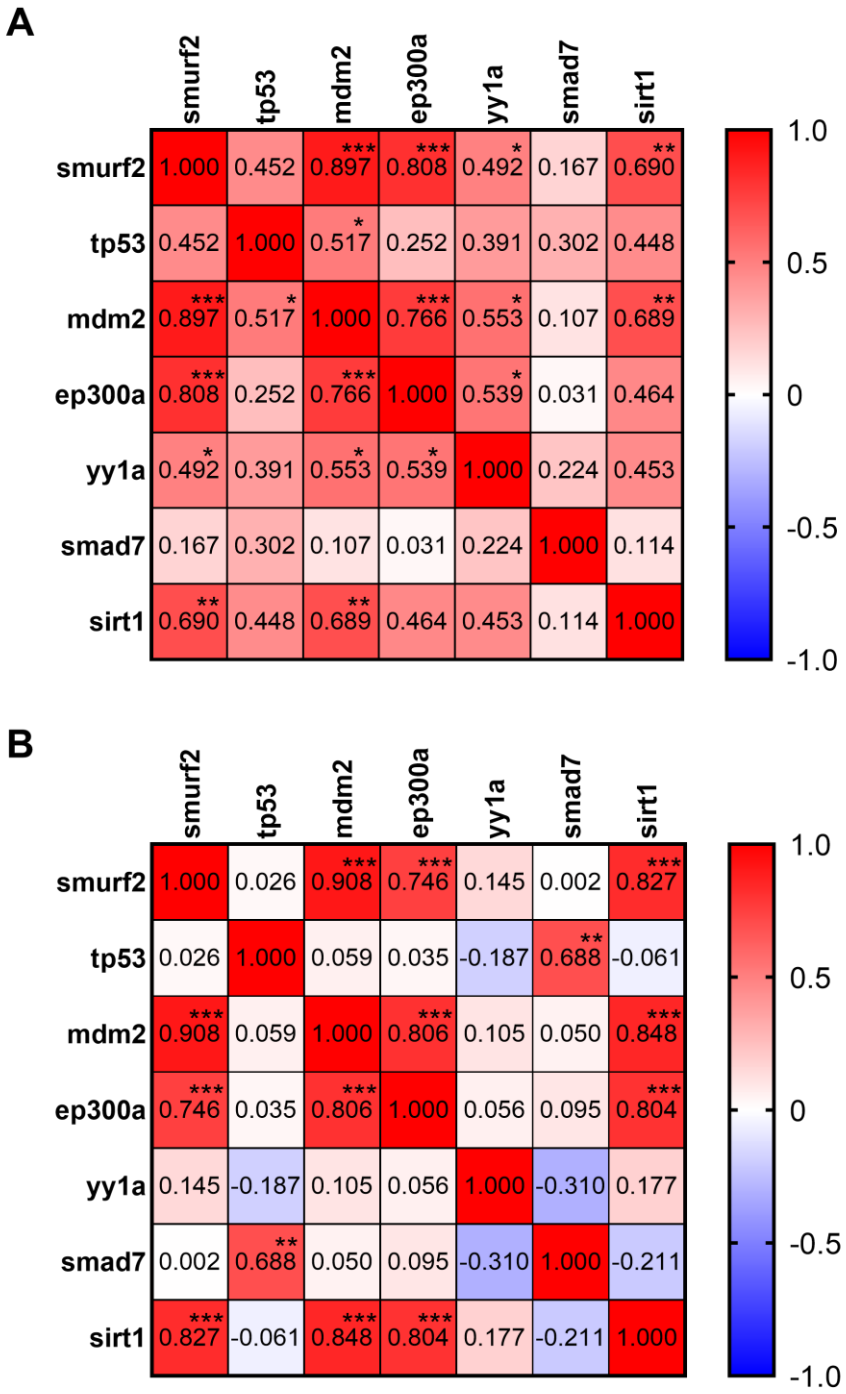

Figure 5.12 Pearson correlation matrices indicated diverse correlations between genes of interest in (A) young and (B) old brains. *: $p<0.05$, **: $p<0.01$, ***: $p<0.001$.

5.1.7 Discussion and Conclusions

This part of the current study aimed to understand the effects of non-genetic dietary interventions during aging on the zebrafish brain in terms of the neuronal proteins and associated proliferation proteins as well as the expression of Smurf2 and its interacting partners. CR diet is a non-genetic intervention which positively affects the lifespan and healthspan in multiple organisms [21], [104], [165]. However, high calorie intake i.e. OF lead to metabolic and cognitive impairments even in young ages [98]–[100]. To our knowledge, the present study is one of research including two opposing dietary regimens, CR and OF in the same experimental conditions during aging analyzed the global protein and gene expression alterations. Our results demonstrated that the body weight and length increased during aging which is expected in the zebrafish model organism since zebrafish continue to grow even in advanced age [79], [92], [146], [147]. Also, both young and old OF groups gained weight and have increased BMI while CR groups had less weight and BMI as compared to age-matched AL fish. The early-differentiated neuronal marker, HuC, decreased with advanced age and this decrease was apparent in the brain of OF and CR-fed fish. On the other hand, DCAMKL1 increased significantly only in OF fish during aging. In order to demonstrate accompanying mechanisms, the global proliferation marker, PCNA, and senescence protein, Smurf2, were analyzed with respect to age and diet. Interestingly, PCNA and Smurf2 protein levels were not altered by age or diet although PCNA levels were highly correlated with DCAMKL1 levels. The gene expression of *smurf2* and its interacting partners were also analyzed; only *tp53* levels decreased in advancing age and especially in the case of CR diet.

Lastly, the correlation among the gene expression levels indicated that the potential balance between the regulatory genes controlling ubiquitination, acetylation and deacetylation could be age and diet dependent in order to maintain the cellular stability.

The body parameters were altered by age and diet in the present study. Firstly, the body weight was analyzed to understand the weight gain or weight loss in response to aging and dietary regimens. Both age and diet affected significantly the body weight. The animal fed with OF tended to have higher body weight as compared to AL-fed fish. In contrast, animals in CR diet lost weight significantly as compared to age-matched AL group which is consistent with previous studies [79], [92]. Moreover, the body length was investigated and the body length increased with advancing age and the dietary regimens lead to the alterations of body length. Previous research has shown that zebrafish can grow even in older ages [146] and thus the body weight and length of aged zebrafish was higher than young animals regardless of diet [79], [92]. However, the study by Arslan-Ergul et al. indicated that 10 week CR diet did not cause significant change in terms of the body length but there was a decreasing trend in CR groups of both young and old fish [79]. Unfortunately, it was not possible to measure the body length of zebrafish without anesthetization and so the body length of each fish was not measured at the beginning of treatment and during 12 weeks diet to prevent the confounding stress and anesthetic effect on the brain. Thus, we could not conclude whether CR diet affect the normal growth of fish. It will be essential to measure the body length at least at the beginning of the study with anesthetization similar to the study by Landgraf et al.

[94] or a camera-equipped system [119], [166] in order to decide body length alteration by CR diet.

The previous studies also utilized the second body parameters, BMI and Fulton K factor, [92]–[94], [148], [149] in order to define the effects of dietary interventions. As expected, in the present study BMI values were altered by age and diet significantly; aged animals tended to have higher BMI values in each diet and there was an opposing trend between OF and CR groups in terms of BMI. A recent study demonstrated that 8 week CR diet decreased BMI value significantly [92] as similar to this study. Another studies indicated that OF fish had significantly higher BMI value than control fed group at the end of 8 week diet [93], [94] and our 12 week diet resembled the same effects on BMI values. Additionally, Fulton K factor changed significantly with dietary regimens; OF increased but CR decreased Fulton K factor. Previous research have shown that after short-term and long-term high fat diet or OF, Fulton K factor increased significantly as compared to normal fat diet or AL, respectively [94], [148], [149]. Also, the study by Ran et al. demonstrated that Fulton K factor of young adult zebrafish fed with CR diet for 8 week was decreased significantly [149]. Moreover, since Landgraf et al. measured the initial body weight and length, they had chance to compare BMI and Fulton K factor at the initiation and at the end of the high fat diet [94]. In order to understand whether the dietary regimens intervene the dynamics of body growth, the initial body parameters should be recorded just before the diet. Also, recent publications has drawn attention to body fat volume ratio could be a better predictor of cognitive impairment than the body parameters [98], [100], [167]. However, in our study we did not examine the adipose

tissues or body fat volume since this study aimed to determine the effects of dietary regimens in the brain aging. Further examination could be done in order to determine the body fat volume ratio and behavioral and cognitive performance in respect to age and diet.

One of the main purposes was to determine the neuronal impacts of aging and dietary interventions. For this aim, the post-mitotic neuronal markers, HuC and DCAMKL1, were analyzed. HuC is known as early-differentiated neuronal marker and can be detected in post-mitotic neurons. It has been shown that HuC positive neuron number declined in the aged zebrafish brain and human brain in a region-specific manner [78], [139]. In concordance with their result [78], [139], HuC protein levels decreased significantly during aging in our study. This age effect was significant especially in OF and CR-fed fish. It may imply that caloric intake has more robust effect than aging in early neuronal differentiation. Immunostaining could be utilized as further steps in order to label HuC positive cells and colocalize with other neuronal markers with respect to age and diet.

On the other hand, in the current study DCAMKL1 protein levels were altered significantly by age and diet interaction; aged OF zebrafish had higher DCAMKL1 expression than young diet-matched animals. Previously published studies conducted with rodent models indicated that DCAMKL1 has persistent expression in adult neuron [152] although this protein is also expressed in immature neuronal cell populations of highly neurogenic regions of the adult brain [168]. So, its balanced expression level is a requirement during neurogenesis [152]. In aged OF zebrafish, this balance may be shifted through upregulation of DCAMKL1 and maybe more

neurogenesis. However, the study by Shu et al. also demonstrated that more DCAMKL1 does not mean more neurogenesis since its ectopic expression leads to a mitotic arrest [152]. It may be interpreted that the negative impacts of high caloric intake may be evident in cell cycle regulation; DCAMKL1 overexpression could suppress the unregulated proliferation through mitotic arrest. In order to unravel this, the cell cycle markers and regulators could be further analyzed.

To understand the effects of age and diet on the global proliferation and senescence, the proliferation marker, PCNA, and the senescence protein, Smurf2 was analyzed. It has been shown that the PCNA, a global proliferation marker, labels the cycling population of neural progenitors [78], [154] and PCNA positive cell number decreased with advancing age in the brain of zebrafish and mouse [78], [134], [135]. However, in our study PCNA protein level was not altered by age and diet. Also, in a recent publication, PCNA levels increased with advancing age however, this age effect was robust in the rapamycin-treated group rather than the AL-fed and CR-fed zebrafish [92]. In the current study, the protein levels was investigated with Western blotting by utilizing whole brain protein lysates, while Jinno et al., Edelmann et al., and Oh et al. [78], [134], [135] utilized the anatomical methods to determine PCNA positive cell number in the brain. Moreover, in the study of Celebi-Birand et al. [92], since the treatment with rapamycin dissolved in dimethyl sulfoxide (DMSO), the AL-fed and CR-fed groups received DMSO in tank water. The anatomical cell counting [78], [134], [135] and the additional component [92] may cause the alterations between our current study and their study. Previously, it has been shown that senescent cells detected with SA-β-gal increases with advancing age [79], [80],

whereas CR diet can prevent the generation of senescent cells [169]. Moreover, it was known that Smurf2 has roles in cellular senescence and its ectopic expression is enough to induce cellular senescence *in vitro* [31]. Recently, it has been demonstrated that *smurf2* gene expression levels increased with advanced age [36], [39] and Smurf2 protein expression increased in the aged zebrafish in a region-specific manner [36]. In the light of these evidences, Smurf2 protein expression was investigated with respect to age and diet. In the current feeding study, the protein level of Smurf2 was not changed in age and diet groups. Similarly, a previous publication revealed that SA-β-gal levels in the brain are not altered by short-term CR diet as compared to age-matched AL animals [79]. In order to unveil the effects of age and diet on the neuronal proliferation or senescence in a comprehensive picture, other proliferation and senescence markers should be further analyzed in the gene and protein levels and also the colocalization of these markers and neuronal markers could be achieved by immunostaining.

Then, in order to relate the neuronal markers with global proliferation and senescence proteins, correlation analysis was conducted. There was overall positive correlation between DCAMKL1 and PCNA which was also conserved in both young and old groups. The possible explanation for this positive correlation can be overlapping temporal expression of PCNA and DCAMKL1 during neurogenesis [152]–[154], [168]. PCNA is expressed in mitotic progenitor cells during whole cell cycle [78], [134], [153], [154]. DCAMKL1 have more diverse and persistent expression in the rodent brain; for example, this protein can be expressed in immature post-mitotic neuronal cells in the neurogenic regions of the adult brain [151], [168],

in mitotic cells [152] and in radial glia cells [168], [170]. Thus, DCAMKL1 levels in whole brain lysates may reflect its protein expression in both neuronal and glial cells. On the other hand, HuC protein levels were negatively related with DCAMKL1 levels independent to age and diet. Nevertheless, this negative regulation was more robust in the aged brain and HuC levels were also negatively correlated with PCNA in the aged brain. This may imply that HuC have non-overlapping expression time with DCAMKL1 and PCNA levels. Moreover, surprisingly the level of Smurf2 protein had a positive correlation with DCAMKL1 in the old brain. In the light of this evidence, it suggests that global proliferation and senescence is dysregulated with advanced age. In order to gain insight into the proliferation and senescence in the context of age and dietary regimens, anatomical analyses will be further conducted and the number of positive cells for each protein of interest or multi-labeled cells with more than one protein of interest will be counted.

In the Chapter 3 of this thesis work, the gene expression of *smurf2* and its interacting partners changed in a region-specific manner (Figure 3.7; [36]). Thus, it could be also beneficial to investigate their expression levels with respect to non-genetic dietary interventions. Interestingly, only *tp53* and *smad7* gene expression levels decreased significantly with advanced age. Previous studies have shown that *smurf2* levels was higher in the aged brain and HSCs [35], [36], [39]. In the current feeding experiment, both gene and protein expression of Smurf2 was not altered by age and diet. The possible reason could be the age differences in aged animals between the current study (23 month old at the time of euthanization) and previous studies (29-35 month old at the time of euthanization, [36], [39]). Since to the best of

our knowledge, this is one of the studies investigated Smurf2 gene and protein levels with respect to different dietary regimens, it was not possible to discuss the dietary pattern but we suggest that the dietary effects may hinder the overall age effect in the whole brain. It should be further analyzed in a region-specific manner with respect to age and diet.

On the other hand, *tp53* expression level decreased significantly during aging with a significant decrease in CR-fed group and a marginally significant decrease in OF-fed zebrafish. In concordance with the current result, previous research conducted with mouse model organism demonstrated a significant decrease in the number of tp53 positive cells in CA1 region with respect to high calorie diet [155] or low calorie, CR diet [156]. However, our previous results indicated that *tp53* levels were not altered with advanced age in the whole brain and specific brain regions [36] similar to mouse studies which indicated no significant alteration in the *tp53* gene expression levels during aging in the brain [157] [158]. Thus, it may imply that *tp53* expression in the brain could be more vulnerable against the dietary alterations rather than aging. Another gene of interest, *mdm2*, whose protein is a negative regulator of tp53 protein [47], was not changed in terms of age and diet in the present work. Our recent publication demonstrated that *mdm2* gene expression level was comparable in the whole brain during aging [36]. However, same study indicated that the level of *mdm2* was altered in a region-specific manner [36]. Also, it was recently shown that *mdm2* gene was expressed differentially among adipose tissues in response to high fat diet [159] while the advanced age decreased the mdm2 mRNA and protein levels in hippocampus [158] and both white and brown adipose tissues [160]. It suggests that

mdm2 expression levels may be a tissue- and brain region-dependent. The further region-specific analysis may give a comprehensive insight into the role of tp53 and mdm2 genes and proteins with respect to dietary regimens. The protein of tp53 is negatively regulated by YY1 via ubiquitin mediated degradation [45]. The levels of *yy1a*, the functional paralogues of human YY1 [57], was not altered by age and diet in the current study. In our recent publication, it has been shown that there was no effect of age and brain regions in the case of *yy1a* expression levels in the zebrafish brain [36]. Another recent study conducted with young mouse model, after short-term high fat diet, YY1 mRNA and protein levels increased in the liver [161]. Moreover, Hakvoort et al. [171] indicated that mouse subjected to 3 days fasting have diverse gene expression profile between brain and four other metabolically active organs, small intestine, kidney, liver and muscle. A set of transcription factors including YY1 may organize the fasting response in four metabolically active organs but not in the brain [171]. Same study concluded that the brain is extremely protected against the fasting [171]. In the light of this evidence, *yy1a* and some other genes of interest have comparable expression levels in terms of brain in order to protect the brain against sudden changes in caloric intake and following alterations in nutrient sensing signaling. The next step should be a multi-organ analysis to unravel the role of metabolically active organs on the protection of brain in response to caloric intake.

In terms of *ep300a* expression levels, there was no effect of age and diet. However, a previous research has been shown that EP300 acetyltransferase is a master regulator of genes dysregulated in OF diet in the case of human and zebrafish adipose tissue and reversed by CR [52]. But, the age at initiation of diet, the dietary

compositions and the duration of diet were different between the study of Nishimura et al. [52] and the present study. On the other hand, our previous result demonstrated that the gene expression levels of *ep300a* was not altered across lifespan in the whole brain but altered in a region-specific manner [36]. Taken all together, *ep300a* expression can be tissue- and brain region-dependent and its expression should be analyzed in multiple organs as well as in specific brain regions.

Although our previous publication indicated no alteration in the levels of *smad7* in both whole brain and specific brain regions [36], the expression level of *smad7* was decreased with age in the current study. However, the overall main effect of age was not robust in any diet groups. A previously published work has shown that *Smad7* mRNA levels are higher in the neurogenic brain regions than the levels in non-neurogenic brain regions since Smad7 regulates the proliferation of neural stem cells in the mouse brain [172], [173]. Hence, the overall decrease with advanced age in our study could be the consequence of less proliferation in the brain during aging. On the other hand, a recent study revealed that long-term high fat diet downregulate the *smad7* expression level in mice pancreas [162]. To learn in detail, the analyses should be extended to the specific brain regions and multiple organs in the zebrafish.

In the present study, the last gene of interest is *sirt1* that regulates lifespan in concert with metabolism [23]. Previous publications has shown that SIRT1 protein levels decrease with aging and cause a subsequent increase in the acetylation of proteins in hippocampus including tp53 [26], [164], [174] while CR diet increases the expression of SIRT1 protein [26], [175]. Also, recent studies showed that high-fat diet in mice leads to downregulation of SIRT1 protein levels in hippocampus whereas

acetylated tp53 protein levels increase because of the inadequate deacetylation via SIRT1 [24], [174]. Last but not least, a study conducted in the brain of juvenile rats demonstrated that the gene expression level of *Sirt1* is higher in both prefrontal cortex and hippocampus than the levels of AL-fed animals while OF diet causes the downregulation of *Sirt1* gene expression in the prefrontal cortex as compared to AL-fed group [25]. Unfortunately, neither aging nor short-term dietary regimens was not influenced the level of *sirt1* in terms of whole brain in the present study. Furthermore, according to our previous experience [36], *sirt1* expression levels was not changed across lifespan in the case of whole brain while its level decreased with aging in the telencephalon. Taken all together, the protein and gene expression levels of Sirt1 could be analyzed in a region-specific manner.

In order to relate the expression levels of genes with each other, Pearson correlation analysis was conducted among the genes of interest. Similar to our previous results [36], the pairwise correlations among *smurf2, mdm2, ep300a* and *sirt1* were observed in this dataset. However, there were differences in terms of the correlation of *tp53* with other genes of interest since *tp53* expression levels could be more prone to the dietary alterations in concordance with its altered gene expression in OF- and CR-fed animals during aging. Moreover, the correlation among *smurf2, mdm2, ep300a* and *sirt1* were mostly conserved in both young and aged brains although the genes of interest were correlated differently during aging for example, *yy1a* was correlated with *smurf2, mdm2* and *ep300a* in only young brains. However, *tp53* were related with *mdm2* in only young brain while *tp53* and *smad7* was correlated only in the aged brain. The age-related alterations could be driven also by

dietary regimens similar to *tp53* expression levels with decreases in aged OF and CR group as compared to their younger counterparts. Because of their roles in diverse PTMs, the relation among *smurf2, mdm2, ep300a* and *sirt1* could be conserved to balance ubiquitination, acetylation and deacetylation during aging. However, this analysis does not enough to understand the causative relationships among gene expression levels in terms of aging and dietary regimens. Their direct interaction and relation should be analyzed with coimmunoprecipitation or colocalization on the brain slices including immunostaining.

In conclusion, in order to understand the effects of non-genetic dietary interventions including high caloric intake i.e. OF and low caloric intake, CR, in the same experimental conditions, both young and old zebrafish were treated with short-term OF and CR diets as well as AL control diet in this part of thesis work. To the best of our knowledge, this current study is one of the first studies to investigate the impacts of opposing caloric intake on the brain in both young and old animals. The present results may be preliminary to unravel the role of high or low caloric intake on the cellular and molecular properties of brain and cognitive abilities. The further analysis on gene and protein expression levels could be necessary to complete the picture of dietary interventions and brain aging.

5.2 The specific inhibitor of HECT E3 ligase, Heclin, altered the expression of *mdm2* and *tp53* in zebrafish embryos

5.2.1 Increasing doses of heclin decreased the survival proportions of embryos

Heclin is a selective inhibitor of HECT-type E3 ligases, Nedd4, Smurf2, and WWP1 [116]. In a recent study, it has been shown that heclin treatment improved short-term memory, consolidation and retrieval [97]. Before treating adult zebrafish with heclin, the dose curve was conducted on zebrafish embryos. The embryos were incubated in one of the different doses of heclin (5 μM, 6.8 μM, 9 μM, 12 μM) or DMSO control (0.2% in E3) or blank (E3) control from 6 hpf to 72 hpf. The doses of heclin was determined according to previous *in vitro* results [116]; heclin inhibited Smurf2 with IC50 values of 6.8 μM and autoubiquitination of the Smurf2 with an IC50 value of 9 μM. One lower (5 μM) and one higher (12 μM) doses were also added in our analysis. The solution was replaced with a fresh solution every day and the dead embryos were removed and recorded for survival analysis. The survival distributions for the interventions were statistically different ($\chi 2(5) = 55.92, p < 0.0001$; Figure 5.13). The survival ratios of embryos for each treatment at 24, 48 and 72 hpf were noted in Table 5.1. Although 6.8 μM and 9 μM doses of heclin can inhibit Smurf2 activity and its ubiquitination, respectively, 45 μM heclin is required to kill 50% of cells *in vitro* [116]. In our embryo treatment, 5 μM and 6.8 μM heclin treatment had similar survival ratios with blank and DMSO controls. With higher doses of 9 μM and 12 μM, the survival ratio was decreased but the highest dose, 12 μM, could not reach the 50% lethality on the embryos. The main aim of this part of

thesis was to evaluate the potential effects of non-genetic inhibition of Smurf2 by heclin, so the downstream genes were investigated in the next section.

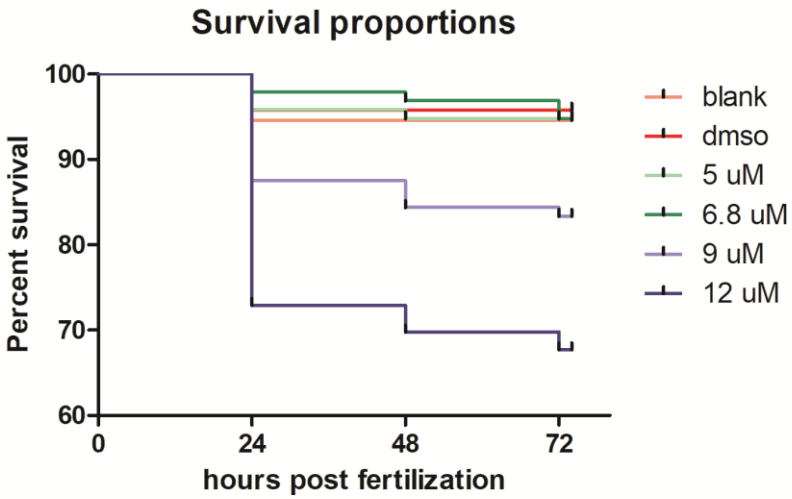

Figure 5.13 Survival analysis indicated that the survival distributions for the interventions were statistically different.

Table 5.1 Survival proportions (%) at the time of 24, 48, and 72 hpf for each treatment solutions. Data expressed as Mean± SEM. hpf: hours post fertilization.

	Blank control	DMSO control	5 µM Heclin	6.8 µM Heclin	9 µM Heclin	12 µM Heclin
24 hpf	94.62 ±2.34%	95.79 ±2.06%	95.83 ±2.04%	97.92 ±1.46%	87.50 ±3.38%	72.92 ±4.54%
48 hpf	94.62 ±2.34%	95.79 ±2.06%	94.79 ±2.27%	96.88 ±1.78%	84.38 ±3.71%	69.79 ±4.69%
72 hpf	94.62 ±2.34%	95.79 ±2.06%	94.79 ±2.27%	94.79 ±2.27%	83.33 ±3.80%	67.71 ±4.77%

5.2.2 Heclin treatment altered the expression of Smurf2 interacting partners, especially in terms of *mdm2*

Since heclin inhibits the activity of HECT E3 ligases *in vitro* [116], it was not expected to see an alteration in the gene expression levels of *smurf2*. The treatment does not changed the *smurf2* expression significantly ($\chi 2(5)=9.440$, $p=0.093$; Figure 5.14A). However, *tp53* gene expression was altered ($\chi 2(5)=12.673$, $p=0.027$; Figure 5.14B). Also, there was a treatment effect in the case of *mdm2* levels ($F(5,18)=12.819$, $p<0.0001$; Figure 5.14C). Pairwise comparisons indicated that 12 μM heclin treated group had differential expression than blank control ($p=0.001$), DMSO control ($p<0.0001$), 5 μM heclin ($p<0.0001$), 6.8 μM heclin ($p=0.001$) and 9 μM heclin ($p=0.001$) treated groups. Heclin does not affect the autoubiquitination of MDM2 *in vitro* [116] however Smurf2 protein enhances the E3 ligase activity of MDM2 which ubiquitinates and degrades tp53 protein [47]. In the depletion of Smurf2 by RNA interference, the *MDM2* and proapoptotic tp53 target gene expression levels increased [47]. Thus, the increase in the embryonic expression of *mdm2* may be the indirect consequence of the inhibition of Smurf2 activity. But heclin treatment did not alter the expression levels of *ep300a* ($F(5,18)=1.092$, $p=0.398$; Figure 5.14D), *yy1a* ($F(5,18)=2.497$, $p=0.069$; Figure 5.14E), and *smad7* ($\chi 2(5)=7.646$, $p=0.177$; Figure 5.14F). Lastly, there was a main effect of treatment in terms of *sirt1* gene expression ($F(5,18)=3.018$, $p=0.038$; Figure 5.14G). This effect was marginally significant between blank control and 12 μM heclin treated embryos ($p=0.067$). In order to gain insight into the senescence and apoptosis mechanism induced by heclin, the gene expression profiles of senescence-

related genes, proapoptotic genes and anti-apoptotic genes could be investigated similar to the study of Nie et al. [47].

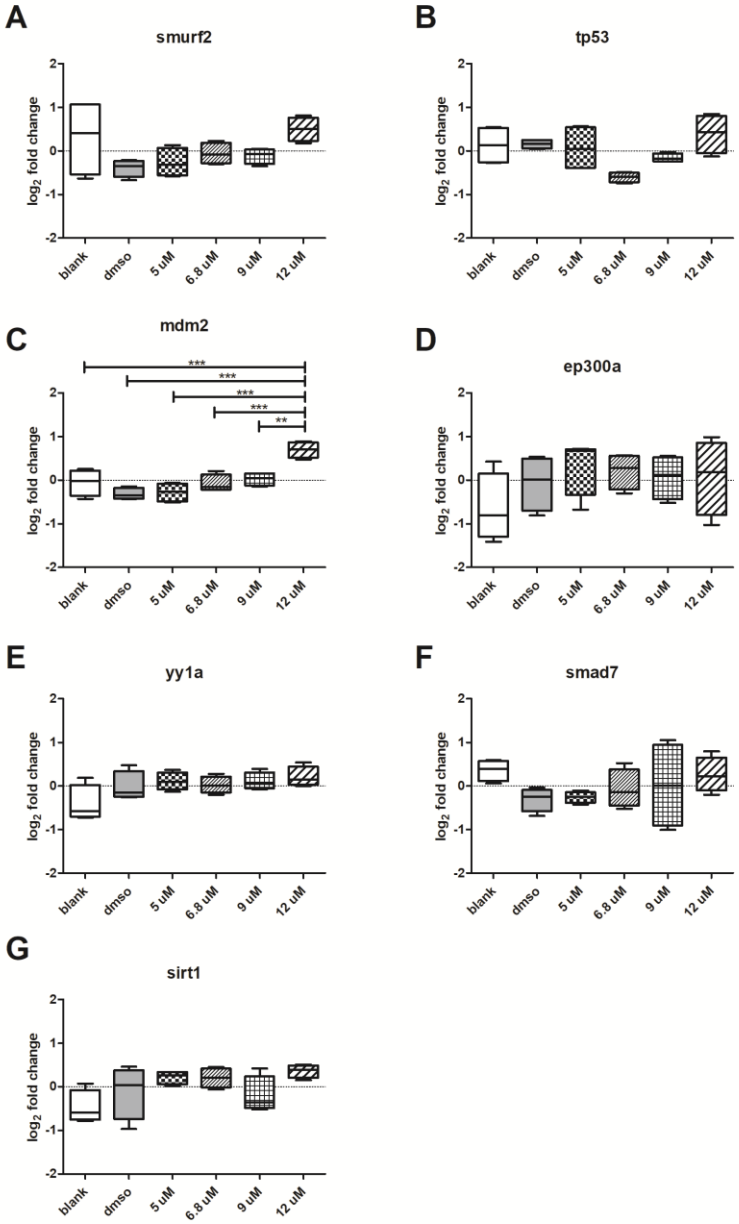

Figure 5.14 The relative gene expression levels of *smurf2* and its interacting partners in whole embryo at 72 hpf after heclin treatment; (A) *smurf2*, (B) *tp53*, (C) *mdm2*, (D) *ep300a*, (E) *yy1a*, (F) *smad7* and (G) *sirt1* . **: p<0.01, ***: p<0.001.

5.2.3 The early-differentiated neuronal marker, HuC, was changed in embryos with respect to the treatment of heclin

According to the results of survival ratios and gene expression profile, 6.8 μM heclin dose was chosen to investigate the neuronal impacts because 12 μM heclin concentration could have some off-target effects to trigger lethality and the alteration in the gene expression levels while 6.8 μM heclin concentration have similar lethality with blank and DMSO controls and the gene expression levels have comparable with other concentrations except *tp53* levels. Previous study conducted with rodent model demonstrated that the inhibiton of HECT E3 ligases in CA1 region of dorsal hippocampus leads to enhancement of short-term memory, consolidation, retrieval and reconsolidation dependent on the administration time of heclin [97]. In order to understand the neuronal and proliferative impacts of HECT ligase inhibition, the embryos were treated with 6.8 μM heclin for 5 days and the embryos were collected at 3 dpf and 5 dpf to isolate proteins. The survival distributions for the interventions (blank control, DMSO control and 6.8 μM heclin) were not statistically different ($\chi 2(2) = 0.6052$, $p = 0.73$; Figure 5.15).

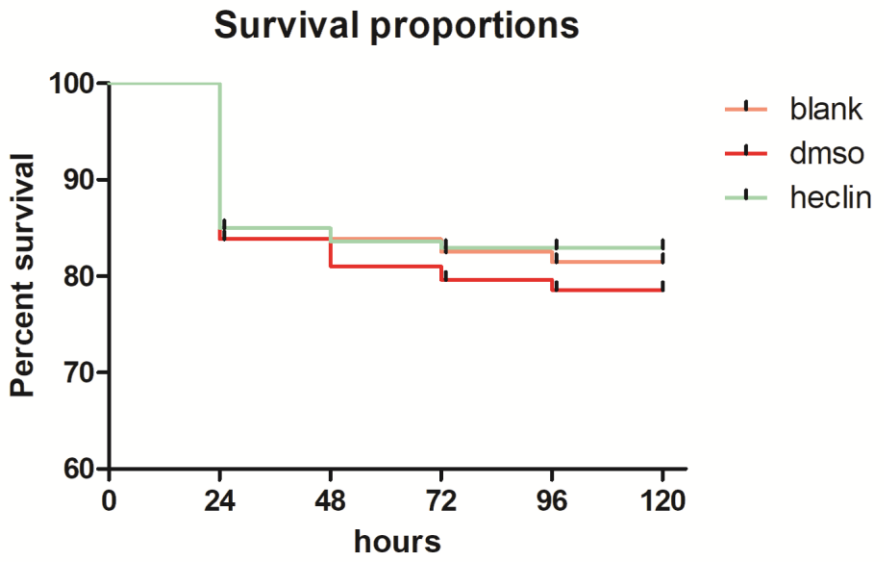

Figure 5.15 Survival analysis indicated that the survival distributions for the interventions for 5 days were not statistically different.

In order to understand the cumulative effect of heclin, the embryos at 3 dpf and 5 dpf were investigated with respect to treatment and time. Similar to gene expression levels of *smurf2*, its protein expression was not altered by heclin treatment ($F(2,12)=0.171$, $p=0.845$; Figure 5.16) because heclin inhibits its activity [116]. Also, there was no main effect of time and an interaction effect between treatment and time ($F(1,12)=4.161$, $p=0.064$ and $F(2,12)=0.145$, $p=0.866$, respectively) in terms of Smurf2 protein levels.

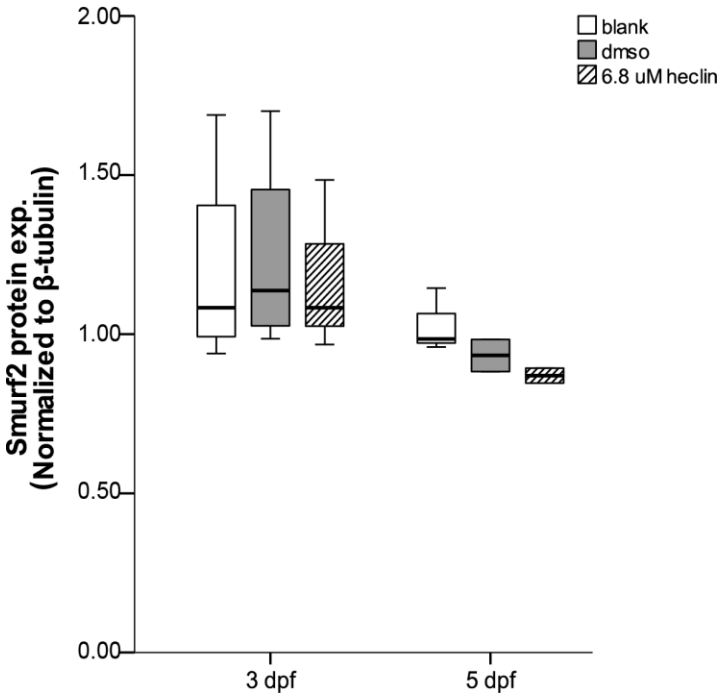

Figure 5.16 Protein expression level of Smurf2 was not altered with respect to heclin treatment and time. Tub-normalized values are indicated.

To unravel the neuronal impact of heclin treatment in the embryos, the early-differentiated neuronal marker, HuC, was analyzed but the treatment did not affect the protein levels of HuC ($F(2,12)=2.532$, $p=0.121$). However, the main effect of time was statistically significant ($F(1,12)=69.073$, $p<0.0001$) with an interaction effect ($F(2,12)=4.882$, $p=0.028$; Figure 5.17A). These were evident between DMSO control and 6.8 μM heclin-treated group ($p=0.012$). Moreover, the protein levels of HuC was significantly higher in 5 dpf embryos than 3 dpf embryos had in the case of blank control ($p=0.003$), DMSO control ($p<0.0001$) and 6.8 μM heclin treatment ($p=0.005$). Interestingly, blank control and DMSO control at 5 dpf was marginally significant ($p=0.066$) with an increased expression in DMSO control. Although DMSO

concentration at the final solution (0.2%) was selected based on a recent paper [176], our result may imply that DMSO concentration also interferes with embryonic development and neuronal proliferation. The other neuronal marker, DCAMKL1 was also investigated and there was a main effect of developmental time ($F(1,12)=66.534$, $p<0.0001$; Figure 5.17B) without a main effect of treatment or an interaction effect ($F(2,12)=0.603$, $p=0.563$ and $F(2,12)=0.426$, $p=0.663$, respectively). The protein levels of DCAMKL1 was significantly lower in 5 dpf embryos than 3 dpf embryos had in the case of blank control ($p<0.0001$), DMSO control ($p=0.001$) and 6.8 μM heclin treatment ($p=0.001$). Similar to DCAMKL1, the protein levels of PCNA was decreased significantly at 5 dpf compared to 3 dpf ($F(1,16)=31.243$, $p<0.0001$; Figure 5.17C) in terms of blank control ($p=0.031$), DMSO control ($p=0.001$) and 6.8 μM heclin treatment ($p=0.005$). There was neither a main effect of treatment nor an interaction effect with respect to PCNA protein levels ($F(2,16)=0.534$, $p=0.596$ and $F(2,16)=0.923$, $p=0.417$, respectively). Taken together, the main effect in the protein levels was the developmental time of embryos rather than the specific inhibitory effect of heclin on Smurf2 protein. Moreover, since DMSO impacts the level of HuC protein, the lower DMSO concentrations but the higher molarity of heclin could be utilized for the next experiments to see drastic effects of Smurf2 inhibition on the neuronal development by investigating same proteins and additional markers.

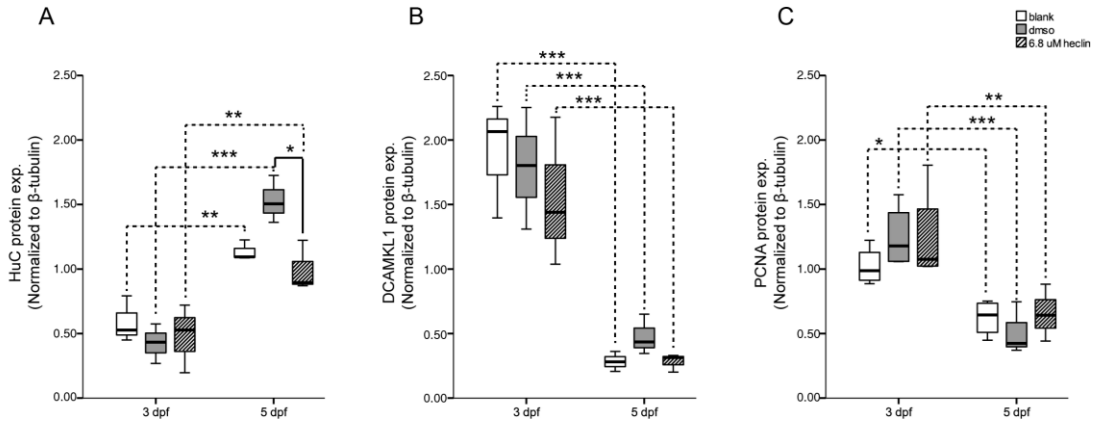

Figure 5.17 Protein expression level of (A) HuC, (B) DCAMKL1 and (C) PCNA was altered with respect to developmental time. Tub-normalized values are indicated. *: $p<0.05$, **: $p<0.01$, ***: $p<0.001$.

5.2.4 Discussion and Conclusions

The main aim of this part was to investigate the impacts of non-genetic drug treatment, which inhibits Smurf2 activity, on the gene expression levels of interacting partners, and the protein levels of neuronal markers and global proliferation marker. Heclin is a reversible selective inhibitor of HECT-type E3 ligases, Nedd4, Smurf2, and WWP1 [97]. Also, a recent study conducted with rat demonstrated that hippocampal injection of heclin leads to improve in short-term memory, consolidation and retrieval [98]. In the current study, firstly heclin treatment was applied to embryos from 6 hpf to 72 hpf and survival ratios were analyzed; increasing heclin dose decrease the survival proportions. Also, the gene expression level of *tp53*, *mdm2*, and *sirt1* was altered by treatment. Since the higher lethality and overall increase in gene expressions in the case of 12 μM heclin concentration, the protein

expression profile experiments were conducted with 6.8 μM heclin-treated embryos as well as control groups. Although there was a significant decrease in heclin-treated group as compared to DMSO control in terms of HuC protein levels, blank control and DMSO control were marginally different. The overall time (developmental) effect was observed in the case of HuC, DCAMKL1 and PCNA protein levels. Since our knowledge on heclin is very limited for now, our preliminary result may give a new perspective about the activity of Smurf2 protein on the neuronal proliferation. In order to gain more insight into the impacts of Smurf2 inhibition, additional neuronal proteins could be analyzed in the embryos with higher concentrations of heclin.

Since it has been shown that HECT E3 ligase inhibition by heclin leads to enhancement in short-term memory in adult rat, after define the dose according to survival analysis and gene expression levels, the neuronal proteins and a global proliferation protein was investigated. Surprisingly, only HuC protein level was altered with heclin treatment compared to DMSO control at 5 dpf while blank control and DMSO control were marginally different. This suggests that DMSO concentration (0.2% v/v) could interfere with neuronal development and heclin treatment may recover its effect on HuC protein level. Moreover, DCAMKL1 and PCNA levels have difference between blank and DMSO control groups whereas heclin treatment, which also included 0.2% (v/v) DMSO in final solution, reverse the protein levels as similar to blank control. To understand the effect of DMSO, it is essential to investigate higher and lower concentrations of DMSO in embryo medium in terms of HuC, DCAMKL1 and PCNA levels.

Our next aim was to perform heclin treatment in the adult zebrafish and observe the effects on adult neurogenesis and aging. In order to achieve this goal, we tried to build an *ex vivo* treatment setup based on recent studies [177], [178] and investigate the levels of genes of interest and neuronal proteins on *ex vivo* treated adult brains. As it has been stated that *ex vivo* drug treatment has several advantages including cost-effectiveness, application to adult brain and last but not least, the direct penetration of drug to the isolated brain due to lack of blood-brain barrier [177], [178]. After the system is set up in our laboratory, this way of treatment will be applied to adult brain of both young and old zebrafish to investigate the neuronal proliferation across lifespan.

CHAPTER 6

OVERALL DISCUSSION AND CONCLUSIONS, AS WELL AS FUTURE PROSPECTIVES

Aging is a normal and natural process that is associated with impairments in cognitive function, including slowing of information processing, declines in memory and cognitive operations [1]. At first, brain aging was thought as a result of neuronal death which disproved in studies conducted with model organisms. It has been shown that the number of neurons in the hippocampus, parahippocampal region and subregions of parahippocampal region does not alter significantly during aging [3], [4]. Rather than the neuronal loss, brain aging is accompanied by specific and relatively subtle synaptic alterations in the hippocampus and prefrontal cortex [5]. Moreover, the neurogenesis occurs in restricted brain regions across lifespan in mammals [7] with a decrease during aging [6], [8]. Moreover, it has been shown that subtle cellular and synaptic alterations have contributions to neurobiological aging [9]–[12]; hence, the molecular and cellular alterations may give more insight into the brain aging process.

The hallmarks of aging are shared features of aging process in different organisms including rodents and zebrafish [13], [14]. These hallmarks are genomic instability, telomere attrition, epigenetic alterations, loss of proteostasis, deregulated nutrient sensing, mitochondrial dysfunction, cellular senescence, stem cell exhaustion, and altered intercellular communication [13]. Several key proteins including *smurf2, tp53, ep300a* and *sirt1* regulate more than one of these hallmarks of

aging [31]–[34], [49]. Taken all together, the investigation of molecular and cellular underpinnings of aging is essential to understand and so prevent the age-related diseases and cognitive decline.

According to previously published studies [35], [39], *smurf2* expression increases with age in brain and bone marrow. Also, its upregulation leads to cellular senescence as a consequence of telomere shortening [31]. Moreover, it has been shown that several E3 ubiquitin ligases have critical roles in neurological disorders for example, Parkinson's disease and Alzheimer's disease [179]–[181]. In the human genome, over 600 genes were identified as E3 ubiquitin ligase coding genes because E3 ligases mediate the substrate specificity and target recognition [182], [183]. 83 of E3 ubiquitin ligase genes were associated with 70 different neurological disorders [180]. For example, mutations in the E3 ligases, LRSAM1, FBXO7 (PARK15), and PARKIN/PARK2 have been identified in Parkinson's disease while mutations in FBXL7, FBXL13 and TTC3 ubiquitin ligases have been associated with Alzheimer's disease [180]. Moreover, E3 ligase Neuralized1 overexpression enhances the memory formation and synaptic plasticity by upregulating the expression of AMPA-type glutamate receptors [179]. Specifically, E3 ligase Smurf2 degrades EZH2 by ubiquitination and thus enhances neuron differentiation after ischemic stroke [184]. As well as the roles of ubiquitin ligases in the neuronal processes, interacting partners of Smurf2 such as tp53, ep300, SIRT1, YY1 have essential roles in central nervous system including synaptic plasticity, learning and memory, and neuroprotection against neurodegenerative diseases [185]–[188]. For example, tau accumulation is under control of several PTMs including ubiquitination by CHIP, acetylation by

ep300 and deacetylation by SIRT1. E3 ligase CHIP polyubiquitinates and degrades phosphorylated tau [189], [190]. However, acetylation of tau by ep300 prevents the degradation of phosphorylated tau [185] similar to the prevention of ubiquitin-mediated degradation of tp53 and smad7 by acetylation [50], [191]. On the other hand, SIRT1-mediated deacetylation of tau allows the ubiquitination and subsequent degradation of phosphorylated tau and prevents tau aggregation which is one of the hallmarks of Alzheimer's disease [185], [188]. Moreover, it has been shown that tp53 levels increase in neurodegenerative diseases (For review, [192]). The network between some of the mentioned proteins, and Smurf2 and its interacting partners were investigated with STRING database and summarized in Figure 6.1 [127]. Although Smurf2 has been well-studied in cancer cells [30], our knowledge about its role in brain aging is very limited. However, it has known that there is a crosstalk between cancer and neurodegenerative diseases [192], [193] similar to cancer and aging have [13]. Cancer is the consequence of the aberrant gain of cellular fitness, i.e., cell survival, while aging and neurodegenerative diseases are characterized with the loss of fitness, cell death [13], [192]. A transcriptomic meta-analyses indicated that the genes upregulated in three neurodegenerative diseases (Alzheimer's disease, Parkinson's disease, and schizophrenia) are significantly overlapped with the downregulated genes in three kinds of cancers (lung, prostate, and colorectal cancer) and vice versa [193]. For example, the p53 pathway is upregulated in cancers, while it is downregulated in neurodegenerative diseases [193]. Importantly, the ubiquitin-proteasome system is downregulated in neurodegenerative diseases whereas it is upregulated in cancers [193]. In the light of these evidences, it is inevitable to investigate Smurf2 and its interacting partners during brain aging.

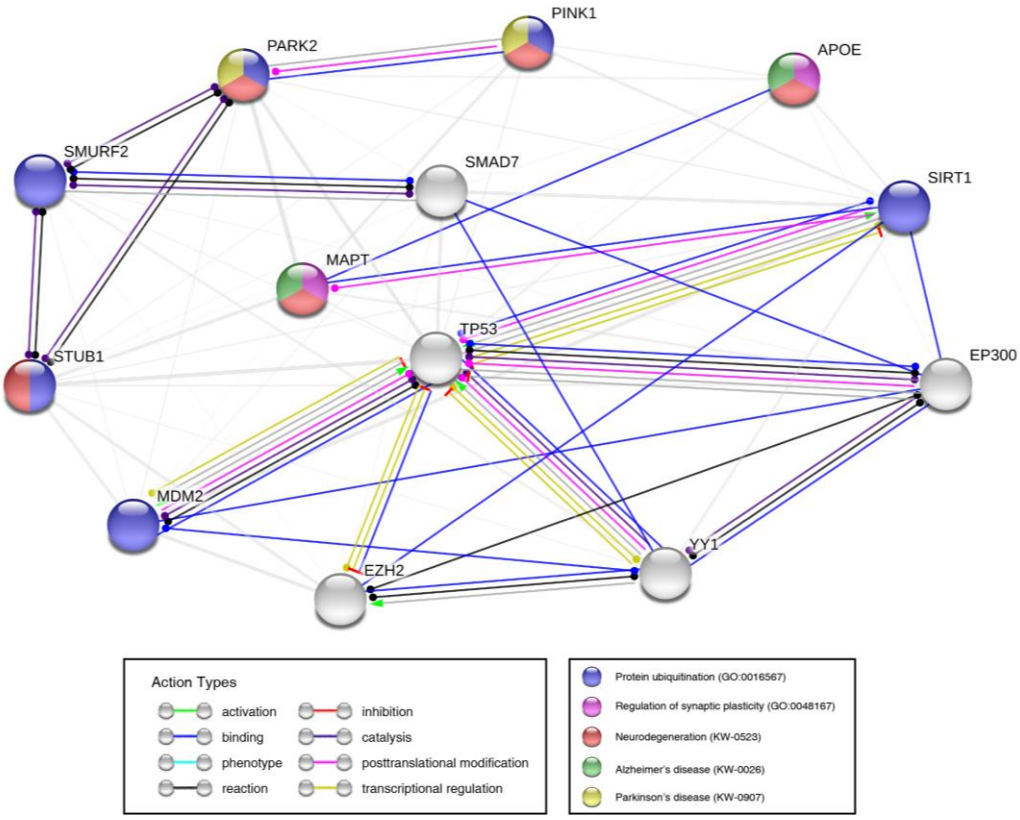

Figure 6.1 STRING analysis of 13 proteins in humans. Nodes represent the proteins and the colors in the nodes represent the specific functional enrichment in the network; blue in node: protein ubiquitination (GO:0016567), purple in node: regulation of synaptic plasticity (GO:0048167), red in node: neurodegeneration (KW-0523), green in node: Alzheimer's disease (KW-0026) and yellow in node: Parkinson's disease (KW-0907). Color lines represent interaction type between nodes; green line: activation, red line: inhibition, blue line: binding, purple line: catalysis, cyan line: phenotype, magenta line: PTM, black line: reaction, yellow line: transcriptional regulation.

The overall aim of this thesis to investigate the alterations in the gene and protein expression level of Smurf2 and its interacting partners with respect to aging, genetic interventions and non-genetic interventions. To the best of our knowledge,

the current study is one of the first studies to investigate Smurf2 gene and protein expression with respect to genetic and non-genetic interventions across lifespan. This overall aim was investigated under three aims; (1) the analysis of the protein and gene expression levels of Smurf2 and its interacting partners during normal brain aging, (2) the investigation of the impacts of genetic interventions on Smurf2, and (3) the examination of non-genetic interventions with respect to Smurf2, its interacting partners and neuronal proteins.

In Chapter 3, Smurf2 protein levels were investigated across lifespan; its expression increased with advanced age in terms of whole brain and specific brain regions, Tel and Ce. Also, its protein was mostly localized in cytosol. Then, Smurf2 and its interacting partners were investigated in terms of gene expression levels. Only *smurf2* gene expression significantly increased in the whole brain however, the brain region-specific analysis demonstrated that *smurf2, mdm2, ep300a* and *sirt1* decreased in the Tel region of aged zebrafish. Interestingly, in spite of the decrease in terms of gene expression in Tel and Ce region, upregulated protein levels were observed in the same regions. These support the idea that Smurf2 accumulated in the aged brain and possibly maintains proteostasis in more vulnerable cognitive regions. In addition, the multivariate analysis demonstrated that *smurf2, mdm2, ep300a,* and *sirt1* were highly correlated and influenced the dataset similarly. This might imply that there is a balance between their proteins with the roles in ubiquitination, acetylation and deacetylation but with advancing age, this balance may disrupt and other regulatory proteins should also take a role to sustain cellular stability. Increasing sample size may improve the results of multivariate analysis, PCA and Pearson correlation. Field

(2015) stated that as a common rule, researchers have at least 10-15 samples per variable in factor analysis while some statisticians argued that 300 is a good sample size [194]. In our analysis, we had a total of 12 animals, 6 young and 6 old, in terms of whole brain whereas a total of 6 fish, 3 young and 3 old, in terms of each brain region. If we would increase the sample size at least in brain region-specific dataset, it may improve our understanding about their relations in specific brain regions and may unravel the age-related contributions of genes of interest. Moreover, since *smurf2*, *mdm2*, *ep300a* and *sirt1* have similar contribution to principal components; their relationship should be investigated in terms of protein expression and protein-protein interaction in order to give a causative meaning of this module conserved in whole brain and Tel. As well, the protein levels of interacting partners and their protein-protein interactions may be further examined in terms of aging.

In Chapter 4, the stable and transient genetic interventions were utilized to upregulate or downregulate the Smurf2 levels. A heat-shock inducible Smurf2 transgenic animal was generated via Tol2 transposase system. The inducible system gives us to overexpress the gene of interest at the desirable time across lifespan rather than the overexpression throughout the life. After we obtain a stable generation, we may induce the overexpression of Smurf2 in the adulthood by heat-shock, especially in the young ages in order to accelerate the aging process and compare them with their age-matched counterparts and older animals. Because of the limitations including time and low frequency of germline transmission, the desired stable transgenic line and potential inducible accelerated aging model could not be generated and tested for the neuronal impacts of Smurf2 overexpression during this

thesis work. In order to increase the frequency of germline transmitted founder fish, new injections can be performed easily with the same vectors which have already generated and found in the laboratory. Moreover, since we have complete Tol2kit, the new constructs could be generated for the different inducible systems or ubiquitous expression throughout the life. For example, to prevent the leakage of *hsp70l* promoter without heat-shock treatment, another heat-shock promoter could be utilized. In a recent publication, HspR promoter, a repression-based system was established to overcome the leaky properties of activation-based heat-shock response system [195]. HspR sequence may be cloned into 5' entry clones with a recombination and then this promoter vector can be merged in a destination vector in order to inject into one-cell stage embryos. Also, autofluorescence signal made difficult to the phenotyping with EGFP signal. It will be corrected with Image Calculator in Fiji ImageJ [196], [197]. Moreover, to overcome the autofluorescence issue during phenotyping, the confocal microscope can be utilized to rather than the stereo microscope. The specific emission filter can block the autofluorescence signal and pass only EGFP signal [198].

Also, same chapter aimed to generate the stable knockout model of Smurf2 by using CRISPR-Cas9 system. Since the knockout of Smurf2 did not cause any phenotypic trait in the embryos or young adults, genotyping methods were necessary to identify the founder fish. Unfortunately, the PCR-based methods could not be optimized until now. After an efficient and reliable method is optimized, new injections will be performed with already prepared gRNA and *cas9* mRNA. Also, rather than the *in vitro* transcribed *cas9* mRNA, Cas9 protein can be co-injected with

gRNAs to increase the efficiency [135]. The generation of Smurf2 knockout could be a beneficial model to study brain aging as well as metabolic aging.

On the other hand, Vivo-morpholino gives an opportunity to knockdown the gene of interest at any time during lifespan. The purpose was the knockdown of Smurf2 expression during adulthood for a short time. Vivo-morpholino solutions were delivered into zebrafish brain via CVMI [90]. The effect of Vivo-morpholino technology is transient that is time- and dose-dependent [90]. The knockdown efficiency was investigated for two different Vivo-morpholinos in the present study. Accordingly, the further analysis will be done at 1 dpi for splice-blocking morpholino but at 1 dpi and/or 2 dpi after the application of translational-blocking morpholino. The future investigations should be performed to observe the neuronal effects of Smurf2 knockdown with Vivo-morpholino.

In Chapter 5, the non-genetic interventions including dietary regimens and inhibitor treatment was employed in order to understand the role of Smurf2 in the brain aging. The OF and CR diet, altered the neuronal markers, HuC and DCAMKL1, without changes in global proliferation protein, PCNA and senescence protein, Smurf2. There was overall positive correlation between DCAMKL1 and PCNA which was also conserved in both young and old groups. On the other hand, HuC protein levels were negatively related with DCAMKL1 levels independent to age and diet. Nevertheless, this negative regulation was more robust in the aged brain and HuC levels were also negatively correlated with PCNA in the aged brain. This may imply that HuC has non-overlapping expression time with DCAMKL1 and PCNA proteins. Moreover, surprisingly the level of Smurf2 protein had a positive

correlation with DCAMKL1 in the old brain. In the light of this evidence, it suggests that global proliferation and senescence is dysregulated with advanced age. Also, gene expression levels of *smurf2* and its partners were not altered significantly except *tp53* expression in the whole brain. However, the correlation among *smurf2, mdm2, ep300a* and *sirt1* were mostly conserved in both young and aged brains as consistent with their relation shown in Chapter 3. This supports our previous implication; there is a balance between the genes regulating ubiquitination, acetylation and deacetylation that is age-dependent in order to maintain the cellular stability.

Lastly, heclin, a specific HECT E3 ligase inhibitor, was utilized to inhibit Smurf2 activity. Before understanding its impacts on adult brain, heclin was applied to embryos. Survival ratios in terms different doses were analyzed; increasing heclin dose decrease the survival proportions. Also, the gene expression level of *tp53*, *mdm2*, and *sirt1* was altered by treatment. The protein expression profile experiments were conducted with 6.8 μM heclin-treated embryos as well as control groups since the higher doses had lower survival ratio. Only HuC protein level was altered with 6.8 μM heclin treatment compared to DMSO control at 5 dpf while blank control and DMSO control were marginally different. This suggests that DMSO concentration (0.2% v/v) could interfere with neuronal development and heclin treatment may recover its effect. To understand the effect of DMSO, it is essential to investigate the higher and lower concentrations of DMSO in embryo medium in terms of HuC, DCAMKL1 and PCNA levels. The next step will be conducted on the adult brain as *ex vivo* treatment in order to observe the potential effects of Smurf2 inhibition on the adult brain and brain aging.

It is inevitable to investigate the protein levels of interacting partners to gain insight into the complete role of Smurf2 during brain aging. Since some publications examined the some of the interacting partners across lifespan or against to non-genetic feeding interventions, their protein levels should be investigated under same conditions with same samples. For example, it will be expected to observe a decrease in terms of Sirt1 protein level in aged brain in a region-specific and maybe gender-specific manner according to previous observations [26], [199], [200]. On the other hand, since the protein level of ep300 decreases in senescent cells [51], there could be a potential decrease in the case of ep300a in the aged brain especially in Tel according to our group's previous observation that senescent cell number increased in aged brain Tel [79]. Since tp53 protein has a short half-life and its activity is tightly regulated by several PTMs [45], [47], [201], its protein expression also may be stable during aging. However, tp53 protein levels increases in hippocampus [158] and in astrocyte cells derived from aged individuals [202]. Thus, the protein levels of tp53 should be investigated in a region-specific and brain cell-specific manner. However, MDM2 protein level decreases slightly in hippocampus in the aged mouse [158]. Furthermore, it was shown that dysregulation in the MDM2-tp53 balance leads to premature aging [43], [49]. YY1 regulates the genes associated with neurodegenerative diseases according to a transcriptional meta-analysis [55] and it is a part of the repressor complex with SIRT1 to suppress microRNA-134 and regulate synaptic plasticity and memory formation [56]. Moreover, YY1 could be a critical mediator in neuronal plasticity by regulating transcription of genes in mature neurons in hippocampus [203], [204]. According to previous literature, we can expect slight alterations in terms of Mdm2 and Yy1a protein levels during brain aging in a region-

specific manner but other consequences of aging could be the changes in their activity and interactions with other proteins including tp53 and Smurf2. In the light of these evidences, the further experiments on proteins of interest including Western blotting, immunohistochemistry, and co-immunoprecipitation, are important to gain a comprehensive picture about brain aging.

Finally, in order to unveil therapeutic implications of Smurf2 expression during aging, the overexpression model could be inevitable because it may show the potency of this protein. In order to rescue potential detrimental effect of Smurf2 in the overexpression model as well as aged WT brain, we could apply some drugs including HECT inhibitor, heclin, proteasome inhibitors such as MG132 [205] or senolytics that decrease the accumulation of senescent cells [111]. To observe the consequences of overexpression of Smurf2 and drug treatment, further experiments may performed in terms of gene and protein expression for example, qRT-PCR, immunohistochemistry, co-immunoprecipitation, Western blotting and SA-β-gal.

In conclusion, in the present thesis it was shown that Smurf2 protein levels increased during aging. Its gene expression and interacting partners' expression were also altered in a region-dependent manner. Also, the stable and transient genetic methods were utilized to alter Smurf2 expression and see its role during aging. Lastly, dietary regimens were altered the levels of neuronal proteins and *tp53* gene expression without change in terms of Smurf2 gene and protein levels. To the best of our knowledge, this study is one of the first studies to investigate the levels of Smurf2 during aging and in response to genetic and non-genetic interventions. The future investigations should be conducted to gain a complete insight into Smurf2 impacts

across lifespan. It could be a promising target to delay the brain aging process and the onset of age-related cognitive decline.

BIBLIOGRAPHY

[1] N. Raz, “Cognitive Aging,” in *Encyclopedia of the Human Brain*, vol. 1, Elsevier, 2002, pp. 829–838.

[2] H. Sontheimer, “Aging, Dementia, and Alzheimer Disease,” in *Diseases of the Nervous System*, Elsevier, 2015, pp. 99–131.

[3] P. R. Rapp and M. Gallagher, “Preserved neuron number in the hippocampus of aged rats with spatial learning deficits.,” *Proc. Natl. Acad. Sci.*, vol. 93, no. 18, pp. 9926–9930, Sep. 1996.

[4] P. R. Rapp, P. S. Deroche, Y. Mao, and R. D. Burwell, “Neuron Number in the Parahippocampal Region is Preserved in Aged Rats with Spatial Learning Deficits,” *Cereb. Cortex*, vol. 12, no. 11, pp. 1171–1179, Nov. 2002.

[5] J. H. Morrison and M. G. Baxter, “The ageing cortical synapse: hallmarks and implications for cognitive decline,” *Nat. Rev. Neurosci.*, vol. 13, no. 4, pp. 240–250, 2012.

[6] O. Lazarov, M. P. Mattson, D. A. Peterson, S. W. Pimplikar, and H. van Praag, “When neurogenesis encounters aging and disease,” *Trends Neurosci.*, vol. 33, no. 12, pp. 569–579, 2010.

[7] G. Ming and H. Song, “Adult Neurogenesis in the Mammalian Brain: Significant Answers and Significant Questions,” *Neuron*, vol. 70, no. 4, pp. 687–702, May 2011.

[8] K. L. Spalding *et al.*, “Dynamics of Hippocampal Neurogenesis in Adult Humans,” *Cell*, vol. 153, no. 6, pp. 1219–1227, Jun. 2013.

[9] O. Ganeshina, R. W. Berry, R. S. Petralia, D. A. Nicholson, and Y. Geinisman, “Differences in the expression of AMPA and NMDA receptors between axospinous perforated and nonperforated synapses are related to the configuration and size of postsynaptic densities,” *J. Comp. Neurol.*, vol. 468, no. 1, pp. 86–95, Jan. 2004.

[10] M. M. Adams *et al.*, “Caloric restriction and age affect synaptic proteins in hippocampal CA3 and spatial learning ability,” *Exp. Neurol.*, vol. 211, no. 1, pp. 141–149, May 2008.

[11] H. D. VanGuilder *et al.*, “Hippocampal dysregulation of synaptic plasticity-associated proteins with age-related cognitive decline,” *Neurobiol. Dis.*, vol. 43, no. 1, pp. 201–212, Jul. 2011.

[12] H. D. VanGuilder, H. Yan, J. A. Farley, W. E. Sonntag, and W. M. Freeman, “Aging alters the expression of neurotransmission-regulating proteins in the hippocampal synaptoproteome,” *J. Neurochem.*, vol. 113, no. 6, p. no-no, Mar. 2010.

[13] C. López-Otín, M. A. Blasco, L. Partridge, M. Serrano, and G. Kroemer, “The Hallmarks of Aging,” *Cell*, vol. 153, no. 6, pp. 1194–1217, Jun. 2013.

[14] J. Van houcke, L. De Groef, E. Dekeyster, and L. Moons, “The zebrafish as a gerontology model in nervous system aging, disease, and repair,” *Ageing Res.*

Rev., vol. 24, pp. 358–368, 2015.

[15] C. J. Lord and A. Ashworth, "The DNA damage response and cancer therapy," *Nature*, vol. 481, no. 7381, pp. 287–294, Jan. 2012.

[16] C. R. Burtner and B. K. Kennedy, "Progeria syndromes and ageing: what is the connection?," *Nat. Rev. Mol. Cell Biol.*, vol. 11, no. 8, pp. 567–578, 2010.

[17] M. Z. Levy, R. C. Allsopp, A. B. Futcher, C. W. Greider, and C. B. Harley, "Telomere end-replication problem and cell aging," *J. Mol. Biol.*, vol. 225, no. 4, pp. 951–960, 1992.

[18] Q. Ain *et al.*, "Cell cycle-dependent and -independent telomere shortening accompanies murine brain aging," *Aging (Albany. NY).*, vol. 10, no. 11, pp. 3397–3420, Nov. 2018.

[19] E. T. Powers, R. I. Morimoto, A. Dillin, J. W. Kelly, and W. E. Balch, "Biological and chemical approaches to diseases of proteostasis deficiency.," *Annu. Rev. Biochem.*, vol. 78, no. August, pp. 959–991, 2009.

[20] H. Koga, S. Kaushik, and A. M. Cuervo, "Protein homeostasis and aging: The importance of exquisite quality control," *Ageing Res. Rev.*, vol. 10, no. 2, pp. 205–215, 2011.

[21] L. Fontana, L. Partridge, and V. D. Longo, "Extending Healthy Life Span--From Yeast to Humans," *Science (80-.).*, vol. 328, no. 5976, pp. 321–326, Apr. 2010.

[22] N. Barzilai, D. M. Huffman, R. H. Muzumdar, and A. Bartke, "The critical

role of metabolic pathways in aging," *Diabetes,* vol. 61, no. 6, pp. 1315–1322, 2012.

[23] L. Guarente, "Sirtuins in Aging and Disease," *Cold Spring Harb. Symp. Quant. Biol.*, vol. 72, no. 1, pp. 483–488, Jan. 2007.

[24] Z. Zhao, M. Yao, L. Wei, and S. Ge, "Obesity caused by a high-fat diet regulates the Sirt1/PGC-1α/FNDC5/BDNF pathway to exacerbate isoflurane-induced postoperative cognitive dysfunction in older mice," *Nutr. Neurosci.*, vol. 0, no. 0, pp. 1–12, 2019.

[25] R. Mychasiuk, H. Hehar, I. Ma, and M. J. Esser, "Dietary intake alters behavioral recovery and gene expression profiles in the brain of juvenile rats that have experienced a concussion," *Front. Behav. Neurosci.*, vol. 9, no. FEB, pp. 1–17, 2015.

[26] A. Quintas, A. J. de Solís, F. J. Díez-Guerra, J. M. Carrascosa, and E. Bogónez, "Age-associated decrease of SIRT1 expression in rat hippocampus: prevention by late onset caloric restriction.," *Exp. Gerontol.*, vol. 47, no. 2, pp. 198–201, Feb. 2012.

[27] J. Campisi and F. d'Adda di Fagagna, "Cellular senescence: when bad things happen to good cells," *Nat. Rev. Mol. Cell Biol.*, vol. 8, no. 9, pp. 729–740, Sep. 2007.

[28] J. Krishnamurthy *et al.*, "Ink4a/Arf expression is a biomarker of aging," *J. Clin. Invest.*, vol. 114, no. 9, pp. 1299–1307, Nov. 2004.

[29] G. P. Dimri *et al.*, “A biomarker that identifies senescent human cells in culture and in aging skin in vivo.,” *Proc. Natl. Acad. Sci.*, vol. 92, no. 20, pp. 9363–9367, Sep. 1995.

[30] D. David, S. A. Nair, and M. R. Pillai, “Smurf E3 ubiquitin ligases at the cross roads of oncogenesis and tumor suppression,” *Biochim. Biophys. Acta - Rev. Cancer*, vol. 1835, no. 1, pp. 119–128, Jan. 2013.

[31] H. Zhang and S. N. Cohen, “Smurf2 up-regulation activates telomere-dependent senescence,” *Genes Dev.*, vol. 18, no. 24, pp. 3028–3040, Dec. 2004.

[32] Y. Kong, H. Cui, and H. Zhang, “Smurf2-mediated ubiquitination and degradation of Id1 regulates p16 expression during senescence,” *Aging Cell*, vol. 10, no. 6, pp. 1038–1046, Dec. 2011.

[33] C. Ramkumar *et al.*, “Smurf2 Regulates the Senescence Response and Suppresses Tumorigenesis in Mice,” *Cancer Res.*, vol. 72, no. 11, pp. 2714–2719, Jun. 2012.

[34] M. Blank, Y. Tang, M. Yamashita, S. S. Burkett, S. Y. Cheng, and Y. E. Zhang, “A tumor suppressor function of Smurf2 associated with controlling chromatin landscape and genome stability through RNF20,” *Nat. Med.*, vol. 18, no. 2, pp. 227–234, Feb. 2012.

[35] C. Ramkumar, Y. Kong, S. E. Trabucco, R. M. Gerstein, and H. Zhang, “Smurf2 regulates hematopoietic stem cell self-renewal and aging,” *Aging*

Cell, vol. 13, no. 3, pp. 478–486, 2014.

[36] M. U. Tuz-Sasik, E. T. Karoglu-Eravsar, M. Kinali, A. Arslan-Ergul, and M. M. Adams, "Expression Levels of SMAD Specific E3 Ubiquitin Protein Ligase 2 (Smurf2) and its Interacting Partners Show Region-specific Alterations During Brain Aging," *Neuroscience*, vol. 436, pp. 46–73, Jun. 2020.

[37] C. Chen and L. E. Matesic, "The Nedd4-like family of E3 ubiquitin ligases and cancer," *Cancer Metastasis Rev.*, vol. 26, no. 3–4, pp. 587–604, Dec. 2007.

[38] Y. Zhang, C. Chang, D. J. Gehling, A. Hemmati-Brivanlou, and R. Derynck, "Regulation of Smad degradation and activity by Smurf2, an E3 ubiquitin ligase," *Proc. Natl. Acad. Sci.*, vol. 98, no. 3, pp. 974–979, Jan. 2001.

[39] A. Arslan-Ergul and M. M. Adams, "Gene expression changes in aging Zebrafish (Danio rerio) brains are sexually dimorphic," *BMC Neurosci.*, vol. 15, no. 1, p. 29, Dec. 2014.

[40] D. P. Lane, "p53, guardian of the genome," *Nature*. 1992.

[41] C. L. Brooks and W. Gu, "Ubiquitination, phosphorylation and acetylation: The molecular basis for p53 regulation," *Curr. Opin. Cell Biol.*, vol. 15, no. 2, pp. 164–171, 2003.

[42] M. Li, J. Luo, C. L. Brooks, and W. Gu, "Acetylation of p53 Inhibits Its Ubiquitination by Mdm2," *J. Biol. Chem.*, vol. 277, no. 52, pp. 50607–50611, Dec. 2002.

[43] D. Lessel *et al.*, "Dysfunction of the MDM2/p53 axis is linked to premature

aging," *J. Clin. Invest.*, vol. 127, no. 10, pp. 3598–3608, Aug. 2017.

[44] E. Grönroos, A. A. Terentiev, T. Punga, and J. Ericsson, "YY1 inhibits the activation of the p53 tumor suppressor in response to genotoxic stress," *Proc. Natl. Acad. Sci.*, vol. 101, no. 33, pp. 12165–12170, 2004.

[45] G. Sui *et al.*, "Yin Yang 1 Is a Negative Regulator of p53," *Cell*, vol. 117, no. 7, pp. 859–872, Jun. 2004.

[46] H. M. Jeong, S. H. Lee, J. Yum, C.-Y. Yeo, and K. Y. Lee, "Smurf2 regulates the degradation of YY1," *Biochim. Biophys. Acta - Mol. Cell Res.*, vol. 1843, no. 9, pp. 2005–2011, Sep. 2014.

[47] J. Nie *et al.*, "Smad Ubiquitylation Regulatory Factor 1/2 (Smurf1/2) Promotes p53 Degradation by Stabilizing the E3 Ligase MDM2," *J. Biol. Chem.*, vol. 285, no. 30, pp. 22818–22830, Jul. 2010.

[48] A. Ito *et al.*, "p300/CBP-mediated p53 acetylation is commonly induced by p53-activating agents and inhibited by MDM2," *EMBO J.*, vol. 20, no. 6, pp. 1331–1340, 2001.

[49] D. Wu and C. Prives, "Relevance of the p53–MDM2 axis to aging," *Cell Death Differ.*, vol. 25, no. 1, pp. 169–179, 2018.

[50] E. Grönroos, U. Hellman, C.-H. Heldin, and J. Ericsson, "Control of Smad7 Stability by Competition between Acetylation and Ubiquitination," *Mol. Cell*, vol. 10, no. 3, pp. 483–493, Sep. 2002.

[51] P. Sen *et al.*, "Histone Acetyltransferase p300 Induces De Novo Super-

Enhancers to Drive Cellular Senescence," *Mol. Cell*, vol. 73, no. 4, pp. 684-698.e8, Feb. 2019.

[52] Y. Nishimura *et al.*, "Systems pharmacology of adiposity reveals inhibition of EP300 as a common therapeutic mechanism of caloric restriction and resveratrol for obesity," *Front. Pharmacol.*, vol. 6, no. SEP, pp. 1–13, 2015.

[53] S. M. K. Glasauer and S. C. F. Neuhauss, "Whole-genome duplication in teleost fishes and its evolutionary consequences," *Mol. Genet. Genomics*, vol. 289, no. 6, pp. 1045–1060, 2014.

[54] A. Babu *et al.*, "Chemical and genetic rescue of an ep300 knockdown model for Rubinstein Taybi Syndrome in zebrafish," *Biochim. Biophys. Acta - Mol. Basis Dis.*, vol. 1864, no. 4, pp. 1203–1215, Apr. 2018.

[55] M. D. Li, T. C. Burns, A. A. Morgan, and P. Khatri, "Integrated multi-cohort transcriptional meta-analysis of neurodegenerative diseases," *Acta Neuropathol. Commun.*, vol. 2, no. 1, p. 93, Dec. 2014.

[56] J. Gao *et al.*, "A novel pathway regulates memory and plasticity via SIRT1 and miR-134," *Nature*, vol. 466, no. 7310, pp. 1105–1109, Aug. 2010.

[57] W.-L. Shiu, K.-R. Huang, J.-C. Hung, J.-L. Wu, and J.-R. Hong, "Knockdown of zebrafish YY1a can downregulate the phosphatidylserine (PS) receptor expression, leading to induce the abnormal brain and heart development," *J. Biomed. Sci.*, vol. 23, no. 1, p. 31, Dec. 2016.

[58] X. Yan, Z. Liu, and Y. Chen, "Regulation of TGF-β signaling by Smad7," *Acta*

Biochim. Biophys. Sin. (Shanghai)., vol. 41, no. 4, pp. 263–272, Apr. 2009.

[59] P. Kavsak *et al.*, "Smad7 Binds to Smurf2 to Form an E3 Ubiquitin Ligase that Targets the TGFβ Receptor for Degradation," *Mol. Cell*, vol. 6, no. 6, pp. 1365–1375, Dec. 2000.

[60] M. Simonsson, C. H. Heldin, J. Ericsson, and E. Grönroos, "The balance between acetylation and deacetylation controls Smad7 stability," *J. Biol. Chem.*, vol. 280, no. 23, pp. 21797–21803, 2005.

[61] Y. Yuan, V. F. Cruzat, P. Newshome, J. Cheng, Y. Chen, and Y. Lu, "Regulation of SIRT1 in aging: Roles in mitochondrial function and biogenesis," *Mechanisms of Ageing and Development*, vol. 155. Elsevier, pp. 10–21, 01-Apr-2016.

[62] H. Vaziri *et al.*, "hSIR2SIRT1 Functions as an NAD-Dependent p53 Deacetylase," *Cell*, vol. 107, no. 2, pp. 149–159, Oct. 2001.

[63] J. M. Solomon *et al.*, "Inhibition of SIRT1 Catalytic Activity Increases p53 Acetylation but Does Not Alter Cell Survival following DNA Damage," *Mol. Cell. Biol.*, vol. 26, no. 1, pp. 28–38, Jan. 2006.

[64] G. S. Gerhard, "Comparative aspects of zebrafish (Danio rerio) as a model for aging research," *Exp. Gerontol.*, vol. 38, no. 11–12, pp. 1333–1341, Nov. 2003.

[65] S. Kishi, J. Uchiyama, A. M. Baughman, T. Goto, M. C. Lin, and S. B. Tsai, "The zebrafish as a vertebrate model of functional aging and very gradual

senescence," *Exp. Gerontol.*, vol. 38, no. 7, pp. 777–786, 2003.

[66] K. Howe *et al.*, "The zebrafish reference genome sequence and its relationship to the human genome," *Nature*, vol. 496, no. 7446, pp. 498–503, Apr. 2013.

[67] C. Saverino and R. Gerlai, "The social zebrafish: Behavioral responses to conspecific, heterospecific, and computer animated fish," *Behav. Brain Res.*, vol. 191, no. 1, pp. 77–87, Aug. 2008.

[68] R. F. Oliveira, "Mind the fish: zebrafish as a model in cognitive social neuroscience," *Front. Neural Circuits*, vol. 7, 2013.

[69] L. Yu, V. Tucci, S. Kishi, and I. V. Zhdanova, "Cognitive Aging in Zebrafish," *PLoS One*, vol. 1, no. 1, p. e14, Dec. 2006.

[70] J. Ganz *et al.*, "Subdivisions of the adult zebrafish pallium based on molecular marker analysis," *F1000Research*, vol. 3, no. May, p. 308, Nov. 2015.

[71] M. F. Wullimann, B. Rupp, and H. Reichert, *Neuroanatomy of the Zebrafish Brain*. Basel: Birkhäuser Basel, 1996.

[72] M. F. Wullimann and T. Mueller, "Teleostean and mammalian forebrains contrasted: Evidence from genes to behavior," *J. Comp. Neurol.*, vol. 475, no. 2, pp. 143–162, Jul. 2004.

[73] R.-H. Nam, W. Kim, and C.-J. Lee, "NMDA receptor-dependent long-term potentiation in the telencephalon of the zebrafish," *Neurosci. Lett.*, vol. 370, no. 2–3, pp. 248–251, Nov. 2004.

[74] M.-C. Ng *et al.*, “Stimulation of the lateral division of the dorsal telencephalon induces synaptic plasticity in the medial division of adult zebrafish,” *Neurosci. Lett.*, vol. 512, no. 2, pp. 109–113, Mar. 2012.

[75] Y. J. Wu *et al.*, “Unilateral stimulation of the lateral division of the dorsal telencephalon induces synaptic plasticity in the bilateral medial division of zebrafish,” *Sci. Rep.*, vol. 7, no. 1, pp. 1–8, 2017.

[76] C. Kizil, J. Kaslin, V. Kroehne, and M. Brand, “Adult neurogenesis and brain regeneration in zebrafish,” *Dev. Neurobiol.*, vol. 72, no. 3, pp. 429–461, Mar. 2012.

[77] H. Grandel, J. Kaslin, J. Ganz, I. Wenzel, and M. Brand, “Neural stem cells and neurogenesis in the adult zebrafish brain: Origin, proliferation dynamics, migration and cell fate,” *Dev. Biol.*, vol. 295, no. 1, pp. 263–277, Jul. 2006.

[78] K. Edelmann *et al.*, “Increased radial glia quiescence, decreased reactivation upon injury and unaltered neuroblast behavior underlie decreased neurogenesis in the aging zebrafish telencephalon,” *J. Comp. Neurol.*, vol. 521, no. 13, pp. 3099–3115, Sep. 2013.

[79] A. Arslan-Ergul, B. Erbaba, E. T. Karoglu, D. O. Halim, and M. M. Adams, “Short-term dietary restriction in old zebrafish changes cell senescence mechanisms,” *Neuroscience*, vol. 334, pp. 64–75, 2016.

[80] S. Kishi *et al.*, “The Identification of Zebrafish Mutants Showing Alterations in Senescence-Associated Biomarkers,” *PLoS Genet.*, vol. 4, no. 8, p.

e1000152, Aug. 2008.

[81] K. M. Kwan *et al.*, "The Tol2kit: A multisite gateway-based construction Kit for Tol2 transposon transgenesis constructs," *Dev. Dyn.*, vol. 236, no. 11, pp. 3088–3099, 2007.

[82] K. Kawakami, "Tol2: A versatile gene transfer vector in vertebrates," *Genome Biol.*, vol. 8, no. SUPPL. 1, pp. 1–10, 2007.

[83] K. Kawakami, K. Asakawa, A. Muto, and H. Wada, *Tol2-mediated transgenesis, gene trapping, enhancer trapping, and Gal4-UAS system*, vol. 135. Elsevier Ltd, 2016.

[84] W. Y. Hwang *et al.*, "Efficient genome editing in zebrafish using a CRISPR-Cas system," *Nat. Biotechnol.*, vol. 31, no. 3, pp. 227–229, Mar. 2013.

[85] M. Li, L. Zhao, P. S. Page-McCaw, and W. Chen, "Zebrafish Genome Engineering Using the CRISPR–Cas9 System," *Trends Genet.*, vol. 32, no. 12, pp. 815–827, 2016.

[86] B. R. Bill, A. M. Petzold, K. J. Clark, L. A. Schimmenti, and S. C. Ekker, "A Primer for Morpholino Use in Zebrafish," *Zebrafish*, vol. 6, no. 1, pp. 69–77, 2009.

[87] J. S. Eisen and J. C. Smith, "Controlling morpholino experiments: don't stop making antisense," *Development*, vol. 135, no. 10, pp. 1735–1743, 2008.

[88] P. A. Morcos, "Achieving targeted and quantifiable alteration of mRNA splicing with Morpholino oligos," *Biochem. Biophys. Res. Commun.*, vol. 358,

no. 2, pp. 521–527, Jun. 2007.

[89] P. A. Morcos, Y. Li, and S. Jiang, “Vivo-Morpholinos: A non-peptide transporter delivers Morpholinos into a wide array of mouse tissues,” *Biotechniques*, vol. 45, no. 6, pp. 613–623, 2008.

[90] C. Kizil and M. Brand, “Cerebroventricular Microinjection (CVMI) into Adult Zebrafish Brain Is an Efficient Misexpression Method for Forebrain Ventricular Cells,” *PLoS One*, vol. 6, no. 11, p. e27395, Nov. 2011.

[91] C. Kizil, A. Iltzsche, J. Kaslin, and M. Brand, “Micromanipulation of gene expression in the adult zebrafish brain using cerebroventricular microinjection of morpholino oligonucleotides.,” *J. Vis. Exp.*, no. 75, p. e50415, 2013.

[92] D. Celebi-Birand, N. I. Ardic, E. T. Karoglu-Eravsar, G. F. Sengul, H. Kafaligonul, and M. M. Adams, “Dietary and Pharmacological Interventions That Inhibit Mammalian Target of Rapamycin Activity Alter the Brain Expression Levels of Neurogenic and Glial Markers in an Age-and Treatment-Dependent Manner,” *Rejuvenation Res.*, vol. XX, no. Xx, p. rej.2019.2297, May 2020.

[93] T. Oka *et al.*, “Diet-induced obesity in zebrafish shares common pathophysiological pathways with mammalian obesity,” *BMC Physiol.*, vol. 10, no. 1, 2010.

[94] K. Landgraf *et al.*, “Short-term overfeeding of zebrafish with normal or high-fat diet as a model for the development of metabolically healthy versus

unhealthy obesity," *BMC Physiol.*, vol. 17, no. 1, pp. 1–10, 2017.

[95] M. Dozawa, H. Kono, Y. Sato, Y. Ito, H. Tanaka, and T. Ohshima, "Valproic acid, a histone deacetylase inhibitor, regulates cell proliferation in the adult zebrafish optic tectum," *Dev. Dyn.*, vol. 243, no. 11, pp. 1401–1415, 2014.

[96] Y. Shimizu, Y. Ueda, and T. Ohshima, "Wnt signaling regulates proliferation and differentiation of radial glia in regenerative processes after stab injury in the optic tectum of adult zebrafish," *Glia*, vol. 66, no. 7, pp. 1382–1394, 2018.

[97] J. Redondo *et al.*, "Hippocampal HECT E3 ligase inhibition facilitates consolidation, retrieval, and reconsolidation, and inhibits extinction of contextual fear memory," *Neurobiol. Learn. Mem.*, vol. 167, no. July 2019, p. 107135, 2020.

[98] S. Hao, A. Dey, X. Yu, and A. M. Stranahan, "Dietary obesity reversibly induces synaptic stripping by microglia and impairs hippocampal plasticity," *Brain. Behav. Immun.*, vol. 51, pp. 230–239, 2016.

[99] V. Kothari *et al.*, "High fat diet induces brain insulin resistance and cognitive impairment in mice.," *Biochim. Biophys. acta. Mol. basis Dis.*, vol. 1863, no. 2, pp. 499–508, Feb. 2017.

[100] S. Meguro, S. Hosoi, and T. Hasumura, "High-fat diet impairs cognitive function of zebrafish," *Sci. Rep.*, vol. 9, no. 1, pp. 1–9, 2019.

[101] World Health Organization, "Noncommunicable diseases country profiles 2018," Chichester, UK: John Wiley & Sons, Ltd, 2018.

[102] M. E. Bocarsly *et al.*, “Obesity diminishes synaptic markers, alters microglial morphology, and impairs cognitive function,” *Proc. Natl. Acad. Sci.*, p. 201511593, 2015.

[103] G. Cavaliere *et al.*, “High-Fat Diet Induces Neuroinflammation and Mitochondrial Impairment in Mice Cerebral Cortex and Synaptic Fraction ,” *Frontiers in Cellular Neuroscience* , vol. 13. p. 509, 2019.

[104] B. Martin, M. P. Mattson, and S. Maudsley, “Caloric restriction and intermittent fasting: Two potential diets for successful brain aging,” *Ageing Res. Rev.*, vol. 5, no. 3, pp. 332–353, Aug. 2006.

[105] S. J. Mitchell *et al.*, “Effects of Sex, Strain, and Energy Intake on Hallmarks of Aging in Mice,” *Cell Metab.*, vol. 23, no. 6, pp. 1093–1112, Jun. 2016.

[106] L. M. Redman and E. Ravussin, “Caloric Restriction in Humans: Impact on Physiological, Psychological, and Behavioral Outcomes,” *Antioxid. Redox Signal.*, vol. 14, no. 2, pp. 275–287, Jan. 2011.

[107] L. Shi *et al.*, “Caloric restriction eliminates the aging-related decline in NMDA and AMPA receptor subunits in the rat hippocampus and induces homeostasis,” *Exp. Neurol.*, vol. 206, no. 1, pp. 70–79, Jul. 2007.

[108] A. L. Markowska and A. Savonenko, “Retardation of cognitive aging by life-long diet restriction: Implications for genetic variance,” *Neurobiol. Aging*, vol. 23, no. 1, pp. 75–86, 2002.

[109] G. Montalbano *et al.*, “Morphological differences in adipose tissue and

changes in BDNF/Trkb expression in brain and gut of a diet induced obese zebrafish model," *Ann. Anat.*, vol. 204, pp. 36–44, Mar. 2016.

[110] A. J. Stankiewicz, E. M. McGowan, L. Yu, and I. V. Zhdanova, "Impaired sleep, circadian rhythms and neurogenesis in diet-induced premature aging," *Int. J. Mol. Sci.*, vol. 18, no. 11, 2017.

[111] M. Ros and J. M. Carrascosa, "Current nutritional and pharmacological anti-aging interventions," *Biochim. Biophys. Acta - Mol. Basis Dis.*, vol. 1866, no. 3, p. 165612, Mar. 2020.

[112] K. T. Howitz *et al.*, "Small molecule activators of sirtuins extend Saccharomyces cerevisiae lifespan," *Nature*, vol. 425, no. 6954, pp. 191–196, 2003.

[113] K. J. Pearson *et al.*, "Resveratrol Delays Age-Related Deterioration and Mimics Transcriptional Aspects of Dietary Restriction without Extending Life Span," *Cell Metab.*, vol. 8, no. 2, pp. 157–168, 2008.

[114] B. B. de Jesus, K. Schneeberger, E. Vera, A. Tejera, C. B. Harley, and M. A. Blasco, "The telomerase activator TA-65 elongates short telomeres and increases health span of adult/old mice without increasing cancer incidence," *Aging Cell*, vol. 10, no. 4, pp. 604–621, 2011.

[115] E. Eitan, A. Tichon, A. Gazit, D. Gitler, S. Slavin, and E. Priel, "Novel telomerase-increasing compound in mouse brain delays the onset of amyotrophic lateral sclerosis," *EMBO Mol. Med.*, vol. 4, no. 4, pp. 313–329,

2012.

[116] T. Mund, M. J. Lewis, S. Maslen, and H. R. Pelham, “Peptide and small molecule inhibitors of HECT-type ubiquitin ligases,” *Proc. Natl. Acad. Sci. U. S. A.*, vol. 111, no. 47, pp. 16736–16741, 2014.

[117] AVMA (American Veterinary Medical Association), *AVMA guidelines for the Euthanasia of Animals: 2013 Edition*, no. January. 2013.

[118] M. Matthews and Z. M. Varga, “Anesthesia and Euthanasia in Zebrafish,” *ILAR J.*, vol. 53, no. 2, pp. 192–204, Jun. 2012.

[119] J. Näslund, “A simple non-invasive method for measuring gross brain size in small live fish with semi-transparent heads,” *PeerJ*, vol. 2, no. 1, p. e586, Sep. 2014.

[120] E. Sezgin *et al.*, “Binding of canonical Wnt ligands to their receptor complexes occurs in ordered plasma membrane environments,” *FEBS J.*, vol. 284, no. 15, pp. 2513–2526, Aug. 2017.

[121] G. M. T. de Oliveira *et al.*, “Transient modulation of acetylcholinesterase activity caused by exposure to dextran-coated iron oxide nanoparticles in brain of adult zebrafish,” *Comp. Biochem. Physiol. Part C Toxicol. Pharmacol.*, vol. 162, no. 1, pp. 77–84, May 2014.

[122] Y. Hua, C. Wang, J. Huang, and K. Wang, “A simple and efficient method for CRISPR/Cas9-induced mutant screening,” *J. Genet. Genomics*, vol. 44, no. 4, pp. 207–213, Apr. 2017.

[123] L. Vouillot, A. Thélie, and N. Pollet, “Comparison of T7E1 and Surveyor Mismatch Cleavage Assays to Detect Mutations Triggered by Engineered Nucleases,” *G3 Genes|Genomes|Genetics*, vol. 5, no. 3, pp. 407–415, Mar. 2015.

[124] B. Dupret, P. Völkel, P. Follet, X. Le Bourhis, and P.-O. Angrand, “Combining genotypic and phenotypic analyses on single mutant zebrafish larvae,” *MethodsX*, vol. 5, pp. 244–256, 2018.

[125] L.-E. Jao, S. R. Wente, and W. Chen, “Efficient multiplex biallelic zebrafish genome editing using a CRISPR nuclease system,” *Proc. Natl. Acad. Sci.*, vol. 110, no. 34, pp. 13904–13909, Aug. 2013.

[126] R. P. Haugland, *Handbook of Fluorescent Probes and Research Products*. 2002.

[127] D. Szklarczyk *et al.*, “STRING v11: protein–protein association networks with increased coverage, supporting functional discovery in genome-wide experimental datasets,” *Nucleic Acids Res.*, vol. 47, no. D1, pp. D607–D613, Jan. 2019.

[128] S. Wiesner *et al.*, “Autoinhibition of the HECT-Type Ubiquitin Ligase Smurf2 through Its C2 Domain,” *Cell*, vol. 130, no. 4, pp. 651–662, Aug. 2007.

[129] B. Cha, Y. Park, B. N. Hwang, S. Kim, and E. Jho, “Protein Arginine Methyltransferase 1 Methylates Smurf2,” *Mol. Cells*, vol. 38, no. 8, pp. 723–728, Aug. 2015.

[130] A. S. Chandhoke, K. Karve, S. Dadakhujaev, S. Netherton, L. Deng, and S. Bonni, “The ubiquitin ligase Smurf2 suppresses TGFβ-induced epithelial-mesenchymal transition in a sumoylation-regulated manner,” *Cell Death Differ.*, vol. 23, no. 5, pp. 876–888, 2016.

[131] K. Inoue, E. A. Fry, and D. P. Frazier, “Transcription factors that interact with p53 and Mdm2,” *Int. J. Cancer*, vol. 138, no. 7, pp. 1577–1585, 2016.

[132] S. Hans, J. Kaslin, D. Freudenreich, and M. Brand, “Temporally-controlled site-specific recombination in zebrafish,” *PLoS One*, vol. 4, no. 2, 2009.

[133] M. LaBonty, N. Pray, and P. C. Yelick, “A Zebrafish Model of Human Fibrodysplasia Ossificans Progressiva,” *Zebrafish*, vol. 14, no. 4, pp. 293–304, Aug. 2017.

[134] S. Jinno, “Decline in adult neurogenesis during aging follows a topographic pattern in the mouse hippocampus,” *J. Comp. Neurol.*, vol. 519, no. 3, pp. 451–466, 2011.

[135] J. M. Oh, J. H. Jeong, S. Y. Park, and S. Chun, “Ginsenoside compound K induces adult hippocampal proliferation and survival of newly generated cells in young and elderly mice,” *Biomolecules*, vol. 10, no. 3, pp. 1–13, 2020.

[136] L. F. Eng, R. S. Ghirnikar, and Y. L. Lee, “Glial Fibrillary Acidic Protein: GFAP-Thirty-One Years (1969–2000),” *Neurochem. Res.*, vol. 25, no. 9, pp. 1439–1451, 2000.

[137] M. M. Boisvert, G. A. Erikson, M. N. Shokhirev, and N. J. Allen, “The Aging

Astrocyte Transcriptome from Multiple Regions of the Mouse Brain," *Cell Rep.*, vol. 22, no. 1, pp. 269–285, Jan. 2018.

[138] G. M. Bernal and D. A. Peterson, "Phenotypic and gene expression modification with normal brain aging in GFAP-positive astrocytes and neural stem cells," *Aging Cell*, vol. 10, no. 3, pp. 466–482, Jun. 2011.

[139] J. Zwirner *et al.*, "Subthalamic nucleus volumes are highly consistent but decrease age-dependently—a combined magnetic resonance imaging and stereology approach in humans," *Hum. Brain Mapp.*, vol. 38, no. 2, pp. 909–922, 2017.

[140] I. Carpentier, B. Coornaert, and R. Beyaert, "Smurf2 is a TRAF2 binding protein that triggers TNF-R2 ubiquitination and TNF-R2-induced JNK activation," *Biochem. Biophys. Res. Commun.*, vol. 374, no. 4, pp. 752–757, 2008.

[141] T. H. Lin *et al.*, "Decreased osteogenesis in mesenchymal stem cells derived from the aged mouse is associated with enhanced NF-κB activity," *J. Orthop. Res.*, vol. 35, no. 2, pp. 281–288, 2017.

[142] J. Chang *et al.*, "NF-κB inhibits osteogenic differentiation of mesenchymal stem cells by promoting β-catenin degradation," *Proc. Natl. Acad. Sci. U. S. A.*, vol. 110, no. 23, pp. 9469–9474, 2013.

[143] Y. Zhang, Z. Zhang, and W. Ge, "An efficient platform for generating somatic point mutations with germline transmission in the zebrafish by CRISPR/Cas9-

mediated gene editing," *J. Biol. Chem.*, vol. 293, no. 17, pp. 6611–6622, Apr. 2018.

[144] F. Carmona-Aldana, H. N. Nuñez-Martinez, C. A. Peralta-Alvarez, G. Tapia-Urzua, and F. Recillas-Targa, "Generation of Functional Genetic Study Models in Zebrafish Using CRISPR-Cas9," in *Cancer Cell Signaling. Methods in Molecular Biology*, vol. 2174, 2021, pp. 255–262.

[145] R. S. Wu, I. I. Lam, H. Clay, D. N. Duong, R. C. Deo, and S. R. Coughlin, "A Rapid Method for Directed Gene Knockout for Screening in G0 Zebrafish," *Dev. Cell*, vol. 46, no. 1, pp. 112-125.e4, Jul. 2018.

[146] G. S. Gerhard *et al.*, "Life spans and senescent phenotypes in two strains of Zebrafish (Danio rerio)," *Exp. Gerontol.*, vol. 37, no. 8–9, pp. 1055–1068, Aug. 2002.

[147] S. B. Tsai *et al.*, "Differential effects of genotoxic stress on both concurrent body growth and gradual senescence in the adult zebrafish," *Aging Cell*, vol. 6, no. 2, pp. 209–224, 2007.

[148] R. Vargas and I. C. Vásquez, "Effects of overfeeding and high-fat diet on cardiosomatic parameters and cardiac structures in young and adult zebrafish," *Fish Physiol. Biochem.*, vol. 43, no. 6, pp. 1761–1773, 2017.

[149] G. Ran *et al.*, "Resveratrol ameliorates diet-induced dysregulation of lipid metabolism in zebrafish (Danio rerio)," *PLoS One*, vol. 12, no. 7, pp. 1–15, 2017.

[150] C.-H. Kim *et al.*, “Zebrafish elav/HuC homologue as a very early neuronal marker,” *Neurosci. Lett.*, vol. 216, no. 2, pp. 109–112, Sep. 1996.

[151] E. Shin *et al.*, “Doublecortin-like kinase enhances dendritic remodelling and negatively regulates synapse maturation,” *Nat. Commun.*, vol. 4, no. May 2012, 2013.

[152] T. Shu *et al.*, “Doublecortin-like kinase controls neurogenesis by regulating mitotic spindles and M phase progression,” *Neuron*, vol. 49, no. 1, pp. 25–39, 2006.

[153] R. Schmidt, U. Strähle, and S. Scholpp, “Neurogenesis in zebrafish - from embryo to adult,” *Neural Dev.*, vol. 8, no. 1, pp. 1–13, 2013.

[154] J. Zhang and J. Jiao, “Molecular Biomarkers for Embryonic and Adult Neural Stem Cell and Neurogenesis,” *Biomed Res. Int.*, vol. 2015, pp. 1–14, 2015.

[155] B. L. Xu *et al.*, “Resveratrol prevents high-calorie diet-induced learning and memory dysfunction in juvenile C57BL/6J mice,” *Neurol. Res.*, vol. 40, no. 8, pp. 709–715, 2018.

[156] B. L. Xu *et al.*, “Comparison of the effects of resveratrol and caloric restriction on learning and memory in juvenile C57BL/6J mice,” *Iran. J. Basic Med. Sci.*, vol. 18, no. 11, pp. 1118–1123, 2015.

[157] M. G. Edwards, R. M. Anderson, M. Yuan, C. M. Kendziorski, R. Weindruch, and T. A. Prolla, “Gene expression profiling of aging reveals activation of a p53-mediated transcriptional program,” *BMC Genomics*, vol. 8, no. 1, p. 80,

2007.

[158] I. Bialuk, M. Cieślińska, O. Kowalczuk, T. A. Bonda, J. Nikliński, and M. M. Winnicka, “IL-6 deficiency attenuates p53 protein accumulation in aged male mouse hippocampus,” *Biogerontology*, vol. 21, no. 1, pp. 29–43, 2020.

[159] T. Loustau, E. Coudiere, E. Karkeni, J. F. Landrier, B. Jover, and C. Riva, “Murine double minute-2 mediates exercise-induced angiogenesis in adipose tissue of diet-induced obese mice,” *Microvasc. Res.*, vol. 130, no. November 2019, p. 104003, 2020.

[160] Z. Liu *et al.*, “The dysfunctional MDM2-p53 axis in adipocytes contributes to aging-related metabolic complications by induction of lipodystrophy,” *Diabetes*, vol. 67, no. 11, pp. 2397–2409, 2018.

[161] Q. Mu *et al.*, “Betulinic acid improves nonalcoholic fatty liver disease through YY1/FAS signaling pathway,” *FASEB J.*, no. July, pp. 1–16, 2020.

[162] T. Ye and R. Liu, “Effect of Octreotide on Pancreatic Fibrosis of High-Fat Diet Induced Obesity in Rats,” *Gastroenterology*, vol. 152, no. 5, p. S895, 2017.

[163] A. Muñoz, C. L. Corrêa, A. Lopez-Lopez, M. A. Costa-Besada, C. Diaz-Ruiz, and J. L. Labandeira-Garcia, “Physical exercise improves aging-related changes in angiotensin, IGF-1, SIRT1, SIRT3, and VEGF in the substantia Nigra,” *Journals Gerontol. - Ser. A Biol. Sci. Med. Sci.*, vol. 73, no. 12, pp. 1594–1601, 2018.

[164] E. Koltai *et al.*, “Combined Exercise and Insulin-Like Growth Factor-1

Supplementation Induces Neurogenesis in Old Rats, but Do Not Attenuate Age-Associated DNA Damage," *Rejuvenation Res.*, vol. 14, no. 6, pp. 585–596, Dec. 2011.

[165] L. Fontana and L. Partridge, "Promoting health and longevity through diet: From model organisms to humans," *Cell*, vol. 161, no. 1, pp. 106–118, 2015.

[166] T. Usui *et al.*, "The French press: A repeatable and high-throughput approach to exercising zebrafish (Danio rerio)," *PeerJ*, vol. 2018, no. 1, pp. 1–12, 2018.

[167] S. Meguro, T. Hasumura, and T. Hase, "Body Fat Accumulation in Zebrafish Is Induced by a Diet Rich in Fat and Reduced by Supplementation with Green Tea Extract," *PLoS One*, vol. 10, no. 3, p. e0120142, Mar. 2015.

[168] D. J. Saaltink, B. Håvik, C. S. Verissimo, P. J. Lucassen, and E. Vreugdenhil, "Doublecortin and doublecortin-like are expressed in overlapping and non-overlapping neuronal cell population: Implications for neurogenesis," *J. Comp. Neurol.*, vol. 520, no. 13, pp. 2805–2823, 2012.

[169] L. Fontana, J. Nehme, and M. Demaria, "Caloric restriction and cellular senescence," *Mech. Ageing Dev.*, vol. 176, no. November, pp. 19–23, Dec. 2018.

[170] E. Vreugdenhil *et al.*, "Doublecortin-like, a microtubule-associated protein expressed in radial glia, is crucial for neuronal precursor division and radial process stability," *Eur. J. Neurosci.*, vol. 25, no. 3, pp. 635–648, 2007.

[171] T. B. M. Hakvoort *et al.*, "Interorgan coordination of the murine adaptive

response to fasting," *J. Biol. Chem.*, vol. 286, no. 18, pp. 16332–16343, 2011.

[172] M. Krampert *et al.*, "Smad7 Regulates the Adult Neural Stem/Progenitor Cell Pool in a Transforming Growth Factor β- and Bone Morphogenetic Protein-Independent Manner," *Mol. Cell. Biol.*, vol. 30, no. 14, pp. 3685–3694, Jul. 2010.

[173] J. Marschallinger, M. Krampert, S. Couillard-Despres, R. Heuchel, U. Bogdahn, and L. Aigner, "Age-dependent and differential effects of Smad7ΔEx1 on neural progenitor cell proliferation and on neurogenesis," *Exp. Gerontol.*, vol. 57, pp. 149–154, Sep. 2014.

[174] H. Liu, J. Yang, K. Wang, T. Niu, and D. Huang, "Moderate- and Low-Dose of Atorvastatin Alleviate Cognition Impairment Induced by High-Fat Diet via Sirt1 Activation," *Neurochem. Res.*, vol. 44, no. 5, pp. 1065–1078, 2019.

[175] H. Y. Cohen *et al.*, "Calorie restriction promotes mammalian cell survival by inducing the SIRT1 deacetylase.," *Science*, vol. 305, no. 5682, pp. 390–2, Jul. 2004.

[176] M. Li, X. Liu, and X. Feng, "Cardiovascular toxicity and anxiety-like behavior induced by deltamethrin in zebrafish (Danio rerio) larvae," *Chemosphere*, vol. 219, pp. 155–164, Mar. 2019.

[177] R. A. Mans, K. D. Hinton, C. H. Payne, G. E. Powers, N. L. Scheuermann, and M. Saint-Jean, "Cholinergic Stimulation of the Adult Zebrafish Brain Induces Phosphorylation of Glycogen Synthase Kinase-3 β and Extracellular Signal-

Regulated Kinase in the Telencephalon," *Front. Mol. Neurosci.*, vol. 12, no. April, Apr. 2019.

[178] Y. Lee, S. Lee, and C.-J. Lee, "Cell Proliferation in the Isolated Brains of Adult Zebrafish Incubated in Artificial Cerebrospinal Fluid," *Zebrafish*, vol. 16, no. 5, pp. 486–489, Oct. 2019.

[179] T. Nakagawa and K. Nakayama, "Protein monoubiquitylation: targets and diverse functions," *Genes to Cells*, vol. 20, no. 7, pp. 543–562, Jul. 2015.

[180] A. J. George, Y. C. Hoffiz, A. J. Charles, Y. Zhu, and A. M. Mabb, "A Comprehensive Atlas of E3 Ubiquitin Ligase Mutations in Neurological Disorders," *Front. Genet.*, vol. 9, no. FEB, pp. 1–17, Feb. 2018.

[181] A. Upadhyay *et al.*, "E3 Ubiquitin Ligases Neurobiological Mechanisms: Development to Degeneration," *Front. Mol. Neurosci.*, vol. 10, no. May, pp. 1–21, May 2017.

[182] F. E. Morreale and H. Walden, "Types of Ubiquitin Ligases," *Cell*, vol. 165, no. 1, pp. 248-248.e1, 2016.

[183] B. Saritas-Yildirim and E. M. Silva, "The role of targeted protein degradation in early neural development," *Genesis*, vol. 52, no. 4, pp. 287–299, 2014.

[184] Y. L. Yu *et al.*, "Smurf2-mediated degradation of EZH2 enhances neuron differentiation and improves functional recovery after ischaemic stroke," *EMBO Mol. Med.*, vol. 5, no. 4, pp. 531–547, 2013.

[185] S.-W. Min *et al.*, "Acetylation of Tau Inhibits Its Degradation and Contributes

to Tauopathy," *Neuron*, vol. 67, no. 6, pp. 953–966, Sep. 2010.

[186] F. Ng, L. Wijaya, and B. L. Tang, "SIRT1 in the brain—connections with aging-associated disorders and lifespan," *Front. Cell. Neurosci.*, vol. 9, no. March, pp. 1–13, 2015.

[187] S. Michan *et al.*, "SIRT1 Is Essential for Normal Cognitive Function and Synaptic Plasticity," *J. Neurosci.*, vol. 30, no. 29, pp. 9695–9707, Jul. 2010.

[188] A. Z. Herskovits and L. Guarente, "SIRT1 in Neurodevelopment and Brain Senescence," *Neuron*, vol. 81, no. 3, pp. 471–483, Feb. 2014.

[189] H. Shimura, D. Schwartz, S. P. Gygi, and K. S. Kosik, "CHIP-Hsc70 Complex Ubiquitinates Phosphorylated Tau and Enhances Cell Survival," *J. Biol. Chem.*, 2004.

[190] L. Petrucelli *et al.*, "CHIP and Hsp70 regulate tau ubiquitination, degradation and aggregation," *Hum. Mol. Genet.*, 2004.

[191] A. Ito *et al.*, "MDM2-HDAC1-mediated deacetylation of p53 is required for its degradation," *EMBO J.*, vol. 21, no. 22, pp. 6236–6245, 2002.

[192] J. Seo and M. Park, "Molecular crosstalk between cancer and neurodegenerative diseases," *Cell. Mol. Life Sci.*, vol. 77, no. 14, pp. 2659–2680, Jul. 2020.

[193] K. Ibáñez, C. Boullosa, R. Tabarés-Seisdedos, A. Baudot, and A. Valencia, "Molecular Evidence for the Inverse Comorbidity between Central Nervous System Disorders and Cancers Detected by Transcriptomic Meta-analyses,"

PLoS Genet., vol. 10, no. 2, p. e1004173, Feb. 2014.

[194] A. Field, *DISCOVERING STATISTICS USING SPSS THIRD EDITION*. 2005.

[195] B. Saltepe, E. U. Bozkurt, N. Hacıosmanoğlu, and U. Ö. Ş. Şeker, "Genetic Circuits To Detect Nanomaterial Triggered Toxicity through Engineered Heat Shock Response Mechanism," *ACS Synth. Biol.*, vol. 8, no. 10, pp. 2404–2417, Oct. 2019.

[196] F. Carmona-Aldana *et al.*, "CTCF knockout reveals an essential role for this protein during the zebrafish development," *Mech. Dev.*, vol. 154, no. April, pp. 51–59, 2018.

[197] J. Schindelin *et al.*, "Fiji: An open-source platform for biological-image analysis," *Nat. Methods*, vol. 9, no. 7, pp. 676–682, 2012.

[198] X. Shi *et al.*, "Probing events with single molecule sensitivity in zebrafish and Drosophila embryos by fluorescence correlation spectroscopy," *Dev. Dyn.*, vol. 238, no. 12, pp. 3156–3167, Dec. 2009.

[199] T. Sasaki, "Age-Associated Weight Gain, Leptin, and SIRT1: A Possible Role for Hypothalamic SIRT1 in the Prevention of Weight Gain and Aging through Modulation of Leptin Sensitivity," *Front. Endocrinol. (Lausanne).*, vol. 6, no. JUL, pp. 1–10, Jul. 2015.

[200] M. Lafontaine-Lacasse, D. Richard, and F. Picard, "Effects of age and gender on Sirt 1 mRNA expressions in the hypothalamus of the mouse," *Neurosci. Lett.*, vol. 480, no. 1, pp. 1–3, Aug. 2010.

[201] K. Hasegawa and K. Yoshikawa, “Necdin Regulates p53 Acetylation via Sirtuin1 to Modulate DNA Damage Response in Cortical Neurons,” *J. Neurosci.*, vol. 28, no. 35, pp. 8772–8784, 2008.

[202] A. Bitto *et al.*, “Stress-induced senescence in human and rodent astrocytes,” *Exp. Cell Res.*, vol. 316, no. 17, pp. 2961–2968, Oct. 2010.

[203] T. Wu and M. E. Donohoe, “Yy1 regulates Senp1 contributing to AMPA receptor GluR1 expression following neuronal depolarization,” *J. Biomed. Sci.*, vol. 26, no. 1, pp. 1–15, 2019.

[204] M. Rylski *et al.*, “Yin Yang 1 is a critical repressor of matrix metalloproteinase-9 expression in brain neurons,” *J. Biol. Chem.*, vol. 283, no. 50, pp. 35140–35153, 2008.

[205] C. Du *et al.*, “A PRMT5-RNF168-SMURF2 Axis Controls H2AX Proteostasis,” *Cell Rep.*, vol. 28, no. 12, pp. 3199-3211.e5, 2019.